MSEL

Materials Science and Engineering Laboratory

CERAMICS

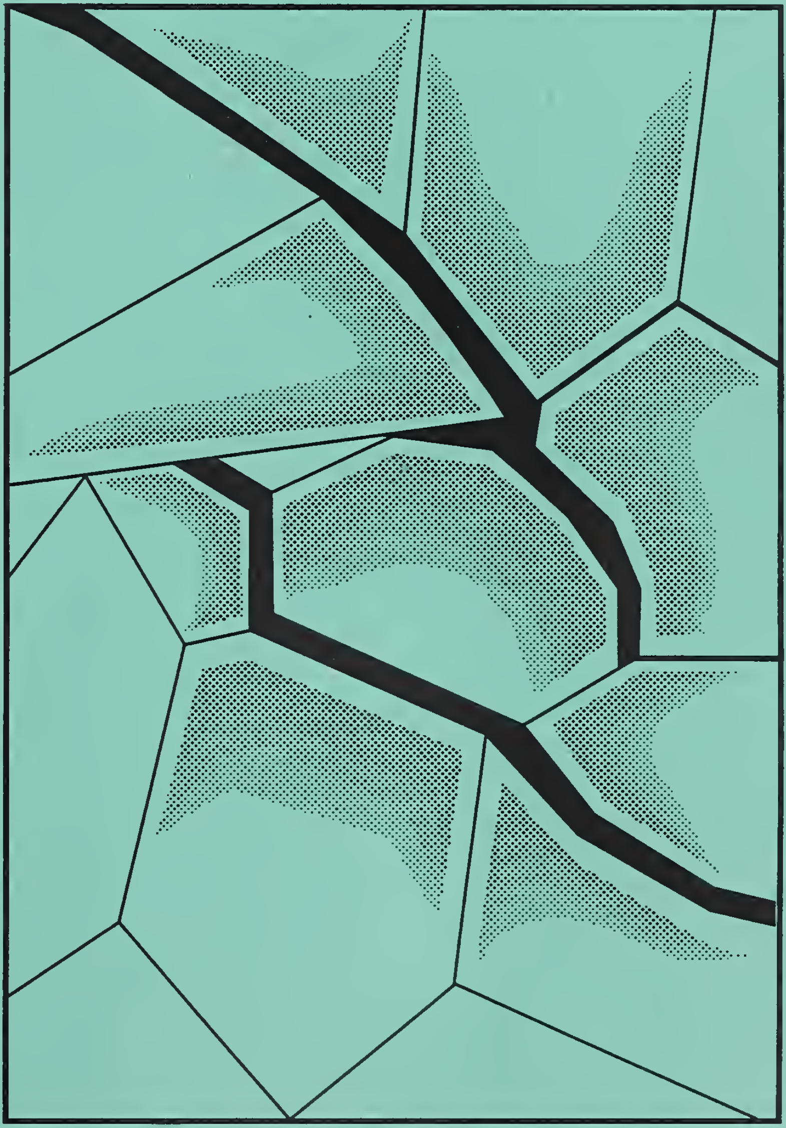

NAS-NRC
Assessment Panel
January 31-February 1, 1991

NISTIR 4394
U.S. Department of Commerce
National Institute of Standards
and Technology

Technical Activities
1990

The cover figure depicts an intergranular crack traversing several grains in aluminum oxide. Some grains in this region remain in contact with both crack interfaces and act effectively as bridges between them. These "grain bridge" include closure forces along the crack flanks which shield the crack top from an external loading, thus imparting additional toughness to the material. Grain bridging is an important toughening mechanism in alumina and other ceramics.

MSEL

Materials Science and Engineering Laboratory

CERAMICS

S.M. Hsu, Chief
S.J. Dapkunas, Deputy Chief

NAS-NRC
Assessment Panel
January 31-February 1, 1991

NISTIR 4394
U.S. Department of Commerce
National Institute of Standards
and Technology

Technical Activities
1990

U.S. DEPARTMENT OF COMMERCE, Robert A. Mosbacher,Secretary
National Institute of Standards and Technology, John W. Lyons, Director

TABLE OF CONTENTS

Page

INTRODUCTION.. 1

TECHNICAL ACTIVITIES.. 5

STRUCTURAL CERAMICS... 7

Overview.. 9
Program Structure... 9
Project Listing... 10
Significant Accomplishments................................... 11
Powder Characterization and Processing...Subhas Malghan....... 13
Mechanical Properties....................David Cranmer........ 33
Tribology................................Said Jahanmir........ 49

FUNCTIONAL CERAMICS... 71

Overview.. 73
Program Structure... 73
Project Listing... 74
Significant Accomplishments................................... 74
Electronic Materials.....................Stephen Freiman...... 77
Optical Materials........................Albert Feldman....... 85
Synchrotron Radiation Analysis...........Masao Kuriyama....... 95

STANDARD AND DATA ACTIVITIES 107

RESEARCH STAFF.. 117

OUTPUTS AND INTERACTIONS...................................... 129

Selected Technical Publications............................... 131

Selected Technical/Professional Committee Leadership......... 155

Industrial and Academic Interactions.......................... 159

Facilities.. 169

APPENDIX

Organizational Chart
National Institute of Standards and Technology

Organizational Chart
Institute for Materials Science and Engineering

INTRODUCTION

In 1990, the Ceramics Division initiated a series of programs to meet the technological needs of the ceramics industry. These programs were developed after extensive interaction with industry in the form of site visits and workshops organized by the Division:

- Test Methodologies for Ceramic Composites
- Research needs in Microelectronics Packaging
- Test Methodologies for Mechanical Property Measurement
- Ceramic Machining

The last workshop, Ceramic Machining, was organized in cooperation with the United States Advanced Ceramics Association. The meetings also augmented our efforts to transfer our research results to industry and academia.

In 1990, technology transfer was accomplished by the preparation and publication of 180 papers, the presentation of 150 talks and the submission of 6 invention disclosures. Many of the outputs were obtained through cooperative programs with guest scientists and research associates from industry.

Leadership of national and international standards activities continued. In addition to ASTM committee participation, Division staff coordinated the International Energy Agency Round Robin on Ceramic Powder Characterization Techniques and the U. S. ceramic activities in the Versailles Agreement on Materials and Standards (VAMAS). This participation strengthened the U.S. position in international standards development. The Structural Ceramics Database (SCD) Version 1.0 which contains evaluated thermomechanical data for industrial designers has been offered for public distribution by the Office of Standard Reference Data. Other database activities continued with the distribution of A Computerized Tribology Information System (ACTIS) and the completion of Volumes 7 and 8 of the NIST/American Ceramic Society Phase Diagrams for Ceramists.

A new activity, an assessment of the New Diamond Technology in Japan was undertaken by division personnel in 1990. This on site study was organized by Dr. Albert Feldman under the auspices of the Office of Science and Technology Policy and included the participation of nine industrial and academic organizations. Following the assessment survey, briefings were held to transmit the findings to U.S. industry.

The Division's research in structural and functional ceramics continued with a focus on the understanding of the chemistry and physics of processing and performance. In the structural materials area, research on the chemistry of ceramic slurries and suspensions has led to identification of mechanisms for coating silicon nitride powders with discrete sintering aids. This paves the way for the development of homogenous microstructures.

Significant advances in our ability to measure surface forces between dissimilar materials were achieved and programs to more comprehensively model behavior of interfaces were expanded. Basic research on bridging effects in fracture have been extended to microstructural design and studies of cyclic fatigue.

In functional materials, phase diagram determinations and studies of the role of processing environments on microstructural features of high temperature superconductors continued. The role of rare earth substitutions on YBaCO properties was evaluated and provided insight into the effect of atomic size of substitutional atoms. Diamond film research has been focused on the development of techniques of measurement of defects and interfacial structure as a function of deposition conditions.

Recognition of Ceramics Division staff contributions resulted in the award of the Department of Commerce Bronze medal to Dr. Debra Kaiser for her research on detwinning of YBaCuO single crystals. Silver medals were awarded to Drs. Roger Horn and Douglas Smith for their application of the Surface Forces Measurement technique to dissimilar materials and to Drs. Subhas Malghan and Alan Dragoo for the IEA Round Robin on Powder Characterization. The Society of Tribologists and Lubrication Engineers presented its National Award to Mr. Marshall Peterson for his contributions to the field of Tribology. Similarly, Dr. William Ruff was elected an Honorary Fellow of ASTM for his dedicated service to that organization.

Staff levels have remained stable but strengthened in the area of performance and reliability prediction and we were able to add two NRC post doctoral fellows this year. Funding remained stable with an increase of 3.5 percent in the funds received from industry, as shown in the following chart.

As we enter 1991 we will continue to address those fundamental needs of cost, reliability and performance prediction for advanced ceramics. Our efforts will focus on machining research required to achieve the above noted objectives for structural ceramics and in the area of functional materials on the measurement of micro stress and micro strain as they relate to component performance. We anticipate close interactions with DOE and industry in this area.

S. M. Hsu
Chief, Ceramics Division

1990 BUDGET – CERAMICS DIVISION

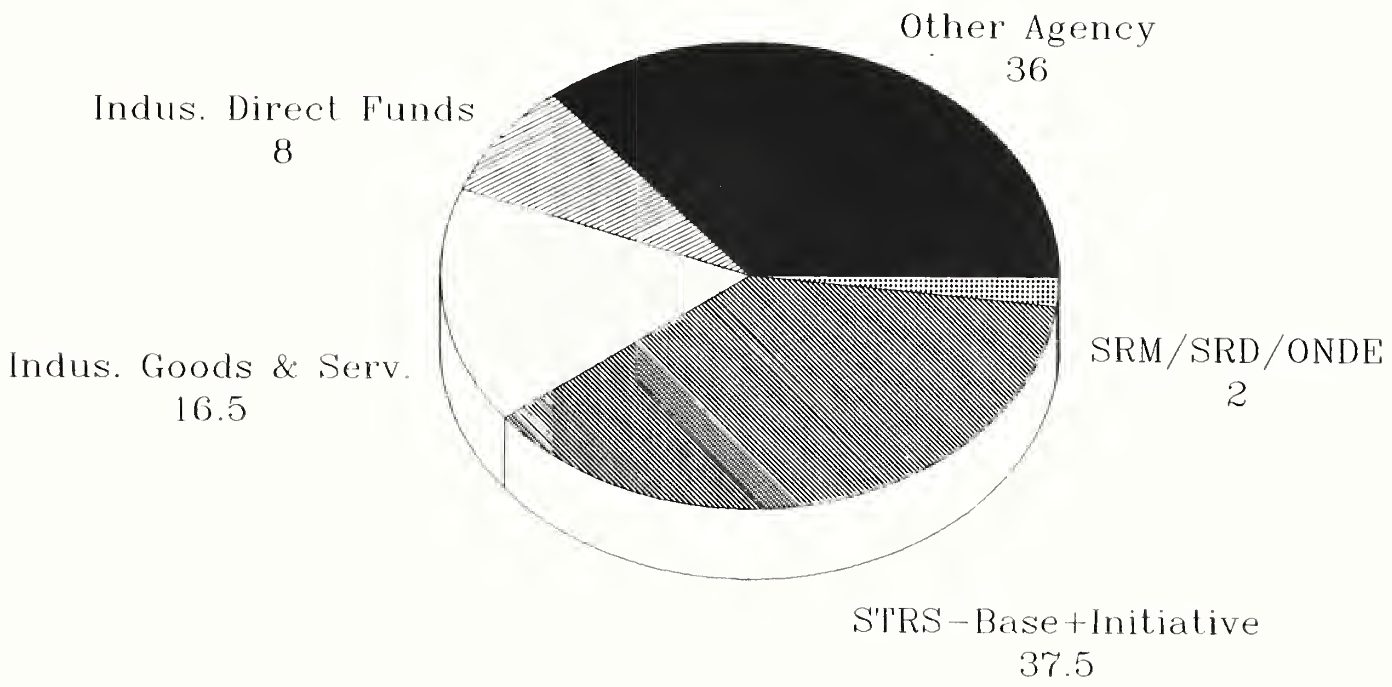

TECHNICAL ACTIVITIES

STRUCTURAL CERAMICS

STRUCTURAL CERAMICS

Overview

Structural ceramics can be defined as those whose primary function is to maintain a mechanical load or force. Recent advances in the design and development of ceramic bearings ceramic heat exchangers and automotive gas turbines and turbochargers have highlighted the improved performance possible through the use of these materials. The United States structural ceramics market (1989) is about $1 Billion. Firms serving this market typically are medium sized or a division of a much larger conglomerate and face intense competition from foreign suppliers. Our Division goal is to provide the standards related research and data required for domestic competiveness.

The structural ceramics program consists of research which addresses the issues of cost, reliability and performance. These issues are addressed through projects which focus on powder characterization, mechanical property measurement and interpretation; and tribological behavior emphasizing the effect of surface physical and chemical mechanisms. Typically, silicon nitride and silicon carbide are the main classes of materials of interest as both monolithics and composites; however, in some instances model materials such as silica and alumina are also used to provide systematic data.

Program Structure

Ceramic powders research utilizes techniques of analysis such as nuclear magnetic resonance (NMR), electrokinetic sonic amplitude and X-ray analysis of powders to identify the role of processing conditions on powder chemistry and morphology. These data provide insight into process controls which impact product cost and performance.

Consolidation and sintering of powder can effect both reliability and performance of ceramic components. Research utilizing small angle neutron scattering is directed toward the sintering of ceramics and has provided data for models describing pore behavior. Models required for control of composite sintering have been developed utilizing X-ray techniques. Related research on high pressure, low temperature consolidation has been initiated to take advantage of the unique properties of nanosized powders.

Mechanical property research has been directed toward the development of test methodologies for creep rupture and analysis of the modes of degradation of silicon carbide and nitride monolithics and composites. Basic research on the role of bridging in fracture of ceramics is underway and is manifested in a program on microstructure design. This effort is complimented by research on the behavior of interfaces in composites.

Tribological research addresses both prediction and mechanisms of wear. Projects are directed to the evaluation of the effects of materials chemistry and microstructure as well as lubricant reactivity. Data from this research is utilized in the development of wear maps which predict performance and mechanisms which impact materials development.

Our emphasis on technology support has increased with the implementation of the NIST mission. To direct our research to appropriate topics we have solicited the ceramics industry for guidance.

This guidance from industry has been gained by industrial visits and NIST sponsored workshops. From these workshops we have initiated changes to include new research on interface science and machining topics which will be emphasized in 1991.

Projects in the following areas comprise the core structural ceramics program.

Powder Characterization

International Round Robin on Ceramic Powder Characterization
Oxidation Kinetics of Ceramic Powders

Powder Processing

Agitation Milling of Powders
NMR Spectroscopy Imaging Technique Development for Powder and Slurries
The Relationship of Processing Properties of Ceramic Matrix Composites
Densification monitoring through Small Angle Neutrons Scattering of Alumina
Fabrication and characterization of nanophase ceramic materials

Performance/Reliability

Assessment of Mechanical Properties Testing Methodology
Microstructural Design of Ceramics
Surface Forces: Contact change transfer and adhesion
Creep and Creep Rupture of Hot Isostatically Pressed Silicon Nitride
Creep and Creep Rupture of Sintered Silicon Nitride
Glass Science and Technology
Ceramic Wear Maps
Tribology of Self Lubricating Composites
Mechanism of Adhesive Wearing Lubricated Contacts
Advanced Liquid Lubricants
Chemical Interactions of Advanced Materials and Lubricants

Significant Accomplishments

- The final report containing data, data analysis, procedures and recommendations on the IEA Subtask 2 program was distributed to the participants. In the continuing phase, 25 procedures were developed in collaboration with the IEA Subtask 6 participants. The samples of five powders were prepared and distributed to the participants. Data development was initiated using the procedures and samples prepared specifically for this purpose.

- Densification of nanosize (10-40 nm) silicon nitride powders at high pressures and low temperatures has been obtained without the addition of sintering aids. The resulting ceramics are transport and show high fracture toughness.

- Solid state nuclear magnetic resonance (NMR) spectroscopy was used to develop liquid imaging for silicon nitride slurry characterization. Qualitative description was developed for the distribution of liquid and solid phases. This information is expected to form a basis for describing the dispersion characteristics of silicon nitride powders.

- Enhanced kinetics were obtained in high energy agitation ball milling of silicon nitride powder. In aqueous environment, the milling kinetics is 8 to 10 times faster than that in a conventional ball mill. However, contamination caused by wear of mill liner is higher than desired.

- Two workshops on testing methodology were held at NIST in 1990. The first was on testing methodology for glass, glass-ceramic, and ceramic matrix composites, the purpose of which was to review and discuss mechanical property measurement techniques for whisker- and continuous-fiber reinforced ceramic composites and their constituents. The second was on mechanical testing methodology for ceramic design and reliability. Its purpose was to assess mechanical property measurement techniques for ceramics for use in component design and lifetime/reliability predictions. Technical areas covered in the workshops included testing for strength, creep and creep rupture, fracture toughness, and fatigue; effects of environment on the fracture and creep processes; lifetime and reliability prediction methods; mechanisms of failure; standardization; statistical experimental design and analysis; and fractography.

- Creep and creep rupture behavior of a hot-isostatically pressed silicon nitride has been characterized in tension using a laser imaging system. Characterization of the damage using analytical electron microscopy has shown the existence of lenticular-shaped cavities at glassy grain boundaries in this material.

- Processing techniques developed in FY 88 for studying residual stresses and distortions in ceramic matrix composites have been applied to both whisker- and fiber-reinforced ceramics. Controlled oxide coatings applied to the fibers by sol-gel techniques have been shown to influence the initiation of sintering stresses.

- Cathodoluminescence was used to measure residual stresses with high precision and with a spatial resolution of better than 5 μm in indented alumina single crystals. Stress induced frequency shifts of the ruby lines were utilized to measure the residual stresses in the region surrounding the indentation. The magnitude of the stresses varied with distance from the center of the indent and also with crystallographic orientation. After annealing at 1600°C for 10 hours, no measurable stresses remained either in the center of the indent or in the surrounding areas.

- A method of quantifying the charge transferred between two dissimilar surfaces in the Surface Force Apparatus has been devised. The method uses two sensitive electrometers to measure the charge on each material. Our technique allows us to measure the area over which the surfaces make contact before they are separated. Since both materials are exceptionally smooth we can equate this geometrical area with the true contact area, and thus calculate the surface charge per unit area, with an unusually high degree of accuracy. The technique also allows us to study the rate at which charge dissipates from the surfaces after they have been separated.

- Test results have shown that the tribological behavior of alpha-alumina in air depends on the contact load and temperature. Four distinct mechanisms were observed: intergranular fracture, tribochemical reaction between water vapor in the environment and the alumina surface, local plastic flow and plowing, and viscous flow of the glassy grain boundary phase. This type of information and the collected data on friction coefficient and wear rate are useful for design and material selection for tribological applications.

POWDER CHARACTERIZATION AND PROCESSING

Subhas Malghan

The manufacture of reliable, cost effective advanced ceramics relies upon the availability and controlled processing of fine powders. These requirements are addressed through development of techniques of powder analysis and data required by industry. This capability is extended to characterization of slurries and microstructural development during consolidation and sintering. The group carries out an integrated effort from the early steps of synthesis of well-characterized, deagglomerated powders to the understanding of processing effects on the microstructure of ceramics.

The group continues to play a key role in an international interlaboratory comparison of powder characterization methods conducted under the auspices of the International Energy Agency (IEA). The results have provided an important basis for the establishment of measurement procedures and standards that are vitally needed for the international commerce of advanced ceramic powders and materials.

Powder Characterization Round Robin

S. G. Malghan, J. F. Kelly, D. B. Minor and L.-S. Lum

International commerce in fine ceramic powders will rely upon the availability of accepted techniques of analysis of these materials. Currently, a variety of methods are used to determine powder size distribution and chemistry, with the extent of comparability and limits of applicability undetermined. This project was established to develop standardized testing and characterization methods for these new materials.

The primary focus of the powder characterization round-robin conducted under the auspices of International Energy Agency (IEA) is on R&D of high temperature structural ceramics for advanced engines and other energy conservation applications. The major objective is the evolution of standardized testing and characterization methods for these new materials.

Participation by the industry is a key aspect of the program. Production and international marketing of ceramic powders and sintered ceramic materials will require proven characterization methods, test procedures, and property standards for use by both manufacturers and users. Hence, researchers from the industry and government laboratories from four participating countries (the U.S., the FRG, Sweden and Japan) worked closely to define the technical scope of work.

The overall objective of the Subtask 6 on powder characterization is enhancement of the quality, reproducibility and reliability of powder characterization measurements and, consequently of ceramic powders. Through a program of interlaboratory comparison of measurements, the participants are engaged in:

- Analysis of ceramic starting powders by using specific procedures developed in this program.

- Establishment of a base of data and analysis experience which would identify unique sets of properties and methods useful for powder evaluation and comparison.

- Determination of the extent of agreement between laboratories.

The analysis of powder characteristics includes particle size distribution by four methods, specific surface area by BET method, crystalline and noncrystalline phase composition, elemental composition of impurities, halides analysis, and a host of surface chemical methods. The five powders included in this program are:

Silicon nitride, Ube SNE-10[1]
Silicon carbide, Starck
Silicon nitride, Starck LC-10
Aluminum nitride, Dow
Zirconia, TOSOH

Representative samples of these powders were prepared by three successive stages of riffling in argon ambient. Approximately 3500 samples were riffled and the sample containers were flame-sealed in glass vials to provide protection against contamination during shipping and storage.

The major emphasis of this program was to develop specific, detailed procedures by which the participants can analyze the samples. Current procedures were collected from the participants. Based on these current procedures, specific procedures were developed for each method of analysis. Subsequently, these specific procedures were ruggedness tested to determine the major variables and their impact on the resulting data. These procedures will be used by all 45 participants in the four participating countries (the U.S., the FRG, Sweden and Japan) to develop analysis data. A total of twenty-five procedures have been developed in this subtask. These procedures will be further refined based on the results of participants testing. The details provided for the physical and bulk chemical properties determination are sufficiently elaborate. However, for the surface chemical methods, sufficient details were not provided since the primary purpose is only to survey the surface chemistry methods.

Another feature of the Subtask 6 program is the flexibility of selecting methods of interest to the participants. Each participant has selected specific powder analysis methods offered under three groups (Physical, Bulk Chemical and Surface Chemical), while satisfying a minimum participation requirement.

During the fourth quarter of 1990, the participants will be analyzing these powder samples using the procedures developed in this program. The results will be compiled and analyzed.

---

[1] Though reference is made throughout the document to industrial firms and their products, such references in no way imply endorsement by the National Institute of Standards and Technology.

Agitation Milling of Powders

D. B. Minor, L.-S. Lum and S. G. Malghan

Machining of ceramic powders constitutes a significant portion of the total cost of processing as well as powder chemistry and resulting microstructure.
One of the major technical challenges in the milling of powders is the enhancement of milling kinetics. This is achieved by optimizing milling variables so that the desired particle size distribution, deagglomeration or surface reactivity is achieved in a short milling time.

Tumbling ball milling is used for achieving enhanced moldability of silicon nitride powders by modification of their surface reactivity, deagglomeration and particle size distribution. An attractive alternative to the conventional tumbling ball mill is a high energy Agitation Ball Mill (ABM). The primary characteristics of the ABM are an enclosed grinding chamber filled with up to 95% of the mill volume with fine sized media and its agitator rotating at 1000-3000 rpm in the vertical or horizontal direction.

Research is underway on the development of milling kinetics data for a silicon nitride powder in the ABM in aqueous and non-aqueous environments. Specifically, the effect of major milling variables on the physical and surface chemical properties of the milled powders are investigated. These data are utilized to develop an understanding of parameters responsible in the preparation of suspensions having a high solids loading.

Milling Variables - Size reduction in the ABM is a complex process, influenced by a number of variables relating to the number and the energy of impacts taking place, the energy transfer to the milling media, rheology of the slurry, hydrodynamics of mixing, residence time distribution and fracture behavior of the particles. Three variables were examined for their anticipated technical importance:

- Agitator speed (1300 to 2600 rpm)
- Suspension feed rate (240 and 480 cc/min)
- Suspending liquid (aqueous and alcohol)

Milling Kinetics - The specific surface area (SSA) of the milled powders at various milling times is shown in Figure 1 for a set of three conditions. Since power draft of the ABM is proportional to the cube of rotor speed, the kinetic energy per unit volume can be increased by increasing the mill rotor speed. The lowest milling rate was obtained when the agitator speed was 2000 rpm. At the same suspension feed rate of 240 cc/min, an increase in the agitator speed to 2600 rpm resulted in doubling the specific surface area at a given milling time. Under the conditions of 240 cc/min slurry feed rate and 2600 rpm mill speed, the SAA of the milled powder increased linearly with the milling time for the present observation times. Apparently, there is no negative effect on the milling kinetics due to the finest sized (< 0.1 μm) particles produced under these conditions.

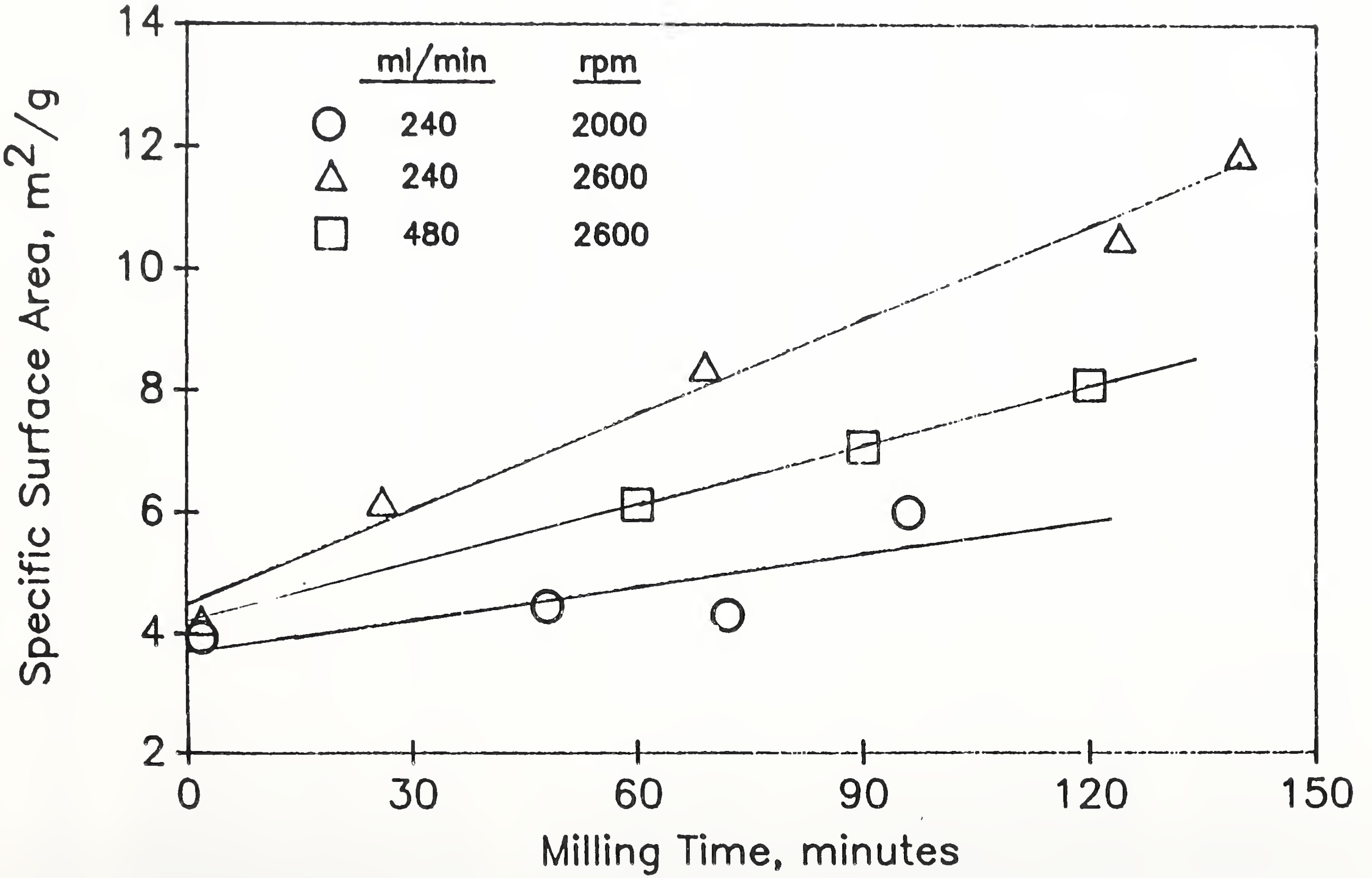

Figure 1. Increase of specific surface area as a function of milling time of 50/50 mixture of Ube SNE-3 and 5 in an aqueous environment containing 150 ppm polyacrylate surfactant and 40% v/v powder loading.

Changing the slurry feed rate changes the residence time for the slurry in the milling volume. Thus, doubling the feed rate doubles the milling time required to achieve a given SSA. This effect can be seen in Figure 1 by comparing, for example, the SSA at 45 min, 240 ml/min, 2600 rpm to the SSA at 90 min, 480 ml/min, 2600 rpm. These data indicate that agitator speed has a more significant effect on the SSA of the powder than the slurry feed rate.

Effect of Milling Fluid - Organic fluids instead of water are used for milling silicon nitride powders to reduce the potential of formation of hard agglomerates during slurry drying. When the water milled powders are dried there is a high energy of adhesion of water to the surface, and as evaporation proceeds the particles tend to be drawn together to give irreversible aggregation. However, the milling fluid has a strong effect on the rheology of the suspension and hence on the kinetics of powder milling. The slurry rheology is also significantly affected by solids loading in a given fluid.

To analyze this effect, the milling kinetics data in water and isopropyl alcohol were compared. At 12% v/v particle loading in isopropyl alcohol, the milling rate was higher than that in the 40% v/v suspension in water. However, by increasing the solids loading to 22% v/v in milling with isopropyl alcohol, the milling rate decreased drastically. The increase of viscosity of alcohol based suspensions as a function of solids loading is much steeper than that in the aqueous suspensions. This increased viscosity of the 22% v/v alcohol based suspensions appears to be the cause of decrease in the milling kinetics.

Chemistry of Milled Powder - Bulk chemistry of the milled suspensions was evaluated by the determination of oxygen and other impurities (Al, Fe, Ca, Mg, and Y) by neutron activation and x-ray fluorescence; whereas, surface chemistry was evaluated by the measurement of isoelectric point using the acoustophoresis technique.

Oxygen content of the powders as a function of their SSA (Figure 2) illustrates the following:

- Higher feed rate increases the rate of oxygen pick up of the powder because of the increased number of milling iterations to achieve the same size reduction as that of the powder milled at a low feed rate.
- Wetting of the unmilled dry powder by an aqueous solution resulted in the increase of oxygen and SSA from 0.98 $\%O_2$ and 4.0 m^2/g to 1.2 $\%O_2$ and 4.2 m^2/g, respectively. The primary reason could be the formation of amorphous surface oxide.

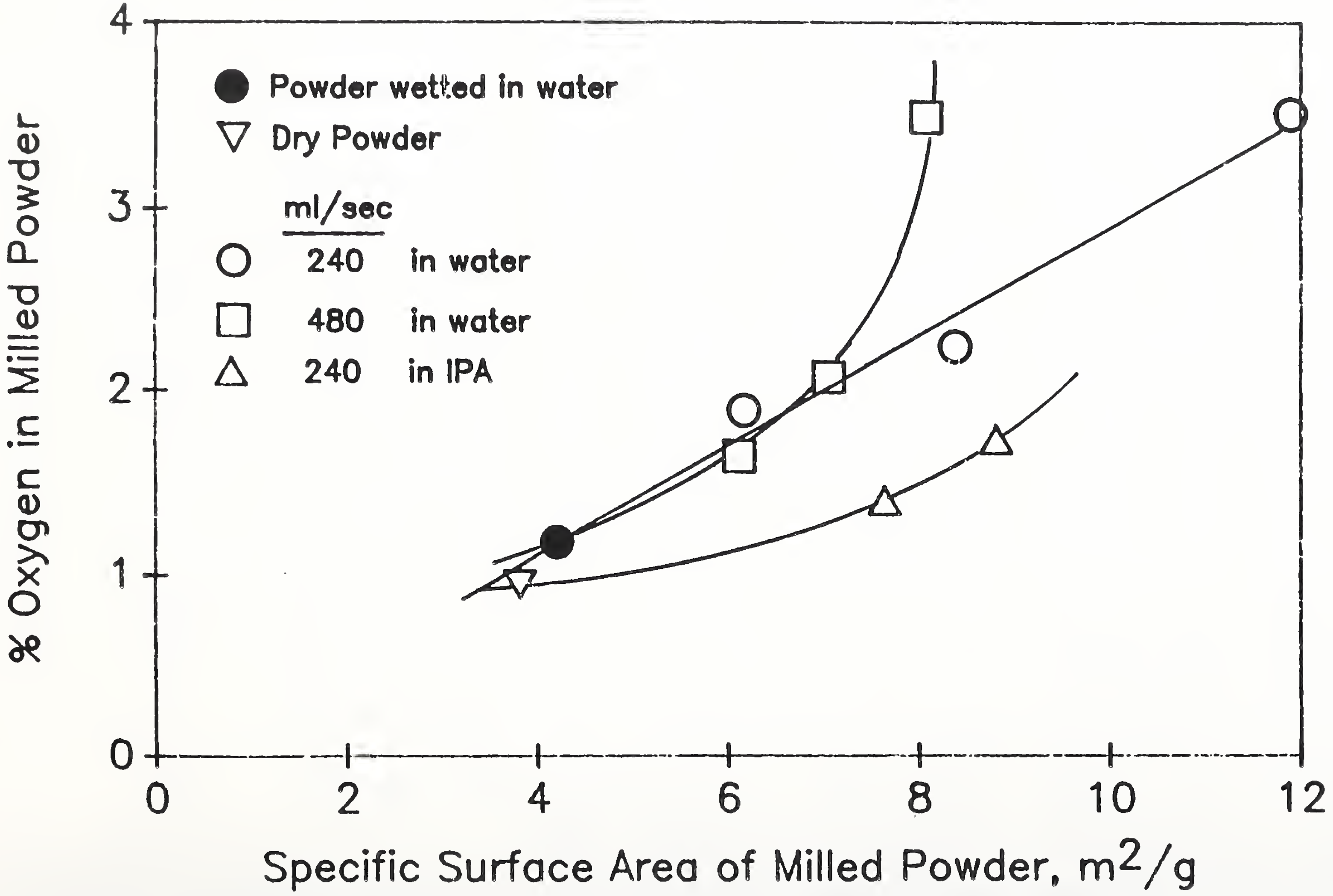

Figure 2. Oxygen concentration of powders as a function of specific surface area by milling at 2600 rpm rotor speed and 40% v/v of suspension.

Uniform Distribution of Sintering Aids

S. G. Malghan, A. Sivakumar[1], P. S. Wang and M. Vaudin

[1]Columbia University

Traditional processing of silicon nitride powders involves the use of sintering aids to achieve complete densification. The sintering aids are added as powders, by hydroxide precipitation or by sol-gel technique. Research is in progress to achieve uniform distribution of the sintering aid, without causing any side effects due to chemical reactions. Of the methods mentioned above, sintering aid addition in the form of powders is not only cost-effective, but also chemically beneficial. However, achieving highly uniform distribution is an important issue. One of the most desirable forms of uniform distributions of sintering aid is that in which the silicon nitride particles are evenly surrounded by the sintering aid particles.

In our study, experiments were conducted to identify suitable conditions under which fine sized alumina and yttria particles can be deposited on the silicon nitride particles. In addition, this research is directed towards the development of techniques for qualitative and quantitative determination of coverage of the silicon nitride surface by the sintering aid particles. Alumina particles were deposited on the silicon nitride particles ($d_{50} = 1.1\ \mu m$, Ube SNE-3) by control of electrostatic attractive forces. The effectiveness and uniformity of the coating was enhanced by increased charge differential between the two types of particles. Therefore, electrostatic charge between the two types of particles was varied as a function of suspension pH. At a pH of 6.0, positively charged alumina particles were deposited on the silicon nitride particles. In addition, the deposition was carried out in the presence of a polycarboxylic acid as a surfactant to maximize negative charge on the silicon nitride particles. In these experiments, surface coverage of deposited alumina particles was not as uniform as when the particles were electrostatically stabilized.

The coating uniformity was evaluated by acoustophoresis, transmission electron microscopy and x-ray photoelectron spectroscopy. The acoustophoresis technique was able to provide information on the amount of surface coverage by comparison of isoelectric points. In addition, this technique was able to identify experimental conditions which showed lack of driving force for deposition.

The TEM examination showed that nanosized alumina particles were equally well deposited on the edges, corners, and surfaces. The XPS data showed that the quantity of deposited alumina increased as the initial concentration of alumina in the starting suspension increased. The thickness of alumina coating and its uniformity was evaluated by XPS by an assessment of the ratio of Si/Al at various regions of coated particles.

Experiments are in progress to address slurry parameters that influence the difference in surface charge between the two types of particles. Also, sensitivity of the coating characterization methods is being evaluated. One of the important issues is when a monolayer coverage of the sintering aid is formed on the silicon nitride particles.

Oxidation Kinetics of Ceramics

P. S. Wang

Surface Oxidation of SiC Platelets

Silicon carbide and silicon nitride are utilized as structural materials both as monolithics and composites. The processing of powders of these materials is often accompanied by surface oxidation of the powders by formation of silica. Silica, or chemical variations thereof, can be retained throughout the processing and result in grain boundary phases which control high temperature mechanical performance. Our program addresses the critical issue of oxidation of these powders to provide guidelines for processing of ceramic powducts with greater control and hence improved reliability and performance.

Silicon carbide as a ceramic has excellent physical and chemical properties for high temperature applications. It has been widely used in both monolithic and composite forms. However, SiC platelets, whiskers, and fibers are commonly used as reinforcements in ceramic composites. In these composites, the interface strength and bonding characteristics between the reinforcements and the matrix are critical in determining fracture behavior, toughness, and reliability. Interface interactions between SiC and other matrix materials often depend on the surface composition and oxidation rate of SiC.

Considerable research has been conducted to investigate the oxidation kinetics of bulk silicon carbide under various conditions. Most of the work was performed in the temperature range from 900°C to 1500°C. Single crystals were used in some of these studies and oxide growth rates were found to vary by a factor of 10 for different crystal faces of SiC. All of the studies on the oxidation kinetics of silicon carbide above ~1000°C have shown that a parabolic rate law is followed in which the rate is diffusion controlled. At lower temperatures; however, the surface chemical reaction will be the dominant rate-determining step and so a linear rate law should apply.

SiC platelets were obtained from C-Axis Technology, Canada. The superfine, high purity (SiC-SF) platelets were heated in alumina crucibles for 0.5, 1.0, 2.0, 4.0 hours at 500°C, 600°C, and 700°C.

The kinetic energy range for the Auger scans include the Bremsstrahlung x-ray induced Si KLL auger peak, as well as the Si 2p and Si 2s photoelectron peaks. These scans also show that boron is detected only on the sample which was heated. The Si 2p photoelectron peak can be deconvoluted into two peaks at binding energies of 100.2eV and 102.3eV identified as SiC and SiO_2, respectively. Similarly, the Si KLL spectra show SiC and SiO_2 peaks at 1609.2 and 1615.5eV kinetic energy, respectively. All these have been detected in our previous study of the whiskers and the results agree very well. The surface oxidation was followed by a change in the oxide to carbide ratio when the samples were heated. The surface oxide thickness, t, can be calculated from:

$$t = -\lambda \ln [R / (R+R^*)] \quad (1)$$

where $R^* = I_c^*/I_o^*$ and $R = I_c/I_o$. I_c and I_o are the carbide and oxide signal intensities, respectively, from the platelets sample. I_c^* is the carbide intensity from a sample with no surface oxide. I_o^* is the oxide intensity from a completely oxidized SiC sample. λ is the mean free path of electrons, which is 29 Å for Si 2p photoelectron, and 38 Å for the Si KLL Auger electron.

Table 1 shows the ratios of the SiO_2 vs. SiC Si KLL Auger intensities for all of the platelet samples analyzed. The corresponding Si 2p data are presented along with the Si KLL data in Table 1. A least-square linear fit to these data gives:

$$I_c = 800 - 3.013\, I_o \qquad (2)$$

$$I_c = 291 - 2.467\, I_o \qquad (3)$$

for Si 2p and Si KLL, respectively. The correlation coefficients are 0.87 and 0.93 for Si 2p and Si KLL, respectively. From the slopes of these lines, we have $R^* = 3.013$ (Si 2p) and 2.467 (Si KLL). The R^* determined from this Si 2p data is larger than that determined for the whisker oxidation study because of the presence of boron oxide in the platelets. The surface oxide films are calculated according to Eqn. 1 and tabulated in Table 1. The oxidation rates deviate from linearity at each temperature. The oxide film thickness calculated from the Auger data are slightly lower than those from the Si 2p. This may be an indication that the literature value of 38 Å for the mean free path of Si KLL electron is low. The study of the surface boron vs. oxide film thickness suggests that the boron is being incorporated into the growing oxide film.

Surface Oxidation of Silicon Nitride Powders with 4% Yttria

Silicon nitride (Si_3N_4) ceramics have found a myriad of applications due to their favorable combination of properties, such as high mechanical strength at high temperature, high fracture toughness, good thermal shock and chemical resistivity, and high wear resistance. However, one significant disadvantage of the Si_3N_4 ceramics is the necessity to use sintering aids to obtain fully dense ceramics.

In the case of Si_3N_4, the binding energy separation between the oxide and nitride silicon 2p peaks is less than 1.5 eV and hence in the XPS studies using non-monochromatic Mg x-rays, these peaks will be unresolved. The silicon KLL Auger peaks from Si_3N_4 and SiO_2, however, have an energy separation of ~3.4 eV and are clearly resolved. The silicon KLL Auger transition, being at ~1610 eV, will not be excited by the characteristic Mg x-rays. Previous studies have shown that higher energy Bremsstrahlung radiation associated with the characteristic radiation can be used to excite Auger transitions that would be otherwise inaccessible. The peak from SiO_2 is at 1608.5±0.3 eV kinetic energy while the peak from Si_3N_4 is at 1611.5±0.2 eV.

The best least-squares fit to the nitride data gives:

$$I_n = -(1.22 \pm 0.11)I_o + (281.4 \pm 9.8) \qquad (4)$$

where I_n and I_o are the Si KLL intensities from Si_3N_4 and SiO_2, respectively. From Equation (4) the value of R^* was calculated to be 1.22 ± 0.19. From the work of Powell a value of 3.8 nm was determined for λ. Table 2 gives the values for the average oxide thicknesses, t, on the silicon nitride particles as well as the errors in these thickness measurements, δt. When the average oxide thicknesses are plotted as a function of heating time for the three different temperatures, the equations for the lines are:

$$900°\text{C}: \quad t = (1.06 \pm 0.27)\ h + (12.28 \pm 0.62) \qquad (5)$$
$$950°\text{C}: \quad t = (2.19 \pm 0.18)\ h + (11.28 \pm 0.41) \qquad (6)$$
$$1000°\text{C}: \quad t = (7.07 \pm 0.45)\ h + (14.01 \pm 1.03) \qquad (7)$$

where h is the heating time in hours. The slopes of these lines are the linear rate constants. The activation energy determined from this plot is 56 ± 1.5 kcal/mole.

It was also found that the measured yttrium level decreased as the average silicon surface oxide thickness on the Si_3N_4 particles increased. The two Y 3d peaks at 160.5 eV and 158.4 eV are due to the spin-orbital splitting of 3/2 and 5/2, respectively. The fact that the logarithm of the normalized yttrium intensity appears to be a linear function of the oxide thickness suggests that there may be an yttrium containing layer formed at the interface between the surface SiO_2 layer and the underlying Si_3N_4. Electron microprobe analysis has shown that an yttrium-rich layer does form at the SiO_2/Si_3N_4 interface on hot-pressed yttria-doped silicon nitride oxidized at 1460°C in 150 Torr O_2. At this temperature, the oxide layer formed was quite thick, ~15 μm. The yttrium-rich layer was believed to be due to crystals of $Y_2Si_2O_7$. Therefore, it appears that the reaction between surface SiO_2 and bulk phase yttria initiates at a much lower temperature than the normal hot pressing temperature of 1700-1850°C. Availability of abundant oxygen for the glass formation reaction to proceed at low temperatures (900-1000°C in this study) could be one of the factors for the formation of an yttrium containing layer on the powder.

Table 1. Surface oxidation data for SiC platelets heated in air. Oxide layer thickness is shown.

Temp. °C	Heating time (hours)	Si 2p R	Si 2p Oxide(Å)	Si KLL R	Si KLL Oxide(Å)
500	0.5	1.573	31.0	2.667	24.9
	1.0	1.407	33.2	2.357	27.2
	2.0	1.368	33.7	2.188	28.7
	4.0	1.336	34.2	2.061	29.9
600	0.5	0.977	40.8	1.500	37.0
	1.0	0.582	52.8	0.999	47.3
	2.0	0.427	60.5	0.770	54.6
	4.0	0.340	62.2	0.667	58.8
700	0.5	0.243	75.3	0.411	74.0
	1.0	0.177	83.9	0.342	80.1
	2.0	0.091	102.4	0.180	102.1
	4.0	0.074	108.2	0.165	105.3

Table 2. Bremsstrahlung-Excited Si KLL Auger Results for Si_3N_4 - 4% Y_2O_3 Powders Heated in Air

Time (Hours)	Temperature (°C)	SiO_2 KLL intensity(cps)	Si_3N_4 KLL intensity(cps)	t(Å)	δt(Å)
0.0	as-received	36.6	179.8	8.4	1.6
0.5	900	65.3	203.4	12.6	2.3
1.0	900	62.7	188.4	13.0	2.2
2.0	900	65.9	162.4	15.3	2.7
4.0	900	90.0	207.2	16.2	2.8
0.6	950	63.9	209.7	12.0	2.2
1.0	950	74.4	203.9	14.0	2.5
2.0	950	81.5	191.7	15.9	2.8
4.0	950	95.5	169.4	19.9	3.2
0.5	1000	76.7	170.7	16.6	2.6
1.0	1000	101.7	164.6	21.3	3.4
2.0	1000	127.5	132.0	29.5	3.8
4.0	1000	148.9	91.0	41.7	4.2

Ceramic Characterization by NMR Spectroscopy and Imaging

P. S. Wang

The binder distribution in a green ceramic and the powder distribution in a slurry are critical parameters of ceramic powders processing which can control the microstructure and hence reliability of final products. A precise, nondestructive analytical method is necessary to investigate homogeneity in these systems. Nuclear magnetic resonance (NMR) imaging provides an unique material diagnostic technique by in-situ, internal mapping not only for the material distribution, but also a profile of the chemical and physical characteristics of these materials.

NMR Imaging

The primary objective of this program is to study the distribution of solid and liquid phases by using the solid state NMR imager. The phase or materials distribution can be monitored by detecting the NMR-active nuclei in the component and the chemical or physical characteristics differentiated from the nuclear spin relaxation times (T_1: nuclear spin-crystal lattice relaxation; T_2: nuclear spin-spin relaxation) for the materials mapped at the same frequency. A liquid NMR imager has to be established before it can be improved to a solid imager due to the nuclear dipole-dipole broadening in solid state NMR. Such a liquid imager will also find its applications in material diffusion, and slurry characterization. To construct a picture from the NMR spectroscopic signals, a set of field gradient coils around the resonant probe coil can control the magnetic field strength and frequencies along the X-, Y-, and Z-coordinate so that the NMR signals can be accumulated along these coordinates. The power and the numbers of selected excitation along X- and Y-coordinates decide the spacial resolution of the picture and Z-coordinate controls the thickness of this internal slicing.

The imaging accessary was built into a Bruker MSL-400 NMR spectrometer. It includes a set of six ^{1}H resonant coils, a set of field gradient coils, two dual-channel power amplifiers, a selective excitation unit, a pre-emphasis unit, an image graphic display processor, a video monitor, a video copy processor, a frequency coupler, and an array processor. The six resonant coils (3, 5, 10, 15, 20, and 25 mm diameter) are insertable to a fixed frequency NMR ^{1}H resonant probe (400.130MHz) for mapping different sample sizes. The selective excitation unit (SEU) generates both "hard pulse" and "soft pulse" to detect NMR signals in the resonant coil. It also provides the pulses to the field gradient coil at chosen frequencies to profile the signal intensities along X-, Y-, and Z-coordinates.

Contour plots of water distribution in a Si_3N_4/H_2O slurry were studied by internal slicing of slurry in a NMR tube. The pictures were taken at proton frequency and water chemical shift. They represent pictures of Si_3N_4 distribution in the slurry of 9.7 mm diameter cross-section (Figure 3). Each point represents an area in which the water concentration is different from its neighbors. A detailed distribution of the silicon nitride in the slurry can be mapped. At any point in a picture, the water intensity profile can also be displayed horizontally or/and vertically. This capability provides a methodology to construct a three dimensional picture by stack plotting numerous profiles in succession.

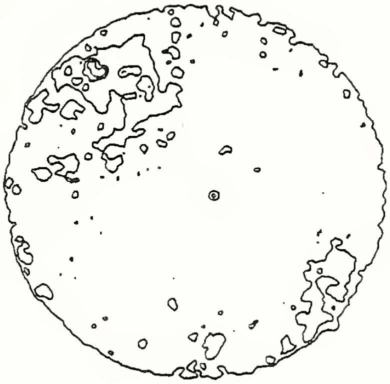

Figure 3. Stack plot of water distribution in a silicon nitride/water slurry.

Chemical Impurity and Phase Composition

Chemical impurities are present in the starting powders due to process related factors. Detailed identification of the chemical and phase composition of the impurities is critical to the improvement of the quality of the advanced ceramics. The ^{29}Si magic angle spinning-NMR spectroscopy is a powerful technique for this application. The chemical shifts of ^{29}Si nuclei are very sensitive to their electronic environment which are related to the chemical and crystal forms. Magic angle spinning (MAS) and cross-polarization (CP) facility have been established in the NMR spectrometer at ^{29}Si (79.460 MHz) and ^{13}C (100.577 MHz) frequencies.

Over 15 different types of Si_3N_4, SiC, and diamond samples have been studied by MAS-NMR at these frequencies. α-phase Si_3N_4 powders were found to have two different chemical shifts due to different Si sites. They were observed at -50.19 and -47.80 parts per million (ppm) as referred to the chemical shift of TMS (tetramethyl silane). Each peak was further split into four peaks probably due to the fine structure. The fine splitting is about 0.3 ppm apart. Figure 4 shows an example of ^{29}Si MAS NMR spectrum from a UBE SNE-5 powder. On the other hand, a nano powder sample shows no structure at all due to its lack of well-defined crystal phase. In addition, the spectrum width is about ten fold of that of the α-phase.

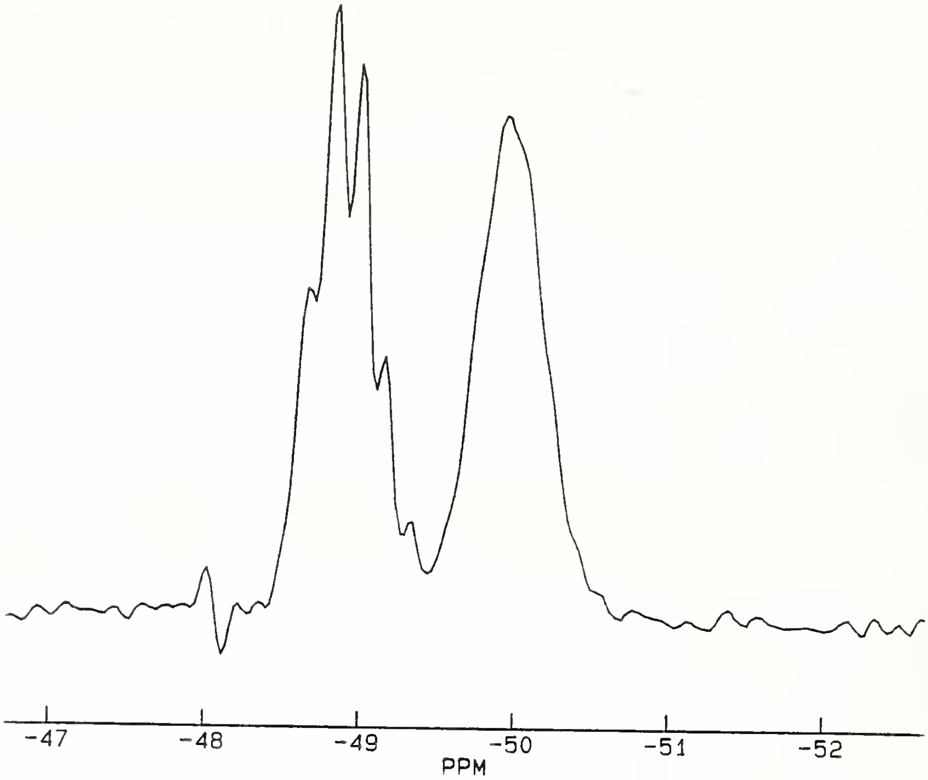

Figure 4. ^{29}Si MAS NMR spectrum of UBE SNE-5 powder showing α-Si_3N_4 chemical shifts.

Organo-Metal Complex Synthesis of A Conductive Oxide Ceramic Powder

J. Ritter, J. Kelly and D. Minor

Current practice in the construction of cathodes for alkaline fuel cells involves the coating of small polytetrafluorethylene (PTFE) particles with 2-5nm gold particles at loadings to assure Au-to-Au contact for electrical conductivity. While fine gold particles are a good electrocatalyst for the cathodic reduction reaction, they tend to sinter when cell temperatures exceed ~80°C, with a concomitant loss in electrocatalytic activity. A new generation of cathodes is under consideration, wherein the PTFE will be replaced by a "conductive particle" lightly loaded with gold. The elimination of extensive Au-Au contact is expected to greatly alleviate the loss of activity at elevated temperatures. Alternatively, if the "conductive particles" show electrocatalytic activity, they could be used directly without the Au deposition. The requirements for these "conductive particles" include, electrical conductivity in the 10^3-10^5/ohm-cm range, 20-70 nm particle size, resistance to chemical attack by 40% aqueous KOH at ~100°C, and stability under cell reduction potentials in the range 0.4-1.2V, Reversible Hydrogen Electrode. Among the candidates considered for this application is a lithium-doped lanthanum nickelate, $La(Li)NiO_x$. The synthetic challenge is to effectively substitute 1 mole percent Li for Ni while maintaining the required particle size.

The known solubility of many lithium compounds in water and other common solvents suggested that coprecipitation would be inappropriate to assure the quantitative inclusion of Li in the product. Thus, an alternative organo-metal complex approach to prepare initial samples of the nickelate was selected. Aqueous nitrate solutions of the metals with molar ratio La : Ni : Li - 1.0 : 0.99 : 0.01, were combined with 1 mole of citric acid per mole of metal ion. Solvent was removed thermally until polymerization occurred. The resultant polymer was calcined up to 500°C, and the desired phase formed at 600-650°C in O_2. Phases were identified by XRPD, surface areas determined with N_2 on a commercial B.E.T. apparatus, Li analysis conducted by flame emission spectroscopy (FES), while powder morphology was examined by SEM. Small portions of the powder were ultrasonicated in 2% (v/v) acetic acid, in an attempt to increase surface area.

Surface area measurements on citrate-derived powders by standard B.E.T. methods give values typically in the 3-6 sq m/g range. Results from FES verified that Li is present at the intended 1 mole % level; whereas, examination of the material by SEM shows a matrix of fused ~100nm particles. After ultrasonication in 2% acetic acid, only 20% of the powder is recovered. However, this recovered material exhibits a surface area of ~15 sq m/g. Examination of the acid washed powder by SEM indicates considerable erosion of the connective links between particles but general retention of the connective structure. Moreover, lithium assay by FES indicates that more than 80% of the original Li is retained.

Studies by other workers [B. Delmon and J. Droguest, Fine Particles; 2nd Int'l Conf., Wm. E. Kuhn ed., Electrochem. Soc. Monograph, (1974), p. 24.], suggest that the polymerization of citric acid-metal complexes form a vitreous phase which contains the metal ions in a random array. It is unlikely that the polymer formation can be controlled to develop a "protostructure" to the ceramic phase, but its chief advantage is its ability to retain ions in a relatively homogeneous dispersion. For the synthesis of the Li-doped lanthanum nickelate, the citrate complex route has the demonstrated advantage of incorporating Li quantitatively. The high Li content of the powder after vigorous acetic acid treatment suggest that a major portion of this dopant is part of the nickelate crystal structure.

Small-Angle Neutron Scattering Measurement of Densification of Alumina

G. G. Long, S. Krueger[1] and R. A. Page[2]

[1]Reactor Radiation Division, NIST
[2]Southwest Research Institute

Densification of ceramics during sintering results from the closure of pores and is effected by both the density of the green body and the chemistry of the material, particularly sintering aids. Control of pore closure is critical for consistent production of microstructures with desired reliability. Small angle neutron scattering provides a means of measuring changes in the size and distribution of small pores.

In the experiments that form the subject of this research the microstructures of pure alumina and of alumina with 0.25 wt. % MgO were investigated as a function of thermal processing to gain insight into the role of this additive during densification. In addition, the effect of green density on microstructure evolution was studied.

Samples were prepared by slip casting, or alternatively by cold pressing. For each green state density, a collection of nearly identical samples were conventionally sintered. During sintering, these samples were removed one by one from the furnace as they achieved intermediate densities, yielding examples of microstructure from the early part of intermediate stage sintering to the latter part of final stage sintering. The microstructure parameters of these samples were derived from multiple small angle neutrons scattering experiments. Figure 5 shows the evolution of the effective pore size as a function of densification, or percent of theoretical density (%TD) for four suites of samples: slip cast alumina, with and without MgO, and cold pressed alumina, with and without MgO. The numbers associated with the left-most symbols in Figure 5 indicate the average green density of each suite of sample. It can be seen that the effective pore radius was nearly constant during the intermediate stage of sintering for each of the suites of samples, independent of doping and green density. This is consistent with a stable topological decay model of porosity during intermediate stage sintering. However, the actual value of the effective pore radius depends inversely on the green density. These results indicate that the connectivity that is established in the alumina green body determines the average pore size throughout the stable intermediate stage, and once this size is determined, it is unvarying as long as isolated porosity has not yet begun to form. At the onset of final stage sintering, the pore radius apparently coarsens abruptly. Part of this apparent coarsening may be due to the pinching-off of pore channels such that the larger dimension of the newly isolated pores comes increasingly within the range of sizes visible to the scattering technique.

Figure 5 also indicates that for the samples with MgO, the intermediate sintering stage remains stable out to significantly higher density (93%TD) than the pure alumina, which remains stable out to 87% TD. Consequently, the pores in the doped sample begin to coarsen later and thus the grains do not suffer the same degree of exaggerated growth evident in the thermal processing of pure alumina, even though the green density was lower in the doped sample.
In summary, it was found that the initial connectivity in the green state plays a dominant role in establishing the channel diameters during the intermediate stage of sintering, and contributes also to determining the onset density at which the final stage of sintering begins. The role of MgO as a sintering aid lies, at least in part in prolonging the stability of intermediate stage sintering such that the body achieves greater density before the transition to final stage sintering, after which isolated pores are formed.

Fabrication and Characterization of Nanophase Ceramic Materials

A. Pechenik

Densification of ceramic powders typically requires high temperature sintering. This step in the processing is accompanied by shrinkage, grain growth and the evolution of phases derived from sintering aids. Elimination of sintering aids, and high temperature processing has the potential to produce fine grained material, while consolidation of nanopowders to nearly full density provides the opportunity to form bodies to near net shape. Both of these aspects can have favorable impacts on cost and reliability.

This research program concentrates on the understanding of fundamental processes involved in the fabrication of nanophase ceramic materials from atomic clusters. Atomic clusters are particles smaller than 100 nm in size. Though size-selected atomic clusters of many ceramic materials in the range of 1-100 nm can be readily synthesized by a variety of techniques, little is known about the methods for production of materials from fine powders consisting of such small particles. Superplasticity, supermodulus, low-temperature ductility, tunable band-gap width,

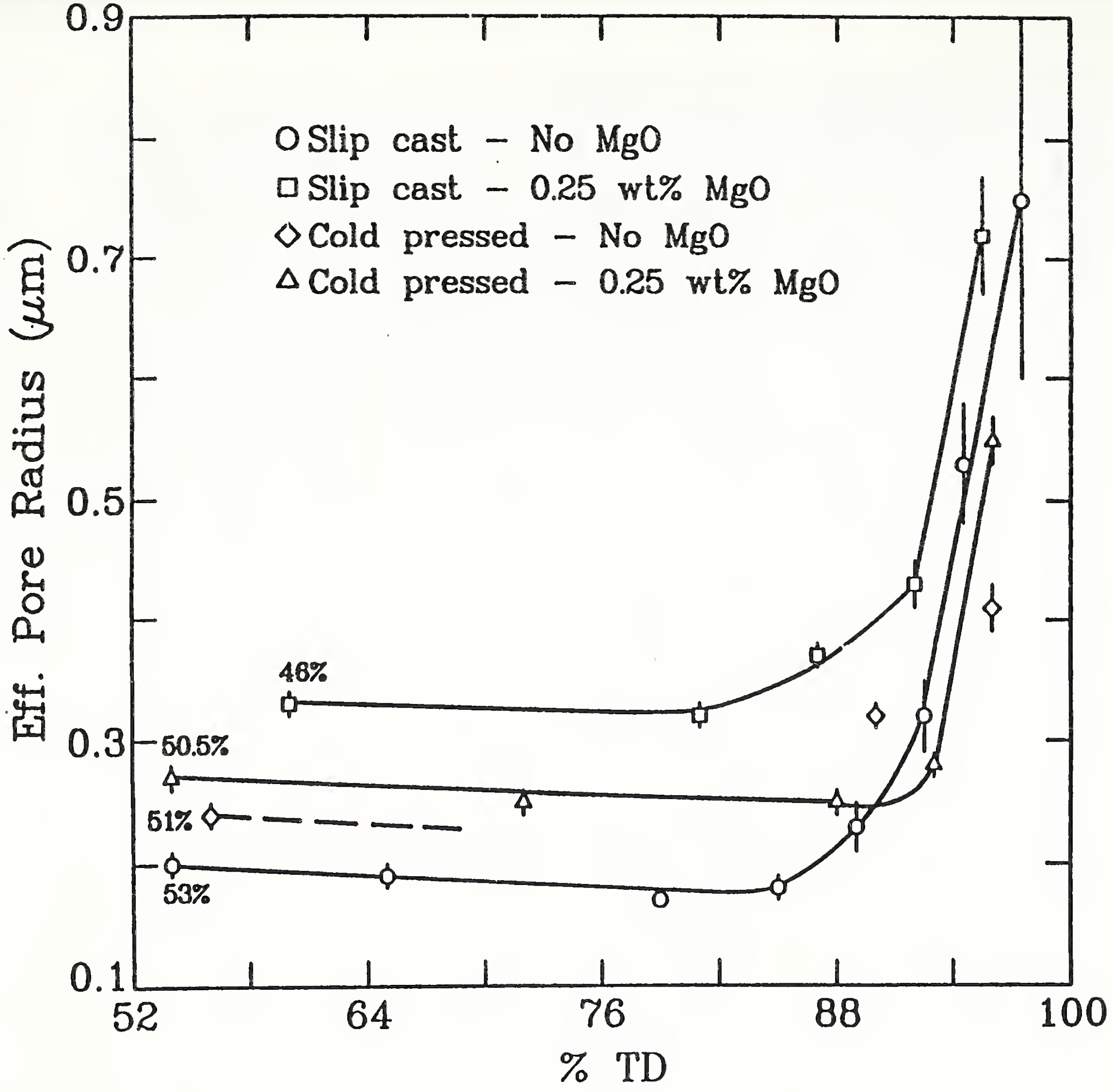

Figure 5. Evolution of effective pore size as a function of theoretical density.

are currently no known techniques, on an industrial or laboratory scale, which would allow fabrication of full-density nanophase ceramic materials without loosing the novel properties entailed by the small size of the individual grains. The main difficulty in the fabrication of nanophase materials is that the high-temperature-sintering commonly utilized for processing of conventional ceramics cannot be used with nano-size particles, because it causes recrystallization and loss of desired properties. In this project we investigate a fundamentally new approach to the fabrication of nanophase ceramic materials utilizing **low temperatures and high pressures**.

To show the usefulness of our approach, we have investigated compaction and densification of an ultra-fine Si_3N_4 powder, a material which is justly termed "unsinterable" in its pure state. We studied compaction of the nano-size silicon nitride powder at industrially-accessible conditions of temperatures below 500°C and pressures not exceeding 5 GPa. The starting powder for this investigation was synthesized at Rutgers University by Prof. Danforth via CO_2-laser-driven gaseous reaction. The powder consisted of 17 nm-size particles of stoichiometric silicon nitride and was amorphous to X-ray and electron diffraction characterization. We compacted this powder under vacuum at room temperature and subsequently sintered at 500°C for 2 hours under 5 GPa of pressure using diamond anvils. This procedure yielded a material with a hardness of 700 kg/mm^2. The material was translucent in the visible range and showed high transmittance in the IR range up to 10 μm. Both the hardness and optical transparency of the material significantly improved when, prior to hot-pressing, the powder was compacted at liquid nitrogen temperature. Optically transparent samples were fabricated by utilizing compaction at liquid nitrogen temperatures followed by sintering at 500°C under 5 GPa. The hardness of these materials increased to 1200 kg/mm^2. When subsequently these samples were sintered **without using** pressure at 1300°C for 2 hours, crystallization took place, the material lost its transparency, and hardness increased to nearly 1800 kg/mm^2, which is essentially equal to the hardness of fully-dense polycrystalline silicon nitride densified with sintering aids. No sintering aids were used in our work except for some oxygen contamination introduced by the exposure to ambient atmosphere. We also started our work on compaction of powders never exposed to the ambient atmosphere. The unexposed powders, which were nearly free of oxygen or moisture, showed improved compacting properties, as manifested by the improved optical transparency of the samples after processing. The prepared materials clearly possess high fracture toughness, as can be emphasized from the fact that no cracks were produced at the corners of Vickers diamond indentations under loads up to 2 kg (the maximum loads that we were able to put on these small samples). Under similar testing conditions, conventional silicon nitride would produce penny-like cracks around the diamond indentation even under loads well below 1 kg.

In addition to its possible industrial significance, this work on nano-size silicon nitride materials has raised a number of fundamental questions about the mechanisms of densification of the fine particles under pressure. The unexpected result that compaction is improved at low temperatures goes somewhat against common intuition, but can be reasoned as the manifestation of the slowing of diffusion and chemical reactions at the interfaces of compacting particles. The diffusion leads to creation of bridges between particles that come in contact and this process is extremely rapid for nano-size particles. In a way, low temperatures decrease the friction forces between particles when the surfaces of the particles are clean from impurities. **Low temperature compaction of nano-size clusters**, is a fundamentally new concept which came from this work. We plan to investigate further the physics of this process.

Investigation of the time-dependence of the compaction process at various temperatures revealed no observable dependence on the duration of pressing. For example, no changes in the optical or mechanical properties of the samples were observed at 500°C when pressing time increased from 2 to 6 hours. This is a rather surprising result since one would expect that the particles should undergo diffusional creep under the applied pressure which should lead to higher density and hardness of the compacts pressed for longer periods of time. Changes in temperature and compacting pressure had a profound effect on mechanical and optical properties of the samples. Reducing pressure from 5 to 2 GPa or decreasing temperature from 500 to 250°C had an effect of decreasing hardness by a factor of two.

TEM examination of the compacts revealed that the small amorphous particles did not change their morphology during compaction, no recrystallization or grain growth has been observed. The particles were compacted into a matrix of densely-packed grains. Some small pores are observed in the TEM micrographs, 5-10nm in size, but no larger pores were detected by TEM, SEM and optical techniques. This unique microstructure is responsible for high fracture toughness, hardness and transparency in the visible range of the nanophase amorphous silicon nitride. Our future goals are:

(1) Investigate sintering of the nanophase silicon nitride to produce the polycrystalline material. If the high density of the amorphous compacts can be retained in the polycrystalline state, this could open the opportunity for fabrication of silicon nitride without using sintering aids.

(2) Study mechanical properties of the prepared compacts at various temperatures and measure creep rates.

(3) Characterize optical properties of the amorphous silicon nitride to assess its possible applications in the field of electro-optics.

(4) Understand and model the physics of low-temperature compaction.

Patent applications have been filed on this method.

MECHANICAL PROPERTIES

David Cranmer

The reliable application of structural ceramics depends upon the ability to control and predict mechanical properties. Knowledge of processing microstructure - property relationships is the basis for this control and is the foces of our program in mechanical properties. Our program on mechanical properties has as its broad objectives: (1) the generation of new theories and data to elucidate fracture and deformation mechanisms in brittle materials; (2) the development of fracture methodology for studying the fundamental forces that exist between two near surfaces; (3) the investigation of ceramic microstructures and their relationship to mechanical behavior; and (4) the understanding of the deformation and fracture properties that govern the mechanical response of ceramics at high temperatures. Specific projects are focussed on the processing-property relations between microstructural features and resulting properties including toughening behavior in structural ceramics and development of models for the fracture behavior of continuous fiber-reinforced, ceramic matrix composites. This latter work involves test development as well as preparation, characterization, and testing of composite systems.

Assessment of Mechanical Properties Testing Methodology

D. C. Cranmer

Evaluation of the methods and methodology used to perform mechanical properties testing for ceramics is an integral part of our program. Successful use of these materials in both monolithic and composite form requires that reliable tests be available to determine specific properties of interest. Accordingly, during FY 1990, we have sponsored two workshops designed to assess the current state-of-the-art in mechanical property testing, and to identify areas where additional test development is required.

Ceramic matrix composites offer the potential of high strength combined with damage tolerance not found in monolithic ceramics. At present, however, the state-of-the-art in fabrication and evaluation of these materials is developmental and our understanding is incomplete. One particular area of concern is the mechanical property testing of composites for structural applications. Consequently, a Workshop on Testing Methodology for Glass, Glass-Ceramic, and Ceramic Matrix Composites was held at NIST on February 8, 1990. The purpose of the workshop was to review and discuss room and elevated temperature mechanical property measurement techniques for whisker- and continuous-fiber reinforced ceramic composites and their constituents. Techniques being used for metal- and polymer-matrix composites as well as those developed exclusively for use with ceramic composites were assessed. Important points include the importance of using a tensile test (not flexure) for strength and creep measurements; the need for different tests for material development versus system design; the need to control test parameters (temperature, temperature gradients, and stress gradients); and the importance of specimen preparation. Additional conclusions were that the same tests used for monolithic ceramics can be used for whisker-reinforced materials with few or no changes, and that an interlaboratory round robin test was needed to determine both laboratory capabilities and material behaviors. Additional research areas identified include long term deformation behavior of composites, environmental effects on material behavior, and the relation of constituent properties to composite properties.

As noted above, successful use of these materials requires that reliable tests be available to determine specific properties of interest. One current limitation is the ability to design with ceramics, based on currently available test procedures and data. Thus, a second workshop, this one on mechanical Testing Methodology for Ceramic Design and Reliability, was held at NIST on September 5-7, 1990. The purpose of the workshop was to assess room- and elevated-temperature mechanical property measurement techniques for ceramics for use in component design and lifetime/reliability predictions. Technical areas covered in the workshop included testing for strength, creep and creep rupture, fracture toughness, and fatigue; effects of environment on the fracture and creep processes; lifetime and reliability prediction methods; mechanisms of failure; standardization; statistical experimental design and analysis; and fractography. Major issues and concerns expressed included the need for extensive fractography, the use of different sets of tests for material development versus component design, continued development of laboratory tests which can be made on a minimal number of specimens to provide an adequate predictive capability, scaling of the data from laboratory specimens to "real" components, and the need for simple techniques to use to create design diagrams. In spite of a significant amount of prior work, there are still major questions regarding the definition, use, and tests for fracture toughness. Significant additional discussion also centered around the process of standardization including interlaboratory comparisons (who does them and when in the process are they done?), the length of time required by the ASTM consensus-type process, and concerns regarding excessive restrictions imposed by a standard. Areas identified for additional research were the effects of the R-curve on lifetime predictions and data analysis, effects of mechanical and thermomechanical fatigue, effects of residual stresses on properties and the interpretation of test results, and nondestructive evaluation of ceramics.

Microstructural Design of Ceramics

B. R. Lawn, S. J. Bennison[1], S. Lathabai[1], J. Rödel[1], L. Braun,[1] N. Padture[1] and J. Runyan[2]

[1]Guest Scientist, Lehigh University
[2]Student, Virginia Polytechnic Institute and State University

This research program is directed toward understanding the governing role of microstructure in the strength and toughness properties of two-phase structural ceramics. With this understanding, we can optimize the mechanical properties for specific applications: i.e. we can "design" our materials. Toughness characteristics of structural ceramics can be a strong function of crack size, i.e. they exhibit "R-curve" behavior. Perhaps the most important practical manifestation of R-curve behavior is an associated "flaw tolerance", i.e. an insensitivity of the strength to the initial crack size. Such flaw tolerance is of special interest in the context of reliability, because it offers the structural engineer the prospect of a well-defined design stress; flaw distributions and statistics are then no longer such critical factors in materials evaluation. Part of our project over the past year has been spent in analyzing these tolerance properties for two-phase composites processed in-house, specifically alumina/aluminum titanate systems. Our results indicate most strongly that, contrary to the prevailing wisdom in the ceramics community, processing philosophies based on the elimination of all flaw populations may be counter-productive; judicial incorporation of defect structures may actually improve strength properties, by enhancing the crack-interface bridging restraints.

Our achievements in this area are summarized as follows. The micromechanical mechanism of R-curve behavior has been physically identified in aluminas and other monophase ceramics as bridging, by interlocking grains at the interface behind the crack tip. This behavior has been mathematically modelled in terms of frictional tractions at the boundary between the interlocking grain and embedding matrix, with thermal expansion mismatch internal stresses the key microstructural element in generating significant energy-dissipative friction. From fits to indentation-strength data, we have been able to evaluate all essential microstructural parameters (grain-matrix friction, internal stress level, etc.) needed to evaluate the complete R-curve. With this "calibration" on "reference" material, the strength and toughness behavior of alumina-based ceramics, including the two-phase aluminum titanate material, has been predicted. Confirmation of these predictions has been obtained by comparing with actual indentation and compact tension crack growth data. The strong level of internal stress in the composite imparts remarkable flaw tolerance characteristics, rendering the strength insensitive to flaws in excess of 100 μm. We are continuing our own processing program, moving to alumina composites with different grain textures, e.g. elongated grains to maximize interlocking and bridging, to test predictions for optimal strength, thence toughness.

Our future goals are:

(i) To strengthen our in-house processing to provide a unique processing-properties approach to designing stronger tougher ceramics. To this end, we will continue a NIST-Lehigh University link, through AFOSR-sponsored funding.

(ii) To extend the bridging principles systematically to more complex two-phase composites, in light of the growing evidence that the bridging mechanism may be a primary source of toughening in most (non-transforming) ceramics. Also, to continue to investigate the micromechanics of bridging using new NIST scanning electron microscope fixture for *in situ* observations of propagating cracks, with particular focus on the micromechanisms of grain pull out.

(iii) To investigate fatigue and wear properties of the same ceramics that show optimal flaw tolerance; recent work in our laboratories suggests that cyclic stressing can degrade the frictional tractions responsible for bridging.

Surface Forces: Contact Charge Transfer and Adhesion

D. T. Smith, R. G. Horn and A. Grabbe

Surface forces play a vital role in as intergranular fracture, the mechanical properties of composite materials, colloidal processing of mixed powders and composites, and the adhesion of coatings. The Surface Force Apparatus has been used very successfully for more than a decade, to make measurements of forces between molecularly smooth mica surfaces in a variety of liquid and vapor environments. Recently at NIST we have devised a method to extend these measurements to silica surfaces. This development greatly extends the range of possible studies which can be made with the apparatus, and in particular it has opened the way to investigating surface forces between dissimilar materials.

In making measurements of the force required to separate two different materials (silica and mica) from contact in vapor, we have observed and identified an important phenomenon which gives a major contribution to their adhesion. The phenomenon is contact charge transfer: when the two materials come into intimate contact, electrical charge transfers across the interface from one to the other. Thus one of the materials acquires a positive charge and the other becomes negative. If the materials are subsequently pulled apart, the two layers of charge must be separated from each other. Work must be done against the electrostatic attraction between the oppositely charged surfaces, which means that the adhesion is considerably stronger than it would have been in the absence of the charge transfer effect.

We had already measured the adhesion between two identical surfaces, both for silica and for mica. It happens that the result is about the same for each. One might therefore expect that if the adhesion arose from nonspecific (e.g. van der Waals) forces, the adhesion between the two different materials would also be the same. However, because of the charge transfer effect it turns out to be at least three times greater.

In order to explore this phenomenon further, we have devised a method of quantifying the charge transferred between silica and mica. This involved building two sensitive electrometers which measure the charge on each material. Our technique allows us to measure the area over which the surfaces make contact before they are separated. Since both materials are exceptionally smooth we can equate this geometrical area with the true contact area, and thus calculate the surface charge per unit area, with an unusually high degree of accuracy. The technique also allows us to study the rate at which charge dissipates from the surfaces after they have been separated.

The familiar phenomenon of static electricity is another manifestation of charge transfer between different insulating materials. Static electrical effects are generally thought to be much reduced in humid air, and we have confirmed that the same is true in our experiments. We are able to keep very close control over the liquid or vapor surrounding the two surfaces. Initial tests conducted in a nitrogen atmosphere show that as the humidity of the atmosphere increases, less electrical charge is transferred when the surfaces are initially separated, and the charge persists for a shorter time.

It is our expectation that charge transfer will generally occur between any two different materials, and so it could be an important factor in adhesion and other interfacial properties which affect the performance of composites, for example. Our aims in pursuing this idea further will be to quantify the electrostatic contribution to adhesion between different pairs of materials, to investigate the mechanisms by which charge is transferred, to study how it is dissipated after an interface is broken, and to find how the charge depends on environmental conditions (such as humidity).

The results of this research are expected to influence how we address areas and phenomena such as dry powder processing, triboelectricity, and fracture in the presence of little or no water.

Toughening Mechanisms in High Performance Ceramic Matrix Composites

C. P. Ostertag, J. Röedel and D. C. Cranmer

One of the advantages of ceramic matrix composites is their ability to tolerate damage without failing catastrophically. Our knowledge and understanding of the toughening mechanisms by which this happens is, however, limited. During FY 90, we have made a number of advances to more clearly elucidate these mechanisms in fiber-reinforced ceramic composites. Specific parameters of interest include how fiber length and/or orientation affect the frictional stresses, the fiber debonding and the fiber pull-out length at the matrix-fiber interface, as well as changes in the crack profile. The effect of incident angle of the propagating crack on the reinforcement orientation plane is also being studied to determine the optimum angle of incidence for maximum toughening.

Model ceramic composites were produced by a controlled processing technique. The processing technique allows us to study the effect of each parameter affecting the toughening mechanism in isolation and furthermore, enables us to produce samples with two dimensional microstructures to study the influence of internal stresses on crack propagation. Samples of duplex microstructures (2-dimensional microstructures of Al_2O_3/Al_2O_3 and ZrO_2/Al_2O_3 layers) and continuous fiber reinforced composites were produced and then pressureless sintered. The processed fiber reinforced composites have different fiber spacing and fiber volume fraction.

A device developed for in-situ SEM examination was used to measure the crack propagation in these samples during loading. Crack propagation was observed in a composite fabricated with duplex microstructure. The samples consisted of layers with fine (ZrO_2-Al_2O_3) and coarse (Al_2O_3) particle sizes. The crack propagation was followed in-situ in the SEM across the interfaces of the two microstructures and inside the layers. In the coarse grained region (alumina layer) strong crack bridging occurred, indicating an R-curve behavior. When the crack approached the interface between the coarse grained (alumina) and fine grained regions (alumina/zirconia), the crack velocity increased. In the fine grained region, no R-curve behavior was observed. The crack bridging zone size depends strongly on the grain size.

The understanding of composite toughening mechanisms achieved in this program can be used to guide development of materials for specific applications, and permit the manufacturer

In-situ High Temperature X-ray Diffraction of Whisker-reinforced Composites

C. P. Ostertag and J. Cline

Ceramic composites are generally produced by hot-pressing in order to achieve full density and good mechanical properties. However, complex shapes cannot be easily fabricated by hot-pressing which therefore is not a viable, cost-effective process. An alternative process for fabricating near-net-shape components is pressureless sintering. The advantage of sintering fiber or whisker-reinforced ceramic composites is the ability to produce complex shapes without the use of expensive machining steps.

Sintering of ceramics reinforced by whiskers or fibers, however, is impeded by stresses generated by the differential shrinkage between the weak, porous ceramic matrix and the dense reinforcing agents. During the sintering of fiber- and whisker-reinforced composites, the ceramic matrix densifies approximately thirty to forty percent by volume, while the fibers, or whiskers, which are already fully dense do not densify at all. Fibers and/or whiskers cause stresses to develop during sintering because of the constraints that they impose on the contracting matrix. During the densification process, the fiber is put under hydrostatic compression. Stresses in the matrix normal to the fiber axis are tensile in the circumferential direction and compressive in the radial direction. Parallel to the fiber axis, stresses in the matrix are tensile because of shrinkage constraints. Stresses that develop due to the presence of fibers or dense inclusions are known as heterogeneity stresses, to differentiate them from the applied stress and from the sintering stress. Heterogeneity stresses occur primarily in the vicinity of the reinforcing agents and cause microcrack formation in the matrix. Heterogeneity stresses also inhibit densification of the composite.

To avoid sintering damage, it is important either to reduce the generation of heterogeneity stresses or to modify the response of the matrix to these stresses such that no microcracks form. To employ effective methods for reducing or avoiding these stresses, it is necessary to know when they initiate and in which stage of the sintering process they are responsible for the crack formations. This research project explores X-ray diffraction techniques for an in-situ high temperature analysis of the evolution of stresses which develop both during the sintering and during the cooling process of whisker reinforced composites. Available equipment includes a Siemens diffractometer equipped with a 3000°C hot stage, a position sensitive detector (PSD), and an incident beam monochromator. The microstresses which are generated during sintering are analyzed using peak shift and peak broadening techniques.

The X-ray diffraction profiles obtained as a function of whisker volume fraction correlate very well with previous results on fiber reinforced ceramic matrix composites in that higher volume fractions of whiskers resulted in larger stresses and the stress development initiated at lower temperatures as the volume fraction increased. One of the key elements in sintering is the sintering atmosphere. The SiC whisker reinforced composites need to be sintered in an inert atmosphere to ensure no degradation of the whiskers. Experiments using different atmospheres (vacuum, N_2, Ar, H_2, CO, and $N_2/2\%\ H_2$) were conducted to determine the effects of sintering atmosphere on chemical compatibility/ reactivity of the whiskers and the matrix. Reactions can change the whisker/matrix interface chemistry, and result in changes in the whisker morphology. Morphological changes were observed in the scanning electron microscope. Qualitatively, we have found that the stress development is strongly dependent on the whisker source, whisker purity and whisker surface morphology. Atmospheres which have higher oxygen concentrations result in greater reactivity between the whisker and matrix, thus introducing new interfacial phases. At the present time, the exact magnitude of the stresses has not been established, nor has the influence of second phases developed due to chemical reaction but these topics are subjects of ongoing investigations.

Measurement of Residual Stresses by Cathodoluminescence

C. P. Ostertag, L. Robins and L. Cook

Residual stresses are present in both monolithic and composite materials and have a strong influence on their mechanical behavior. As an example, the increasing resistance to crack propagation with crack length (R-curve behavior) in alumina is attributed to the interlocking grains which are clamped into the matrix on either side of the crack interface by internal thermal expansion mismatch stresses. In composite materials, the toughness depends strongly on residual stresses (clamping stress) between reinforcement and matrix, and hence, recent discussions have identified the need to assess the residual stress field effect on fiber debonding. Knowledge of these stresses, specifically their magnitude, is important. Unfortunately, there are few nondestructive evaluation (NDE) methods to measure residual stresses in ceramic materials with high spatial resolution.

Cathodoluminescence (CL) was used as a tool to measure residual stresses with high precision and with a spatial resolution of better than 5 μm. This is a phenomenon of light emission from specimens as a result of an interaction with an electron beam. In insulating crystals, the origin of the luminescence arises from impurity atoms (e.g., transition metals or rare earths) in the lattice. Using an electron microscope to produce the electron beam, the spatial distribution of luminescent sites can be observed with sub-micrometer resolution, and correlated with features of the specimen morphology or microstructure.

As the initial step in this project, alumina single crystals indented with a Vickers hardness indenter were investigated by CL imaging and spectroscopy in a scanning electron microscope. The spatial resolution of the CL images was approximately 0.4 μm. CL spectra were measured with wavelength resolution of 1.0 nm in the wavelength range of 200 to 900 nm; in the immediate region of the ruby lines, spectra were measured with a resolution of 0.15 nm. Stress induced frequency shifts of the ruby lines were utilized to measure the residual stresses in the region surrounding the indentation. Both hydrostatic and non-hydrostatic stresses were measured. The magnitude of the stresses was observed to vary with distance from the center of the indent and also with crystallographic orientation. After the samples were annealed at 1600°C for 10 hours, no measurable stresses remained either in the center of the indent or in the surrounding areas.

Future studies based on this work will be conducted with the intention of refining the technique to achieve greater measurement precision, and application to other materials of interest.

Micro-Mechanical Aspects of Asperity-Controlled Friction in Fiber-Toughened Ceramic Composites.

W. C. Carter, E. P. Butler[1] and E. R. Fuller, Jr.

[1] Guest scientist, Lehigh University

The role of friction as an energy dissipation mechanism is an important aspect of fiber-reinforcement toughening of ceramic matrix composites. Friction in most theoretical treatments of composite toughening is characterized by Coulombic friction between the sliding fiber and matrix without regard to the microstructural aspects of the interface. Recent mechanical and microscopical observations by P. D. Jero and R. J. Kerans have indicated the importance of fiber surface roughness on the frictional behavior of the interface. In research initiated this year, we have confirmed these empirical observations and addressed a few fundamental aspects of the role of asperities by developing a micro-mechanical model for interfacial friction.

Microstructural evidence (scanning electron microscopy) and mechanical evidence (re-seating load drops) show that asperities are present in our model composite system and that they play an important role in interface friction. There is an hierarchy of asperity size scales: the smallest result from chemical-vapor fiber-production processes; the medium-sized result from composite fabrication; and the largest occur from crack deviation during fiber-matrix debonding. The largest asperity present at the tip of the debonded region will dominate; furthermore, asperities which can lock the interface are much more effective at shear transfer.

A micro-mechanical model was developed which illustrates the basic phenomenon of asperity-controlled friction. Both the asperities and their matching "seats" were modelled as spherical caps of material on both sides of the interface. Initially, asperities on the fiber are wedged into the interstices (the "seats") in the matrix with a force which is relatable to the clamping pressure derived from composite processing (e.g., arising from differences in coefficients of thermal expansion upon cooling). The deformation of each asperity/seat was calculated with the Hertzian theory. As an asperity is pulled past its seat, increased elastic Hertzian stresses arise; if we assume a local Coulombic coefficient of friction at each asperity/seat, we can calculate the axial force exerted by each asperity as a function of relative displacement. This axial force determines the shear transfer between the fiber and the matrix. Elastic deformation of the asperities is reversible and does not contribute to the overall strain-energy-release rate. However, the localized elastic deformation of asperities is responsible for effects which take place over very small distances, e.g., the observed seating drops.

We expect asperity friction to be an important factor in the toughening of matrices with fibers. We have shown that fibers which have as-manufactured smooth surfaces form a much more inhomogeneous surface when used in a composite. These rough interfaces slide over one another via a mechanism of asperity lock and friction. As these asperity locks make fiber pull-out a more energy dissipative process, fabrication strategies involving roughened fibers (but still smooth enough to debond and pull-out without breaking) could lead to tougher composites. Our observations confirm the presence of asperities and that they can result from both fiber and composite fabrication, or from debonding itself. Our model demonstrates the basic role of asperities during pull-out.

Creep and Creep Rupture of Hot Isostatically Pressed Silicon Nitride

D. C. Cranmer, B. J. Hockey and S. M. Wiederhorn[1]

[1]MSEL, Institute Scientist

High temperature applications for ceramic materials generally lie in the range of ≈1000°C to ≈1500°C. At the low end of this range are turbochargers used in some current models of automobiles; at the high end are gas turbines being developed for cruise missiles and automobile engines. Current ceramics for these applications are mainly two phase materials such as silicon nitride or SIALON, in which hard refractory grains are bonded by either a glassy phase or a soft crystalline phase. These materials are attractive for high temperature applications because of their low thermal expansion, which improves their resistance to thermal shock.

Successful development of these new ceramics holds promise for use in high efficiency, enhanced performance of structural systems in high temperature, stress-bearing environments. However, before ceramics can be used in these industrial applications, issues concerning reliability and service life remain to be resolved. In this collaborative program with Norton/TRW, the creep and creep rupture behavior of a hot-isostatically pressed silicon nitride has been examined as a function of temperature and applied stress. In the initial specimen, an applied stress of 100 mPa was used at temperatures of 1300, 1325, 1350, 1375 and 1400°C. Each temperature-load combination was maintained until steady-state creep was attained. For subsequent specimens, only one temperature (1300, 1325, 1350 and 1375°C) and one applied stress (75, 100, 112.5, 125 and 150 MPa) was maintained until the specimen failed or the test was interrupted. The material exhibits an activation energy for creep of 1,183 kJ/mol. The creep stress exponent for the material is 4.7. This material exhibits a Monkman-Grant behavior with a slope of about -1.28. Using a power-law expression for the time-to-failure (t_f), following the Monkman-Grant formulation,

$$t_f = A\ \epsilon^m$$

and an expression for the creep rate (ϵ) as a function of applied stress,

$$\epsilon = B\ \sigma^n\ \exp(-\Delta H/RT)$$

a combined stress-rupture formulation containing the Monkman-Grant exponent (m), the creep stress exponent (n), and the temperature dependence for creep can be created,

$$t_f = A\ B^m\ \sigma^{mn}\ \exp(-m\Delta H/RT)$$

Using this expression, preliminary lifetime predictions for this material indicate that it can withstand a combined stress and temperature of 50 MPa and 1370°C for a period of about 1 year. The temperature of 1370°C and lifetime of 1 year are typical of those expected in advanced heat engines.

Optical examination of polished sections from a series of samples that failed at 1375°C under different loads, together with two other samples that survived for periods of 1100 and 2000 hrs, revealed no evidence of distributed creep cracks. From this result, it appears that rupture occurs by unstable crack growth, presumably once a critical density of cavities is developed. This conclusion is supported by TEM studies, which although preliminary, have shown the existence of extensive, widely distributed grain boundary cavitation in crept samples. In this material, the cavities are preferentially distributed on grain boundaries that are normal to the tensile stress axis, and are generally in the form of isolated, lens-shaped cavities, showing apparent diffusive growth into the adjacent silicon nitride grains. So far, evidence for full-facet cavitation has only rarely been found. While the identification of these features as creep cavities was confirmed by comparison with samples taken from the stress-free regions, the processes involved in cavity nucleation and growth remain a subject of further study.

Creep and Creep Rupture of Sintered Silicon Carbide

S. M. Wiederhorn[1], R. F. Krause, Jr. and D. C. Cranmer

[1]MSEL, Institute Scientist

The development of new ceramics holds promise for use of high efficiency, enhanced performance of structural systems in high temperature, stress-bearing environments. However, before ceramics can be used in industrial applications, issues concerning reliability and service life remain to be resolved. Accordingly, we have been studying the creep and creep rupture behavior of model ceramics at elevated temperatures. One of the more promising materials is sintered silicon carbide, which exhibits very low creep rates at elevated temperatures in inert environments. At temperatures below 1500°C, the material appears to fail via a slow crack growth mechanism. This material exhibits good strength at elevated temperatures and has a high thermal conductivity.

For this program, tensile creep tests were attempted at 1500°C at applied stresses between 100 and 200 MPa, and creep rates between 8.6×10^{-10} and 1.0×10^{-9} s^{-1} were measured at applied stresses between 100 and 150 MPa. These are approximately the same creep rates as would be predicted for Coors SCRB 210 siliconized silicon carbide at 1150°C. Additional tests at 1475 and 1525°C at an applied stress of 150 MPa gave creep rates of 1.2×10^{-9} and 2.7×10^{-9} s^{-1}, respectively. The activation energy for tensile creep is about 630 kJ/mol, based on the 150 MPa applied stress data. Comparison of these data with compressive creep data appears to show no difference in creep rate between compression and tension. This suggests that predictions of the creep behavior can be made from a limited amount of experimental data obtained from a combination of tension, flexure, or compression tests.

Flexural creep tests were conducted at 1500°C at applied stresses between 160 and 310 MPa. The steady-state creep rates vary from 5.8×10^{-10} s^{-1} at 160 MPa to 3.3×10^{-9} s^{-1} at 310 MPa. An analysis method for evaluating the power-law creep parameters for tensile creep at elevated temperatures was developed. Steady-state displacement rate was measured versus load on flexure specimens and combined with compressive creep data. The analysis takes into account the fact that the material may behave differently in tension and compression. The power-law parameters for compressive creep were evaluated directly from strain rate versus stress data. Using these values for compressive creep, those for tensile creep were evaluated from displacement rate versus bending moment from the flexure tests. The compressive and tensile creep properties of the material determine the curvature and neutral-axis position in the flexure specimen under a given bending moment. The power-law parameters for creep of sintered α-SiC have been evaluated and provide a reasonable prediction of the experimental tensile creep data obtained.

Microstructural examination of the α-SiC showed that initially it consists primarily of the 6H polytype, and has a fine grain, equiaxed structure. It also contains some large inclusions of excess carbon, often in the form of pyrolytic graphite, which are generally situated on the triple (or multi) grain junctions. Preliminary high resolution TEM indicates the presence of a grain boundary interphase of ≤ 1 nm in thickness. There are isolated pores throughout the microstructure, and cracks of 1-10 micrometers situated at the carbon/graphite inclusions. After creep, optical examination of polished sections revealed a distribution of short creep cracks in only one tensile sample. There is also evidence of possible crack initiation from the initial porosity, but there is no clear indication of distributed cavitation found in this preliminary examination.

Processing-Property Relations in Whisker-Reinforced Ceramic Matrix Composites

R. F. Krause, Jr., D. C. Cranmer and E. R. Fuller, Jr.

The primary objective of this program is the experimental determination of the relationships between the performance of whisker-reinforced, ceramic matrix composites and their chemistry, microstructure, and properties. The increased understanding of the fracture process will be used to develop strong, damage-tolerant materials. Low and high-temperature structural performance of ceramic matrix composites is controlled by the chemistry, microstructure, and properties of the material. A vacuum hot press (loads to 500 kN and temperatures to 2100°C) was used to fabricate billets of silicon carbide whisker-reinforced alumina composites. The relation of processing conditions to microstructure, mechanical properties, and performance is being evaluated.

The experimental conditions were determined using a one-half fractional factorial. During FY 90, we have fabricated additional billets of material having different whisker contents (20 and 30 volume %), two different blending procedures, two different whisker types, as well as some confirmatory billets to reproduce earlier work. Densities vary from 3681 to 3818 kg/m^3 with standard deviations ranging from about 5 to 38 kg/m^3. Four-point bend strengths vary from 425 to 598 MPa with standard deviations ranging from 8 to 20 MPa. The strength and density measurements show that we have obtained a range of properties consistent with our expectations from the processing conditions. Machining performance measurements have been completed and will be correlated with the microstructure (density, alumina grain size, homogeneity), mechanical properties (hardness, flexural strength, fracture toughness), and processing parameters. Additional work to conclude the study includes determination of grain size, chemical homogeneity, fracture toughness, and hardness. These measurements and the regression analyses will be completed in FY 91.

Glass Science and Technology

D. C. Cranmer, D. H. Blackburn[1] and D. A. Kauffman

[1] Consultant

The area of glass science and technology is one in which NIST has been involved since 1910-11, and included the large-scale production of material for a variety of lenses and mirrors. The present efforts are driven by the desire to use unique glasses as analytical standards, and devices, sensors, and components of more complex systems.

Europium-based glasses have been identified as potential optical components. Changes in the optical properties as a function of Eu concentration and host glass composition have been observed in our previous work in this area. The host glass in this prior work was a silicate-based material. The results obtained on these materials indicated the need to more closely examine the relations between refractive index (n), its change with temperature (dn/dT), and elastic modulus. To achieve this, during FY 90, two new PbO-SiO_2 glasses having a high refractive index and high dn/dT were prepared, as was a Ta_2O_5-containing silicate glass, which has a high elastic modulus. These glasses were sent to the Center for Laser Research at Oklahoma State University for evaluation of the laser-induced refractive index grating properties. Results obtained to date indicate that the Pb-based glasses exhibit much smaller transient times to write the grating but they also do not retain the grating as long as previously examined compositions.

In an application area examined initially in FY 89, we found that there are presently no completely acceptable materials available for use as a thermal neutron absorber. Choosing a thermal neutron shielding material for neutron scattering instruments or prompt gamma-ray activation analysis (PGAA) instruments is often difficult. The ideal neutron shield is one which attenuates the neutron beam rapidly without creating additional background. But the materials which are most attractive for attenuating the thermal neutrons, such as boron and cadmium, produce gamma-rays in the neutron capture process. Although this gamma-ray background might be tolerated near some neutron scattering instruments, it quickly degrades the quality of a PGAA instrument.

The nuclide ^6Li is more attractive than other nuclides as a thermal neutron shield because it has a large absorption cross section, 941 barns, and the primary neutron capture reaction is the (n, α) charges particle reaction. There is only a small prompt gamma-ray branch (0.0004% of the total). Enriched ^6Li can thus provide rapid attenuation of the neutron beam without producing significant background problems.

A disadvantage of using $^6Li_2CO_3$ has been the lack of a suitable host matrix. Fused $^6Li_2CO_3$ is one common form but it is prone to attack by moisture and has poor structural properties. Sintered ^6LiF is a better material for shielding since fluorine has a low absorption cross section and will not contribute substantially to the gamma-ray background. Structural properties of sintered ^6LiF are also better than those of lithium carbonate, as it is not prone to attack by moisture and is less brittle. This material, though, is not easily formed into irregular shapes and cannot be easily machined.

We have developed a ^6Li silicate glass for use as a thermal neutron shield.

There are only two components to the glass: SiO_2 and $^6Li_2O$. Lithium silicate glasses tend to become susceptible to crystallization at higher Li_2O concentrations. Glasses have been successfully prepared with ^6LiO concentrations of up to 18 weight percent with no evidence of crystallization. This glass provides a thermal neutron attenuation of 76% per mm of glass. To further increase the concentration of Li_2O in the glass, alkaline earth or other divalent oxides can be added to the melt. We have been successful in creating a ^6Li glass containing as much as 22 weight percent by adding 8 weight percent Al_2O_3. The thermal neutron attenuation for this alumina-doped lithium silicate glass is 82% per mm. Long-term irradiation tests have been performed on the ^6Li silicate glass. A one by one cm piece of glass, with a thickness of one mm, was cut from a larger sample of glass and then polished. This glass was irradiated in the 1PH1 pneumatic beam tube of the MITR-2 reactor at the Massachusetts Institute of Technology. The neutron current density in this beam tube is $8x10^{12}$ neutrons/cm^2s and the cadmium ratio is 400. To irradiate the sample, the glass was wrapped in Al foil and placed in a polyethylene rabbit that was packed with polystyrene packing material. Short irradiations, lasting from a few seconds to 15 minutes, were performed to determine whether the heat generated by the glass was a problem. The heat generated by the glass did not cause too much heating of the polyethylene rabbit and the rabbit temperature was stable after a 15 minute irradiation. Following these short irradiations, the sample was irradiated for 10 hours. Two weeks after the end of irradiation, the glass was unpacked and inspected. Some localized charring of the polystyrene was observed within ca. 2 mm of the glass sample. The glass showed no detectable change in appearance other than a discoloration from color centers produced by charged particle recoil.

Much of the usefulness of this glass is in external beam environments, where the neutron current densities are lower, on the order of 10^9 neutrons/cm^2s, and the beams have much lower gamma-ray and fast neutron components. The irradiation studies described above were equivalent to an external beam irradiation of at least seven years. This lithium glass is more applicable as a thermal neutron shield than other shielding materials: it can be cast into a variety of shapes and sizes, and it can be machined using ordinary glass machining techniques into shapes with close tolerances. A patent disclosure has been filed for this material.

The ability to control the chemistry and crystallization behavior of many glasses has led to the creation of the class of materials known as glass-ceramics. One interesting area where these materials are finding new applications is in dental technology. The problem of providing improved dental materials which have improved structural properties while maintaining tooth appearance is one which has beset the dental materials community for a number of years. Previous research in this area has identified a family of glass-ceramics which might be applied to other structural materials and provide the appropriate visual characteristics. Three appropriate glasses which can be heat treated to form glass-ceramics have been melted and provided to the American Dental Association's Health Foundation (This effort is conducted at NIST.) Promising compositions will be modified as needed to maintain appearance.

A number of analytical instruments require the use of standard glass disks, spheres, and particulates. Using conventional glass melting techniques and a unique apparatus for making spheres, we provide a number of glasses in a variety of shapes for use in instrument calibration. The glasses are provided to the

NIST Center for Analytical Chemistry's Gas and Particulate Science Division. During this year, we have provided 11 glasses in various forms to the CAC for development of new microanalytical standards. This particular effort has resulted in the issuance of 13 glass standards in the past 11 years. These kinds of standards can be used to characterize a variety of air pollutants.

Environmentally Enhanced Fracture of ZBLAN

D. C. Cranmer, S. W. Freiman, G. S. White and A. S. Raynes

Evaluation of the mechanical properties of new glasses for optical applications forms a important component of our work. This year, a heavy metal fluoride glass was examined to determine the effects of different environments on the crack growth properties of the glass. We determined the initial strength distribution of a representative fluoride glass composition (ZBLAN), as well as the environmental parameters B' and n, based on dynamic fatigue testing of the glass, and constructed a design diagram for the ZBLAN glass.

To obtain the inert strength distribution, twenty polished disks were tested in biaxial flexure (6 mm diameter flat on 3 ball) at a rapid loading rate. For the dynamic fatigue tests, 30 squares of the glass were indented with a Vickers diamond to introduce a controlled flaw into the tensile surface of the specimen. These squares were then fractured in biaxial flexure in either of two environments (room ambient [about 20%] or 85% relative humidity) at two widely varying stressing rates (2×10^{-3} and 1.5×10^{3} s^{-1}). The strength of each disk was calculated from the dimensions of the sample and the load at failure. The data were rank-ordered, low to high, and the probability of failure, F, computed using:

$$F = \frac{i}{N + 1}$$

where N is the number of samples and i is the rank. The value of m, the Weibull slope, calculated from the data is 2, indicating a wide range of strengths for this material. Given the machining conditions for these samples, this value of m is not surprising and can be raised significantly by better grinding and polishing.

The values of B' and n are obtained by fitting the dynamic fatigue data to a straight line of the form

$$\ln \hat{\sigma} = a_0 + a_1 \ln \dot{\sigma}$$

where

$$a_0 = \frac{\ln [B'(n' + 1)] + (n' - 2) \ln \sigma_i}{n' + 1}, \quad a_1 = \frac{1}{n' + 1}$$

and n' is the apparent environmental constant. The values of n obtained for environments containing 20 and 80% relative humidity are 175 and 75, respectively. From the above equation, Ln B' is then -230 and -71, respectively. Data previously obtained for heavy metal fluoride glass indicated n values in excess of 200. It should be noted that the differences in slow crack growth are not readily apparent once the n value has exceeded approximately 60.

Given the values for ln B', n, m, and ln σ_0, the lifetime of the glass can be predicted for a given applied stress condition and desired reliability (i.e., acceptable percentage of failures). This has been done for the ZBLAN glass for each humidity condition (20 and 80%) and a failure probability of 0.1 (that is, 10% of the pieces in a given group will fail). For these types of glasses, there appears to be little effect of atmospheric humidity, hence the design diagram indicates that failure in service is not likely until an applied stress of about 10 MPa is reached. Comparing this value with finite element calculations shows that the glass would need to be thicker than 2.5 cm, *if* the Weibull parameters of the polished glass are the same as the test pieces used in this program.

TRIBOLOGY

Said Jahanmir

Structural ceramics are increasingly used in a variety of applications where wear resistance in required. However, their reliable use depends upon the availability of data which describes performance and provides guidelines for material design. The primary focus in our research is on the characterization of the tribological interface including analysis of chemical reactions and formation of tribochemical films, physical and mechanical behavior of surface films, and the microstructural aspects of deformation and fracture process leading to wear and failure.

Ceramic Wear Maps

S. M. Hsu, P. I. Lacey[1], S. W. Lee[2] and Y. Wang[1]

[1] Guest Scientist, University of Maryland
[2] Guest Scientist, University of Illinois at Chicago

Advanced ceramic materials offer innovative design opportunities in tribological applications. However, the successful application of ceramics may be inhibited by the need for evaluated materials properties. In addition, friction and wear are not intrinsic materials parameters, rather they are a combined function of material, system geometry, environment and contact conditions. In the present study, a unified test methodology was developed to examine the tribology of ceramic materials in a systematic manner.

This technique allows the representation of material wear as a simultaneous function of any two variables. The more informative combinations include: speed and load, speed and test duration, load and temperature etc. The maps delineate the useful application range for each material, as well as providing a unified data format to allow comparison of different materials under the full spectrum of tribological conditions. The self consistent test methodology also facilitates comparison of the wear mechanism from different materials. A range of polycrystalline ceramics have now been examined in this manner. The result is a data base that collectively provides a comprehensive representation of the wear properties of each material.

The predominant wear mechanisms observed for each of the polycrystalline ceramics were broadly similar. In lightly stressed contacts, typically characterized by low speed and load, a mild wear rate is produced. High temperatures (created by frictional heating) combined with great hydrostatic pressure (created by the material hardness) combine to produce localized plastic deformation of the normally brittle material. Initially increasing the contact stress produces a slight increase in the rate of material removal. On attaining a critical level of stress an abrupt transition occurs. During the transition the wear rate becomes erratic and often increases by several orders of magnitude. Tensile forces formed at the rear of the contact induce crack propagation through the grain boundary matrix. Complete grains and even clusters of grains are detached to form a rough and irregular surface.

The onset of brittle fracture controlled wear delineates the practical application range of each material. A semi-empirical model, based on fracture mechanics was developed to examine the critical parameters required for transition in more detail. This model indicates that to optimize the wear transition resistance of ceramic materials it is necessary to refine the grain size, avoid internal tensile stresses and if possible, induce internal compressive stresses in the near surface region, while maintaining high indentation hardness.

The experimental conditions required for brittle fracture controlled wear were determined from the wear maps of several materials under dry sliding and are plotted in Figure 6. Clearly, the test conditions required for wear transition are strongly influenced by materials parameters. The wear transition for zirconia is highly speed dependant. This material is a good insulator and material removal is probably aided by a large thermal gradient in the near surface region. However, the addition of silicon carbide whiskers to alumina produces a composite ceramic with excellent wear characteristics. The elongated whiskers extend the path required for crack propagation through the material, delaying the onset of fracture.

Monolithic silicon nitride was among the most effective untoughened materials examined. A combination of both α and ß phase grains produce a microstructure which resists fracture of the surface. Relatively severe conditions were required for wear transition in dry sliding and no transition was observed in the presence of a liquid lubricant. Liquid lubricants remove excess heat and reduce the tangential stress at the contact interface. As a result, the onset of transition was delayed for each of the remaining materials examined, as shown in Figure 6b.

Because of the potential of ceramic materials in heat engine applications the high temperature performance of each material is also being examined. Elevated temperatures reduced the effectiveness of silicon nitride (Figure 7) and caused a wear transition similar to that produced by increasing sliding speed. This is probably due to a similar decrement in material properties with either increasing asperity tip flash temperature or ambient test temperature.

Systematic analysis of the wear mechanism in this manner produces a more effective basis for wear modelling and the development of more successful tribomaterials. In addition, the self consistent data base will enhance the ability of designers to select the materials most appropriate to their operating conditions.

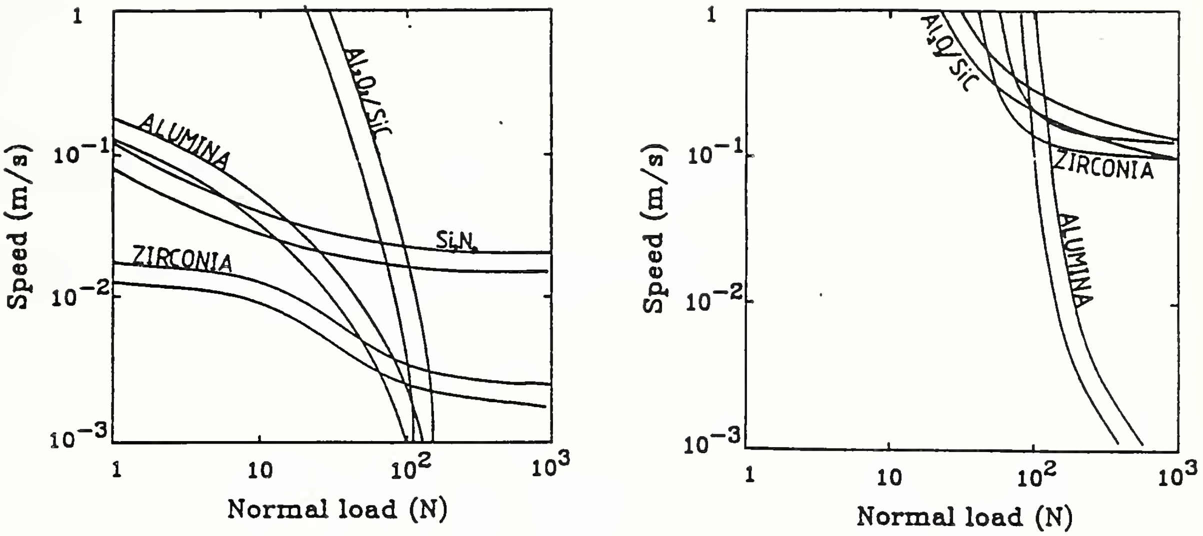

a)

b)

Figure 6. Wear transition maps for a number of materials at room temperature.

a) Unlubricated conditions
b) Lubricated with paraffin oil

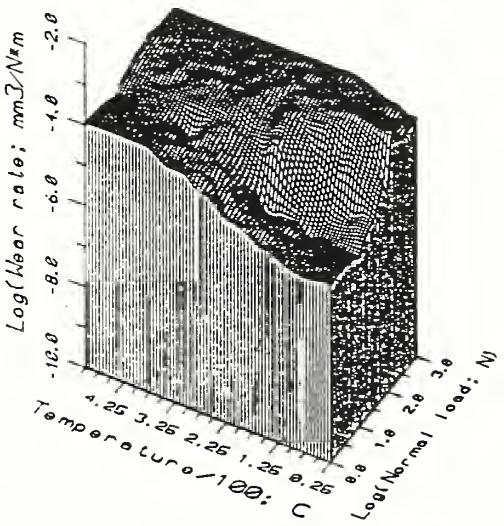

Figure 7. Wear map for unlubricated silicon nitride as a simultaneous function of normal load and test temperature. Wear Mechanisms of Advanced Ceramics.

Ceramic Wear Transition Maps

S. Jahanmir, X. Dong[1] and S. M. Hsu

[1] Guest Scientist, University of Maryland

Advanced engineering ceramics offer unique capabilities as tribomaterials. These materials are being used currently in diverse applications requiring wear resistance and chemical stability at elevated temperatures. They are also being considered for advanced applications in future high efficiency engines and other mechanical systems. Design and selection of ceramics for these applications require reliable data and mechanistic information on the effect of temperature, load and environment on the tribological behavior. The purpose of this project is to determine the wear mechanisms of various advanced ceramics as a function of temperature and contact load.

Our results have shown that the tribological characteristics of alpha-alumina sliding on a similar material under dry sliding conditions can be divided into four distinct regimes. At low temperatures, $T < 200°C$, tribochemical reactions between the alumina surface and water vapor in the environment control the tribological performance. The coefficient of friction in this temperature range is approximately 0.40 and the wear coefficient is less than 10^{-6}, independent of contact load. At intermediate temperatures, $200°C < T < 800°C$, the wear behavior depends on the contact load. At low loads wear occurs by plastic flow and plowing; the coefficient of friction is approximately 0.50 and the wear coefficient is less than 10^{-6}. At loads higher than a threshold value, severe wear occurs by intergranular fracture. The coefficient of friction increases to 0.85 and the wear coefficient increases to 10^{-4}. At temperatures above 800°C, formation of a silicon-rich layer on the wear track by viscous flow and diffusion of the grain boundary phase reduces the coefficient of friction to 0.40, and the wear coefficient is reduced to a value less than 10^{-6}. The results of the wear tests and observations of the fundamental mechanisms controlling the tribological behavior of this material are consolidated in a simple wear transition diagram, shown in Figure 8.

Reasons for these observed transitions have been identified. The transition from Region I to Region IV is controlled by tribochemical reactions between alumina and water vapor. The adsorption tendency of water is reduced as the temperature is increased and the formation of oxides are favored over the hydroxides. This transition occurs in the temperature range of 100°C to 200°C, because aluminum hydroxide is either not formed or is unstable at higher temperatures. This transition boundary may be shifted to lower temperatures at larger loads and higher speeds, due to increased contact temperatures.

The transition from Region II to Region IV is controlled by the fracture strength of the material. A contact mechanics model, based on linear elastic fracture mechanics, was used to show that propagation of cracks from pre-existing flaws controls the onset of severe wear. This transition can be prevented by the reduction of the normal load, reduction of the friction coefficient, or an increase in the fracture toughness of the contacting materials. This transition boundary may be shifted to lower loads at higher speeds, by thermoelastic stresses developed at the contact due to the low thermal diffusivity of alumina.

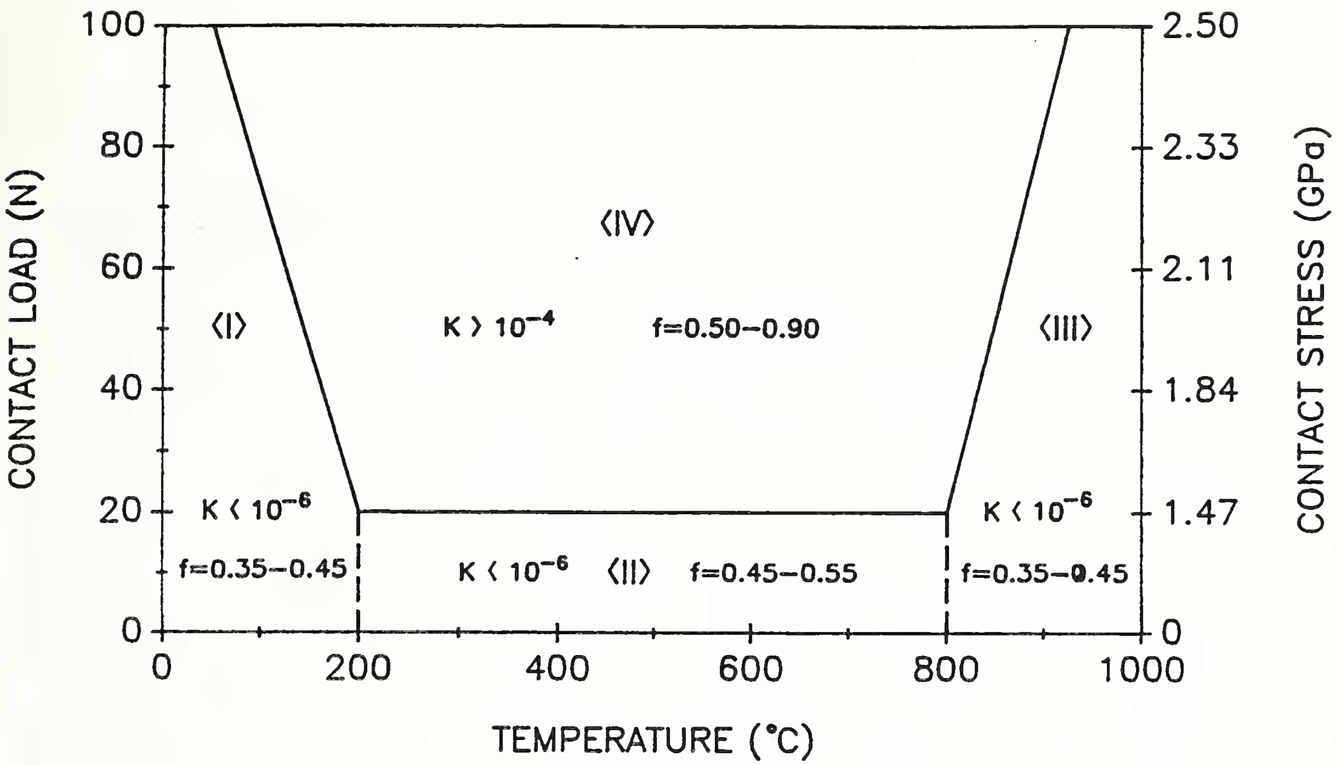

Figure 8. Wear Transition diagram for dry sliding wear of alpha-alumina.

The transition from Region III to Region IV is controlled by diffusion and viscous flow of the glassy grain boundary phase. Since both of these processes are thermally activated, an increase in the sliding speed or the contact load may shift the transition boundary to lower temperatures. However, the thermoelastic stresses generated at higher speeds and increased wear at larger loads may override the beneficial effects.

The wear transition diagram for alpha-alumina clearly shows that the tribological performance of this material can be controlled by a proper selection of operating conditions. The fundamental understanding also can be used to improve the performance of this material by making changes in the composition and/or microstructure. First, any modifications that increase the fracture toughness should result in beneficial effects. Secondly, changes in the composition of the grain boundary phase might produce a material that could spread easily on the surface under certain operating conditions. Finally, the tribological performance can be controlled by lowering the coefficient of friction. This can be achieved by solid-lubricant coatings, self-lubricating ceramic matrix composites, liquid lubrication, or reaction of the surfaces with the environment.

Tribology of Self-Lubricating Composites

M. B. Peterson, A. W. Ruff and W. W. Duvall[1]

[1] Student, University of Maryland

An important area of materials investigation in tribology concerns the factors that determine friction, wear, and durability of solid lubricant films on sliding contact surfaces. In a program sponsored by the Air Force Materials Laboratory, it is planned to use solid lubricant pre-coated surfaces in bearing systems associated with sophisticated components in space satellites. Such coatings must have long life, steady friction, and low wear, all without any possibility of regular maintenance. NIST has the responsibility in its project to develop an understanding of the tribology of self-lubricating composites and to identify potential materials for actual hardware systems. Such materials would offer the advantage of repairing any damage to the solid lubricant surface film by acting as a source for new solid lubricant through controlled wear during operation.

The NIST project has identified key processes responsible for wear in such materials, and has prepared and examined a number of candidate materials. Inert materials such as gold alloy coatings have also been studied and been shown to have very good properties in combination with solid lubricant coated surfaces. Measurements of wear and friction have been carried out under appropriate sliding conditions to provide data for eventual design purposes. Composite materials consisting of both copper-matrix and bronze-matrix with solid lubricant phases of either intercalated ($NiCl_2$) graphite or molybdenum disulfide have been prepared and studied in sliding wear. Both uncoated and MoS_2 pre-coated type 440C stainless steel rings were used as counterface materials. Sliding wear tests were carried out using a pin-on-ring tribological test system at normal temperatures in both air and dry argon gas. The load was 33 N, sliding speed 0.14 m/s, and sliding distance from 790 to 1900 m. Specimen pins were fabricated by several methods. Compaction of powders was done in a hydraulic press using a die at forces of 5,000 to 10,000 lbf (22 to 44 kN). Compacts of pre-mixed powder combinations of matrix material and solid lubricant were made. Two types of manufactured composites were also used: one containing a series of holes in a hexagonal arrangement with different hole diameters and separations, and the other contained a central slit with different widths. These size variations permitted different effective area and volume percentages of solid lubricant under controlled phase shape and spacing. Selected commercial composites were also studied for comparison.

In all specimens, wear led to the generation of wear debris particles some of which remained in the contact gap and established an interfacial film. These characteristic features are important in determining the wear and friction mechanisms involved in the tribology of self-lubricating composites. One method of comparing material performances is shown in Figure 9 which plots average wear rate and average friction coefficient obtained for each case sliding against pre-coated steel in argon gas. Results for both the commercial materials and composites prepared at NIST are shown. Recommendations are being made to the Air Force for deciding on hardware design and production procedures. Project work continues to better understand the fundamental mechanisms and to optimize the composites in other respects such as processing and mechanical strength.

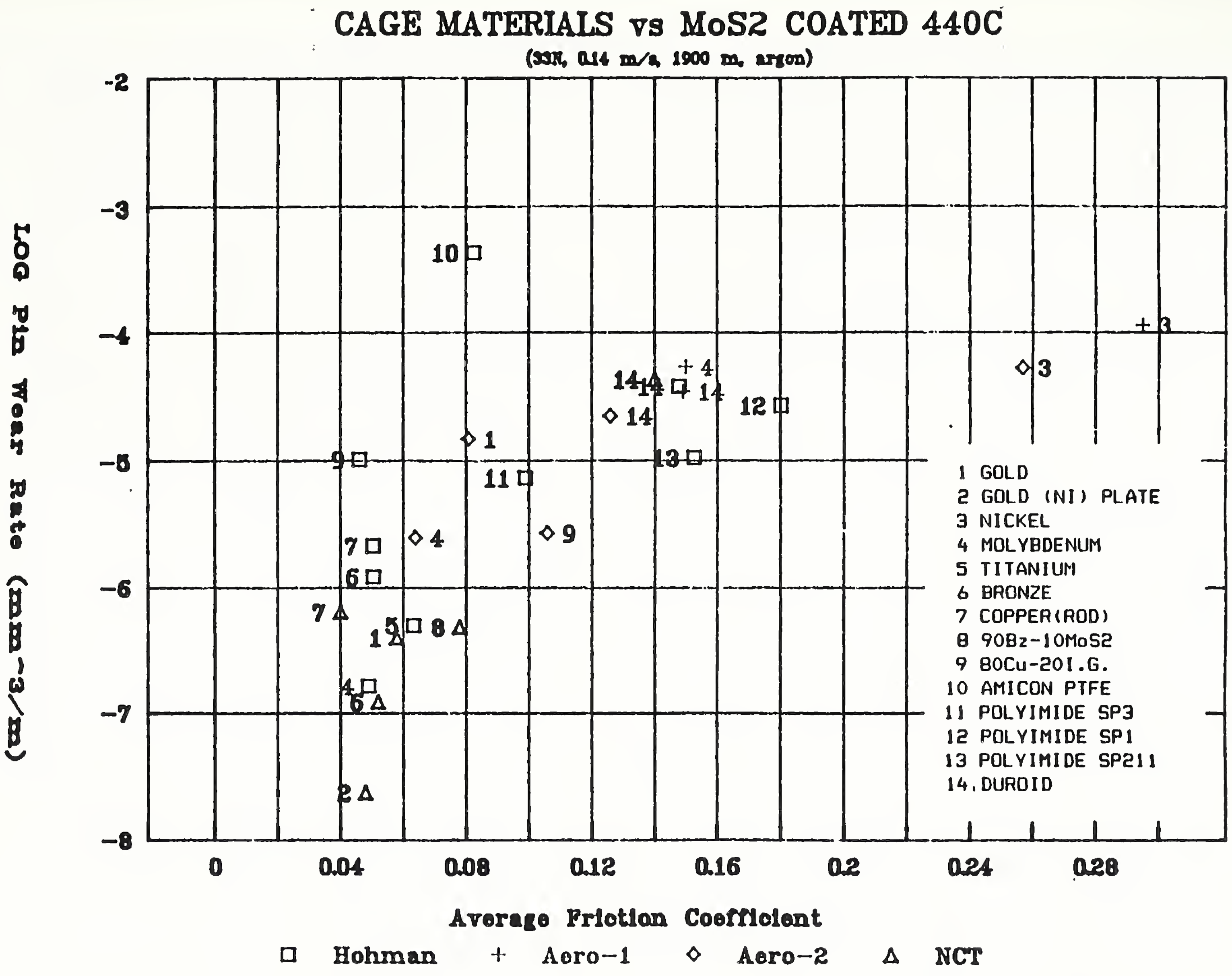

Figure 9. Comparison of wear rate and friction coefficient for different NIST-produced and commercial materials, including self-lubricating composites.

Tribological Films and Coatings

A. W. Ruff, M. B. Peterson, L. K. Ives and E. P. Whitenton

This project examines the role of tribological films in sliding contacts and determines the principal mechanisms and the effects of material variables. Studies are being conducted to identify the nature of oxide films formed at sliding contacts. The purpose of this work is to identify the important properties of effective films (either lubricating or wear resisting) to provide the technology base for improved tribological materials. Studies have been conducted with metals sliding against ceramic substrates in a variety of environments to generate surface transfer films. These films have been analyzed as to composition and morphology. Friction behavior is compared with applied films of known composition to identify which films control friction behavior. Special attention is being given to hydrated oxide and hydroxide films which are hypothesized to control friction and wear at lower temperatures.

To investigate this phenomenon in greater detail sliding tests have been devised to generate surface films in a variety of environments. Pure metal pins are loaded against rotating Al_2O_3 disks to generate the transfer films. Typical friction coefficients are given in Table 3. The results were unexpected in that the friction coefficients in water were much lower than those in air and very little transfer took place. Analysis of the films and data indicated that much of the frictional behavior could be attributed to lubrication of the aluminum oxide either due to the formation of aluminum hydroxide or due to the adsorption of active ions on alumina surface. This however does not appear to be the case for rhenium which gave a value of 0.17 in air and water, and 0.30 in H_2O_2. Reaction films have been hypothesized for each combination and friction tests will be run with those films applied as powders.

Studies of tribological characteristics of composition-modulated alloys (CMA) have also continued. The alloys, alternate oriented layers of nickel and copper in coating form, were made at NIST and deposited on steel substrates. The total coating thickness was from 4 to 25 μm. Sliding wear measurements were carried out under both unlubricated and lubricated conditions against 52100 bearing steel counterfaces using a crossed-cylinder geometry. It was found that the CMA Ni-Cu alloys had significantly more wear resistance than pure copper and nickel. The smallest layer thickness CMA (3.8 nm) shows the greatest wear resistance. Further, results show a load threshold for each CMA above which wear takes place at a rate more similar to that for Ni and Cu. A simple model of dislocation behavior in a layer microstructure during the plastic deformation associated with wear has been applied to explain these results. The model allows for three effects associated with these unique microstructures: 1) layer spacing effects (smaller spacings give greater wear resistance), 2) dislocation line energy difference effects, associated with layer composition, and 3) layer interface thickness and structure difference effects.

These results should provide the needed understanding for future development of wear-resistant metals, coatings, and surface treatments for practical applications. Such developments can have a significant impact, since in many applications it is not possible to use liquid lubricants and thus the materials themselves must have suitable wear and friction properties.

Table 3. Friction Coefficients of Various Pure Metals and Alumina Sliding Against Al_2O_3

	Environment				
Material	NH_4OH	H_2O_2	H_2SO_4	Air	H_2O
Mo		.26		.75	.30
Re		.30		.17	.17
Ni	.13	.20	.08	.60	.20
Cu				.65	.40
Fe				.65	.40
Al				.75	.35
Al_2O_3					.30

Nanoindentation and Scratch Testing

A. W. Ruff and E. P. Whitenton

Indentation testing is an established method to measure mechanical behavior of materials. At microscopic levels, it is especially useful for measuring either small quantities of material or micrometer sized regions within a given sample. The method is routinely applied at quasi-static rates to measure the hardness (resistance to indentation deformation) of materials. Both fracture at the site of the impression and plastic flow can be studied. The effect of strain rate and load on the deformation behavior of materials can be investigated using different indenter shapes, e.g., spherical or pyramidal.

A new project was initiated to construct and use a nanoindentation/scratch system to provide both indentation measurements and scratch measurements on materials, particularly in the form of thin surface films and coatings. This technique is also suited for bulk materials that are inhomogeneous in structure and properties in both the normal direction to the surface and laterally in the surface plane. The instrument can perform indentations using loading times ranging from 0.001 to 100 seconds, over loads from 0.001 g to 1000 g, and record both the instantaneous load and penetration of the indenter into the sample. In addition, it can translate the specimens under load to produce controlled scratches. The load waveform can be held constant during the translation, or it can be varied in a pre-set pattern. The scratching resistance force is measured by a transducer. All control and data analysis are carried out by a dedicated lab computer, using software developed within the project.

Preliminary results from a study of wear of copper vs. MoS_2 coated steel are shown in Figure 10 where the change in elastic and plastic properties (measured by indentation) of the tribological film formed during sliding relative to that of the substrate are indicated. The tester will permit measurements of material properties such as microhardness, elastic modulus, yield strength, ductility, toughness, friction coefficient, plowing resistance, and others, including rate effects of these properties. Microscopic examination of the indentations and scratches during and afterward will provide further information. The instrument will be applied to characterization of solid films present in tribological contacts. It may offer previously unavailable information on micromechanical properties of tribological coatings, coating wear and friction properties, and coating/substrate adhesion. Such characterization will include chemical, mechanical, and structural information, all on a sub-micrometer level. An improved understanding concerning the role of solid surface films in controlling the tribological behavior of materials would open up new avenues for the development of engineering materials, leading to improved performance and reduced failure and maintenance costs.

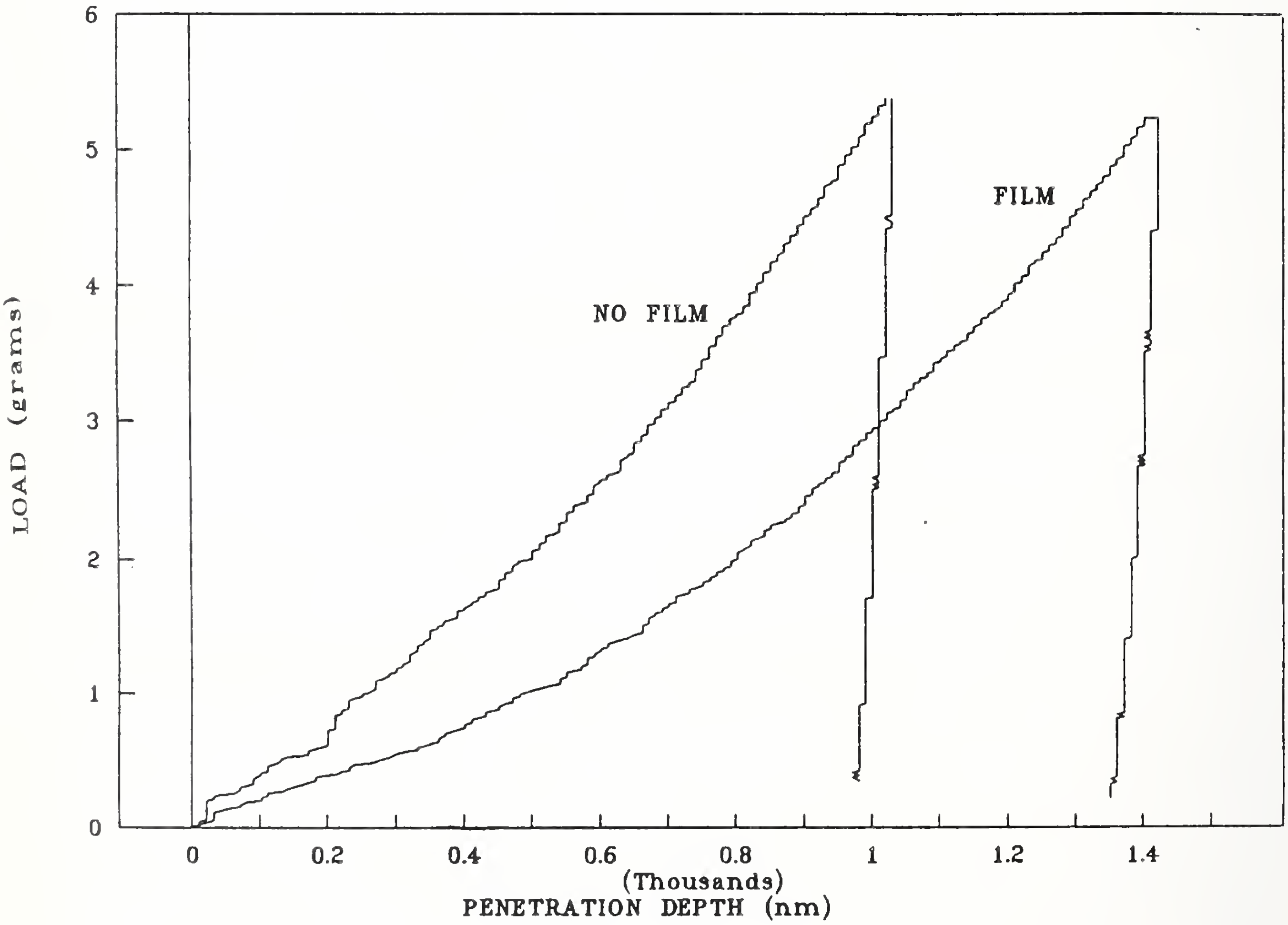

Figure 10. Load vs. indentation depth measurements from a copper/MOS_2 tribological film showing both plastic and elastic effects of film.

Mechanism of Abrasive Wear in Lubricated Contacts

L. K. Ives, M. B. Peterson and E. P. Whitenton

Wear by extraneous abrasive particles is the predominant mode of wear experienced by lubricated components. The purpose of this project is to study the mechanisms which are responsible for this form of wear. A number of different mechanisms can be postulated. These include direct abrasion of the surfaces by hard particles, enhanced wear due to surface roughening and mechanisms involvingeffects associated with the disruption or prevention of the formation of protective lubricating films.

Current research in this project is sponsored by the Fossil Energy Materials Program of the Department of Energy. The Department of Energy is supporting the development of diesel engines capable of operating directly on pulverized coal, primarily in the form of a slurry consisting of 50% water and 50% coal. Efficient combustion has been demonstrated with this fuel; however, operating engines have experienced an extremely high rate of wear. One critical area of wear is at the piston/ring cylinder wall contact. The high wear rate is directly associated with the presence of coal fuel and combustion particles which enter the contact during sliding. Mineral matter in the coal rather than the hydrocarbon in coal is generally thought to be the main agent responsible for wear.

Previously, work on this project has focussed on determining the nature of combustion particulates that are responsible for wear. By examining particulates obtained from prototype diesel engines operating on different types of coal-fuel, it was established that several different types of particles were present. The hardest and probably the most aggressive in terms of abrasion were found to be silicates and quartz, with quartz usually being the hardest mineral present.

The primary emphasis of current research is to determine the influence of contact parameters, to assess the response to different lubricants, and to determine the effect of abrasive and component materials properties on wear processes. Relatively simple laboratory test methods are used for this evaluation. Figure 11 shows results obtained from a pin-on-disk test utilizing 52100 steel test specimens. In the figure a comparison is made of the wear rates obtained when three different types of particulates were mixed at a concentration of 10 wt. % with paraffinic mineral oil. Relative to the wear rate measured without added particles, unburned coal-fuel particles resulted in a 70% increase, coal-fuel combustion particles caused a six times greater wear rate, and mineral matter particles that were extracted during preparation of the coal-fuel increased the wear rate by 35 times. Other parameters being investigated include the effect of lubricant additives, specimen geometry, and atmospheric environment.

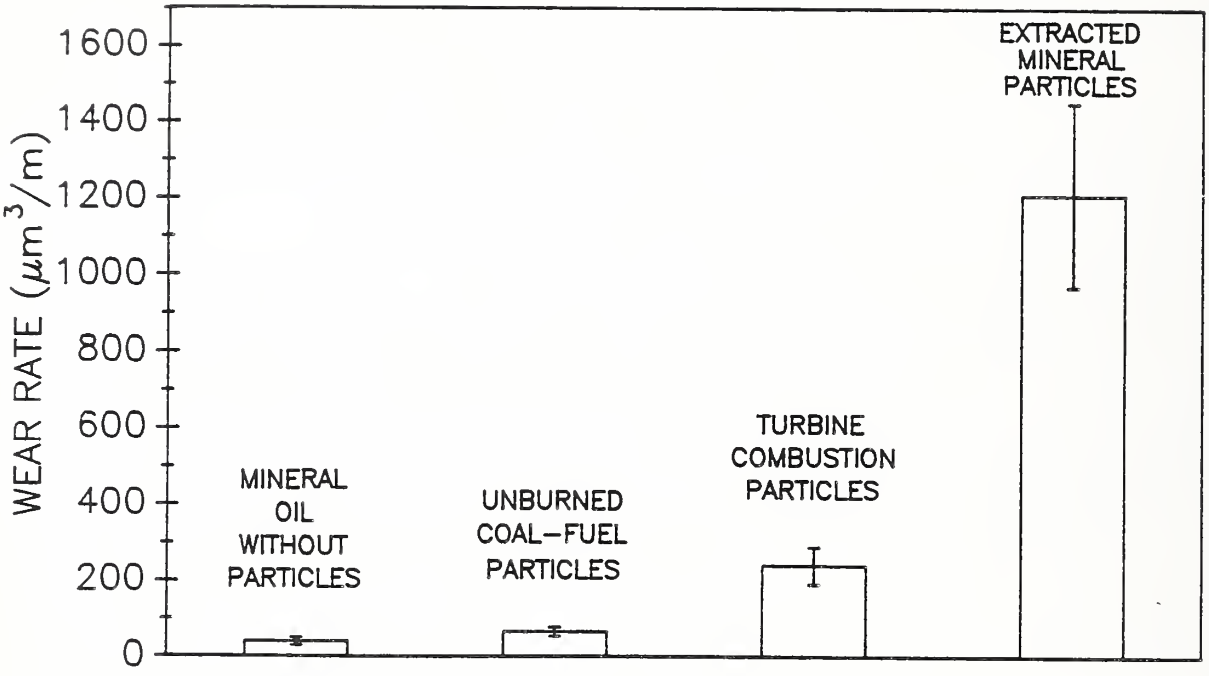

Figure 11. Wear results for various environments.

Fracture Mechanics Analysis of Near-Surface Cracks

S. Jahanmir, J. W. Dally[1] and Y.-M. Chen[1]

[1] Guest Scientists, University of Maryland

The purpose of this project is to develop a qualitative understanding of the propagation of cracks relevant to the formation of wear particles in an elastically deforming stress field. A shallow subsurface crack oriented parallel to the boundary and a vertical surface-breaking crack were analyzed. Three different series of photoelastic experiments were conducted on each crack type and results for the stress intensity factors for both the opening mode K_I, and the shearing mode K_{II}, were determined. The relative signs of K_I and K_{II}, which depend on the location of crack tip with respect to the point of load application, were used to predict the crack trajectories.

Depending on the location of the crack tip with respect to the neutral line, the results of the experiments give the potential crack propagation trajectory of a vertical surface-breaking crack as shown in Figure 12a. If the tip of a vertical surface-breaking crack is located in the tensile zone, $K_{II} < 0$, and the crack will turn to the right toward the direction of applied friction force. However, when the crack tip is in the compression zone, the cracks extend without turning due to mode II. If the crack tip is located near the neutral line the crack may be redirected opposite to the applied friction force depending on the sign of K_{II}.

Results of the subsurface crack experiments indicated that if the crack tip is removed from the neutral line the sign of K_I and K_{II} are the same. However, in the vicinity of the neutral line the sign of K_I and K_{II} may be different. The implication of the relative sign between K_I and K_{II} on the crack trajectory is schematically shown in Figure 12b. According to the influence of K_{II} on crack trajectory, cracks that are located in the tension zone with $K_{II} > 0$ are redirected away from the free surface. However, if the crack tip is located in the vicinity of the neutral line, $K_{II} < 0$ and the crack is redirected toward the surface. Cracks located in the compression zone will not propagate by the opening mode, since K_I is negative, but they may propagate parallel to the surface due to K_{II}.

The result of the analysis implies that subsurface cracks located in the tension zone propagate in a zig-zag pattern. The implication of these results on the process of wear particle formation in elastic materials is of particular interest. In these materials, especially ceramics, the effect of friction is very important. Since the magnitude of the tensile stress and the size of the tensile zone are proportional to the friction coefficient, a large friction coefficient results in a relatively large tensile zone. Vertical surface-breaking cracks may be redirected in this zone by crack curvature and become parallel to the surface. These cracks and other subsurface cracks propagate in a zig-zag pattern at large depths, producing large wear particles. However, when the friction coefficient is small, vertical cracks and subsurface cracks located near the surface are activated to produce small wear particles. Longer vertical cracks with the crack tips located in the compression zone propagate away from the surface and arrest.

Subsurface cracks located at large depths, in the compression zone, do not propagate. The net result is that the size and possibly the number of wear debris are related to the coefficient of friction. Reduction and control of the friction coefficient is of paramount importance in reducing wear of ceramic materials.

Advanced Liquid Lubricants

S. M. Hsu, J. M. Perez, C. S. Ku, D. E. Deckman, Y. Zhang[1] and P. Pei

[1] Guest Scientist, University of Maryland

The lubricant research project is exploring novel chemical structural concepts to provide a technology base necessary for the development of liquid lubricants for new technology applications. Current efforts are aimed at lubricants for energy efficient conversion systems. The low heat rejection engine (LHRE) concept is an example of an advanced technology in which the availability of advanced lubricants is a critical barrier for successful implementation. Increased pressure on environmental issues have resulted in significant industry interest in lubricant chemistry and tribochemical systems. Research is needed on cleaner burning diesel fuels and lubricants. Reduction of the lubricant contribution to emissions can make a significant impact on the level of particulate emissions. Alternative fuels require new lubricant concepts to insure long durability engines. The lubricant also plays a significant role in the use of alternative refrigerants that are being considered to reduce the ozone layer depletion by chloroflorohydrocarbons (CFC's). In a number of these areas, the limiting factor is the lack of knowledge in use of additives and

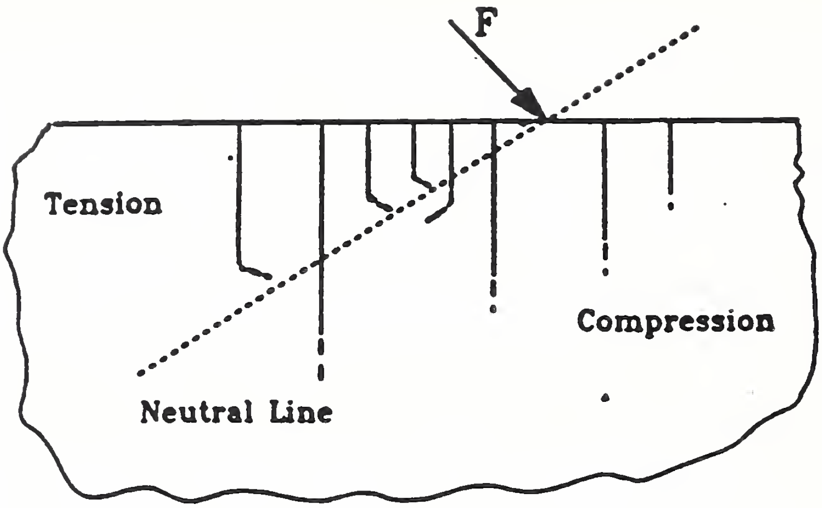

Figure 12a. Schematic representation of crack trajectories for a vertical crack.

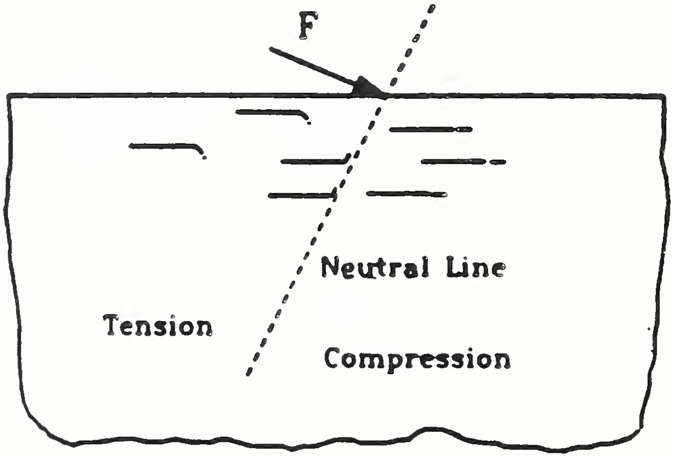

Figure 12b. Schematic representation of crack trajectories for a subsurface.

friction and wear control through lubrication. This project is providing relevant information on solubility and compatibility of additives, thermal stability and oxidative stability and deposit forming tendencies of fluids.

During previous years, we have developed information on thermal and oxidative properties of a number of synthetic fluids, the interactions of lubricants with various materials, and research on the chemistry of high temperature additives. The basic information has resulted in considerable involvement with industry.

As new lubricants evolve, the test methodology used to evaluate the materials needs to be improved. This year, a more sensitive way to evaluate engine deposit formation tendencies was developed through a new sample reactor for the pressurized differential calorimeter. The sensitivity of the system and the reproducibility of the method were significantly improved. Comparisons with industry engine test results, including vehicle field tests were quite successful.

Research on the interactions of additives and materials continued as did the search for stable high temperature additives that are effective in reducing high temperature oxidation and in providing good ceramic lubrication. The research on high temperature liquid lubricants has resulted in a stable fluid with excellent friction and wear properties. When compared to commercial fluids in a time-to-failure test and in 200°C tests on ceramic materials the NIST formulation performed significantly better, as shown in Figure 13.

Much of the research is being carried out cooperatively with industry. Evaluation of fluids and additives has resulted in a high temperature liquid formulation that is currently awaiting engine testing on a LHRE prototype engine.

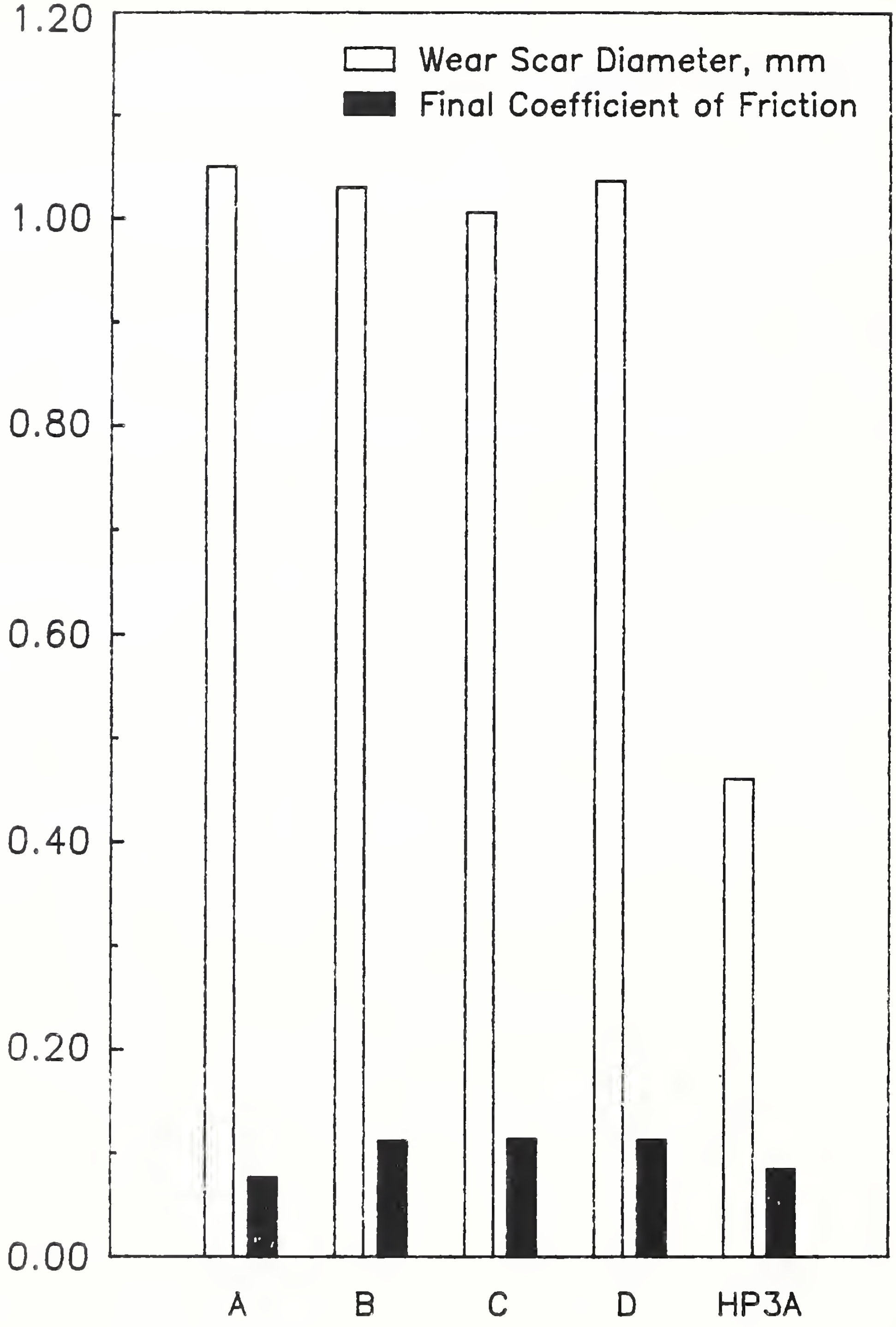

Figure 13. Friction and wear of high temperature formulations on SiC at 200°C, 600 rpm, 40 kg and 1 hr.

Chemical Interactions of Advanced Materials and Lubricants

D. Deckman, R. Gates and M. Shen[1]

[1] Guest Scientist, University of Illinois

Successful use of advanced ceramics in many tribological applications requires an understanding of the physical, chemical, and mechanical properties of the material. Physical and mechanical data are relatively abundant for most ceramics. However, information on the chemical interactions of ceramics is scarce. This is especially true for chemical interactions with regard to lubrication of these materials.

In the past year this project has been investigating the interactions of specific chemical compound classes with ceramic surfaces in a tribocontact. Silicon nitride and silicon carbide were chosen as initial candidates because of their promise in many structural applications.

The chemical interactions between chemical compounds and ceramic surfaces has been investigated using a ball-on-three-flat (BTF) wear tester under a specific set of conditions (Table 4). By comparing friction and wear test results for a purified paraffin oil (PPO) blended with 1.0% (wt) of selected chemical compounds, the effect of these compounds on boundary lubrication was assessed. In addition, post test analyses on the lubricant and ceramic surfaces helped to indicate the extent of ceramic-compound interaction.

A summary of the effect of 1% additions of selected chemical compounds on the friction and wear of Si_3N_4 is shown in Figure 14. Here the friction and wear data are each plotted along an axis to allow for a quick assessment of each of these performance parameters for each compound. The friction and wear performance of the purified paraffin oil without any additives is provided as a reference for the influence of the individual chemical compounds.

Tests with phosphorus containing additives on Si_3N_4 indicate that all phosphorus containing compounds reduce friction and wear under these conditions. The low wear results were associated with the formation of reaction films in and near the wear scar. Subsequent SEM, EDX, and Auger depth profiling analyses of the surface and reaction products suggest that the reaction films are approximately 100 Å thick and they are mixtures of wear debris and phosphorus enriched materials. As compared to PPO tests, sulfur containing compounds generally show little or no different friction and wear behavior. The oxygen containing compounds show that some of them are effective antiwear additives while others actually increase friction and wear. Chlorine containing additives all tended to increase friction and wear.

The results obtained with silicon carbide tests are summarized and shown in Figure 15. In general, few additives simultaneously reduce both friction and wear under the test conditions selected. Additives containing only sulfur have shown to be ineffective antiwear compounds by forming fine pits within the wear scars from corrosive reaction. The corrosion is probably caused by the formation of sulfur dioxide as a result of thermal or oxidative degradation of the molecules in the bulk fluid. Again, the interactions with the ceramic surfaces introduced by only a small amount of these chemical compounds to alter friction and wear behavior are clearly shown.

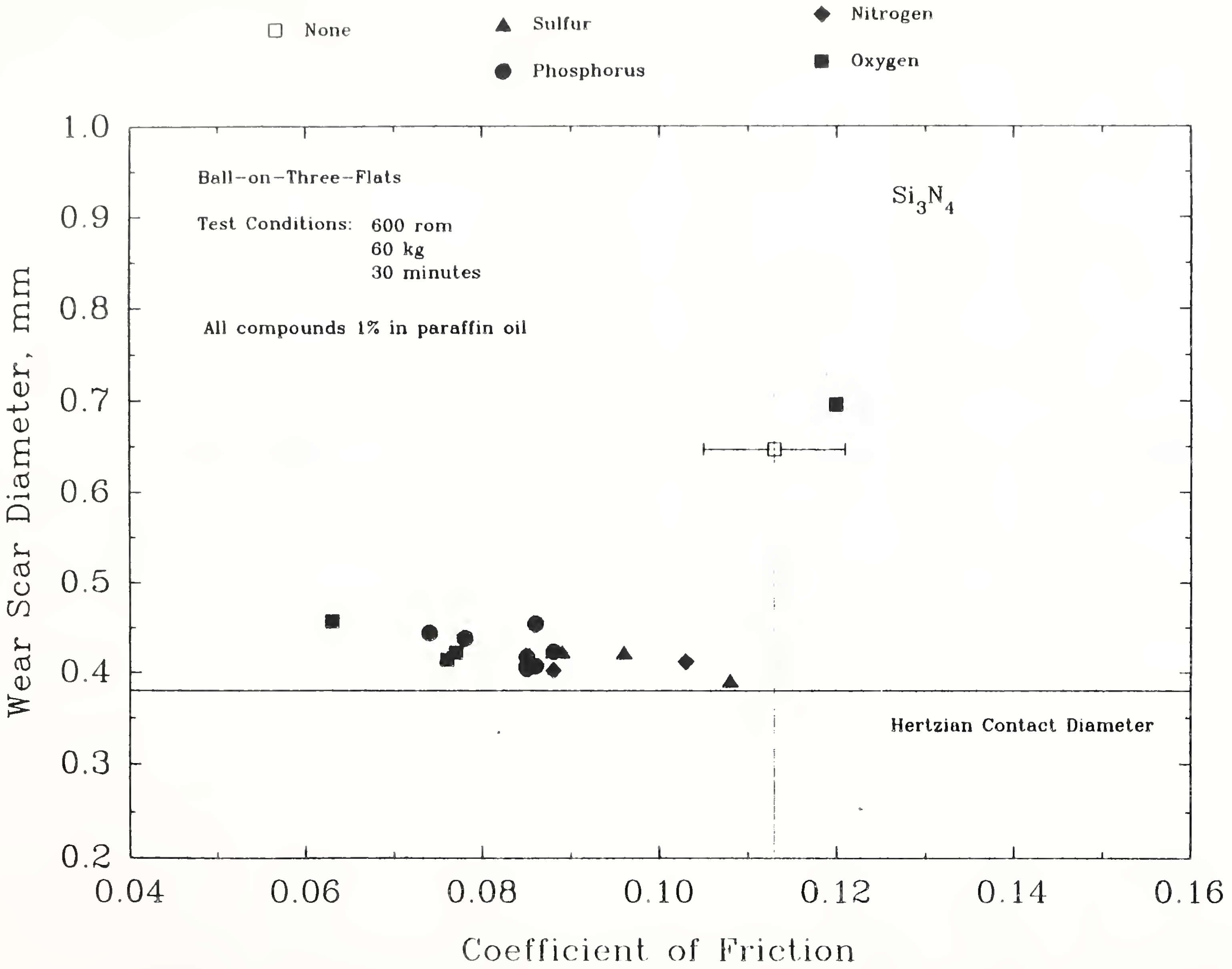

Figure 14. Friction and Wear Evaluations of Si_3N_4.

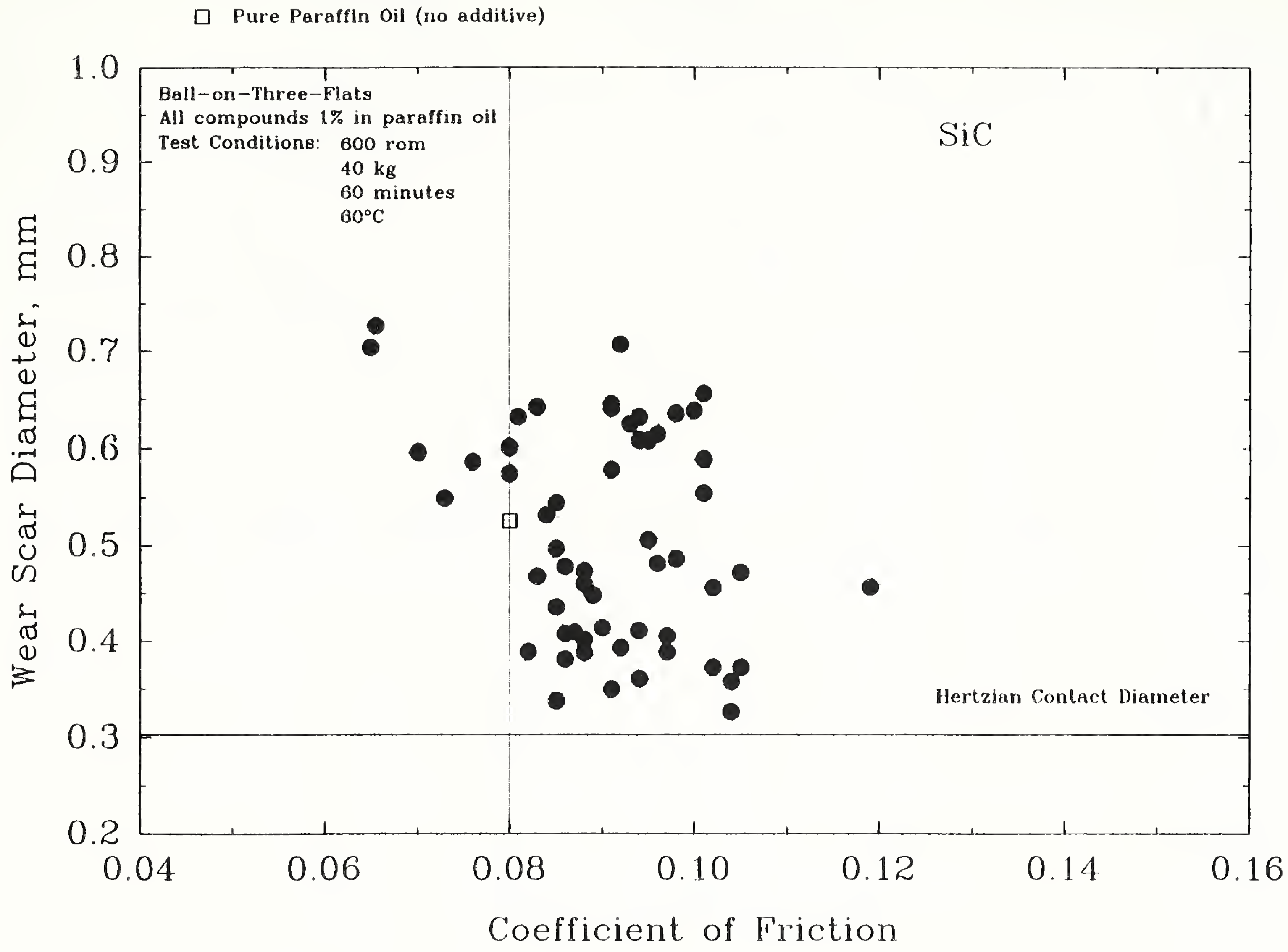

Figure 15. Friction and Wear Evaluations of SiC.

The ability of the ceramics to withstand high temperatures makes them natural candidates for high temperature applications. The additives tested in room temperature have also been evaluated at elevated temperature (200°C). Seven compounds and the PPO base oil were evaluated in both SiC and Si_3N_4 at 200°C. A comparison of the results is shown in Figure 16. The wear index is the ratio of the wear for the compound of interest to the wear obtained for PPO itself. In general, the compounds that result in low wear for one material are also effective for the other. The two exceptions are the chlorine compound that is more effective on SiC and Mo-S-P compound that is more effective on Si_3N_4.

Table 4

Wear Test Condition

	SiC	Si_3N_4
OPERATING CONDITIONS		
Speed (rpm)	600	600
Load (kg)	40	60
Temperature (C)	60	21
Duration (minutes)	60	30
TEST REPEATABILITY		
# of PPO Tests Conducted	3	7
PPO Wear Scar Diameter (mm)		
Range	0.513 - 0.540	0.642 - 0.652
Average	0.526	0.647
σ	0.013	0.004
PPO COF at End of Test		
Range	0.082 - 0.088	0.101 - 0.123
Average	0.084	0.113
σ	0.003	0.008

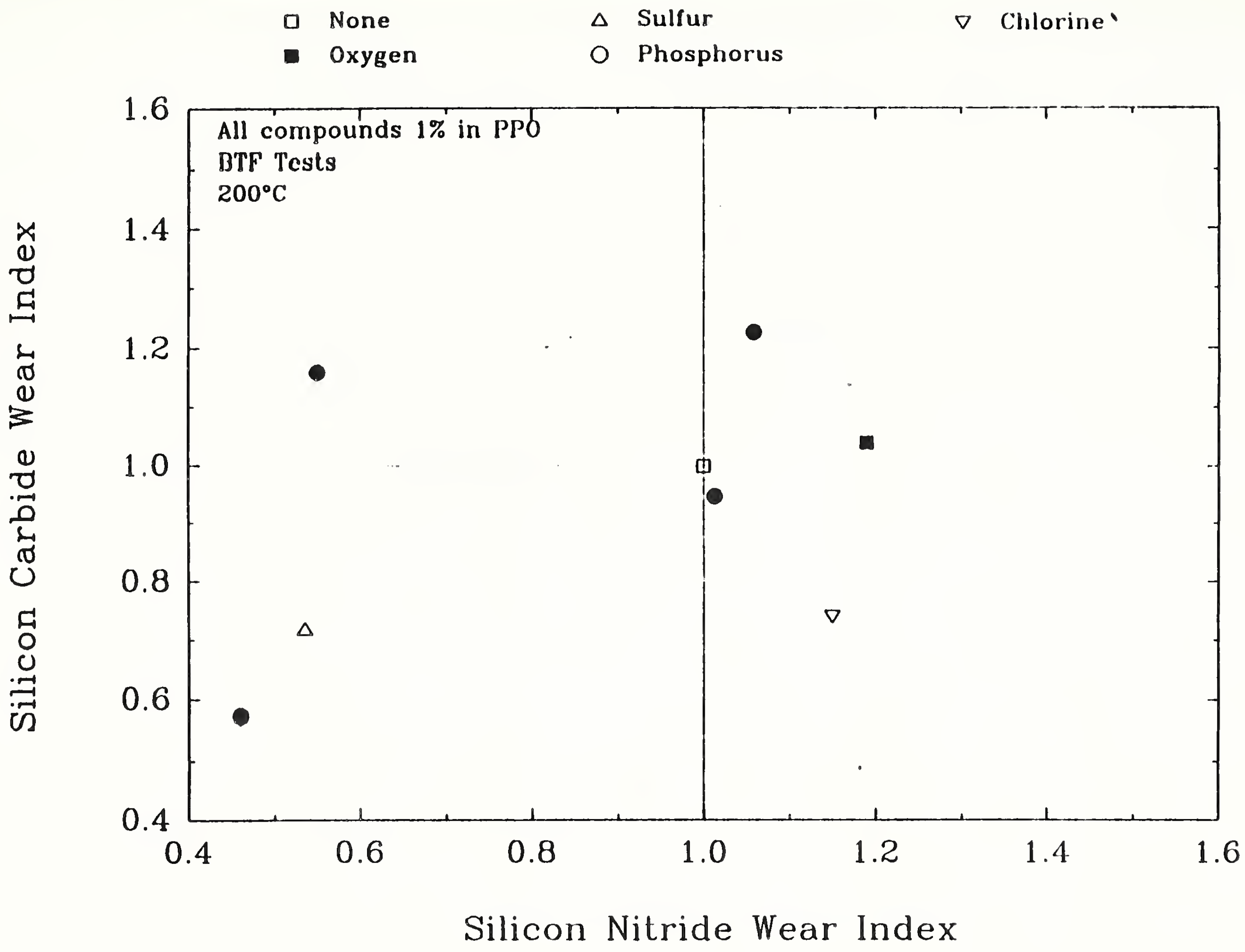

Figure 16. The Comparison of High Temperature Data.

The wear index is defined as the wear scar diameter divided by the PPO wear scar diameter.

FUNCTIONAL CERAMICS

FUNCTIONAL CERAMICS

Overview

Functional ceramics can be defined as those whose primary purpose is in non-load-bearing applications. More specifically, the electrical/electronic, magnetic, optical, properties of ceramics are important for many technical applications. Roughly $3.5B in sales in 1988 by the U.S. ceramics industry were for functional ceramics. The U.S. ceramics industry is aware of the many technological advances produced both in this country and abroad in the area of new materials. The Ceramics Division's program in functional ceramics is structured to assist U.S. industry in assimilating new technology into the manufacture of existing products through the conduct of standards related research which will reduce cost or improve quality and to prepare for the development of new products. The Division's program in functional ceramics works within the technology infrastructure addressing critical issues.

Program Structure

The current Ceramics Division program in functional ceramics involves research in superconducting ceramics, multilayer capacitors, transducers, electronics packaging, ferroelectric films, and diamond films.

In superconducting ceramics a primary need is understanding how the materials can be fabricated into useful components. Divisional efforts emphasize aspects of the processing-structure-properties relationship not apt to be addressed by industry or other government programs. For example, the phase equilibria diagrams for superconducting ceramic systems represent important guidelines to the processor. A significant effort is placed on understanding the relationship between phase equilibria and kinetics in these systems and the current densities attainable in final products.

The program on dielectrics, electronic packaging, and semiconductors reflects the importance of such materials to the electronics industry. The current emphasis is being placed on the mechanical reliability of such components as related to the chemistry and microstructure of the materials. Division scientists work in collaboration with U.S. industry to develop an understanding of this relationship.

The area of photonic materials (optoelectronic and electrooptic) has been recognized as a major growth area. Thus work was begun on developing a system for producing electrooptic materials by metalorganic chemical vapor deposition. In addition, the Ceramics Division in collaboration with the Metallurgy Division has initiated work on the relationship between processing, phase equilibria, and properties of ferroelectric oxide films produced by laser ablation.

Work on diamond thin film technology was occasioned by the recent discovery of ways of producing such films and the realization of the enormous potential of such films in electronic, optical and wear applications. The program in the Ceramics Division involves the use of new characterization techniques to determine the relation of film quality to processing variables.

Nondestructive evaluation techniques primarily affect cost and reliability and are becoming more important as the competitive pressures on the U.S. ceramics industry increase. Work is underway on a number of fronts aimed at developing NDE techniques to detect residual stresses in functional ceramic components as well as to determine the thermal and dielectric properties of materials as a function of location in a component. For example, there is ongoing work on the use of thermal wave approaches for nondestructively characterizing near-surface regions of ceramics.

Finally, a significant effort with respect to reference data is a long-standing cooperative project with the American Ceramic Society (ACerS) aimed at providing the world ceramics community with the most accurate phase diagrams available. In this program, diagrams taken from published literature are evaluated and the results published as volumes in the series Phase Diagrams for Ceramists. This work is described in the standards and Data Activities Section of this report.

Project Listing

Projects comprising the functional ceramics program are as follows:

High Temperature Superconductors:

Thermomechanical Detwinning of Superconducting $YBa_2Cu_3O_{6+x}$
Single Crystals
Crystal Chemistry and Phase Equilibria Studies
Processing High T_c Superconductors
Strength of Superconducting Ceramics
Electrical Properties of High T_c Superconducting Ceramics

Electronic Materials:

Electrostrictive Effects on Crack Growth
Molecular Orbital Calculations of Strained Si-O Bonds
Synchrotron Diffraction Imaging Analysis of Advanced Single Crystals
Advanced Synchrotron Radiation Analysis of Polycrystalline Ceramics
X-ray Imaging for Studies of Interfaces
Cyclic Fatigue of PZT Transducers

Optical Materials:

Diamond Films Processing
Characterization of CVD-Grown Diamond Films
High Pressure Zinc Sulfide Studies
Processing of Lead-Niobate-Titanate for IR Detectors

Significant Accomplishments

- Completed all of the binary and ternary portions of the Sr-Ca-Bi-Cu-O phase equilibrium diagram which contains two superconducting compounds.

- Demonstrated a sharp 106 K transition in Pb-Sr-Ca-Bi-Cu-O superconducting ceramics prepared by a glass-ceramic technique.

- Conducted cyclic fatigue studies on lead zirconate titanate used in high power transducers, which showed that new types of damage can be generated in cyclic loading compared to static tension.

- Developed a procedure for measuring the crystallographic orientation of individual grains in a ceramic in real time using electron back scatter diffraction patterns obtained in an SEM.

- A technique to prepare unsupported transparent films of CVD diamond has been developed. The high transparency and low optical scatter in the infrared and visible regions are correlated with a high nucleation density and low surface roughness of the films.

- Spectral features in the Raman, cathodoluminscence, and photoluminescence spectra of CVD diamond have been found to vary systematically from sample to sample. High quality films are usually associated with an intense and narrow diamond Raman peak, a negligible diamondlike carbon peak, a weak subbandgap excited photoluminescence background, and strong cathodoluminescence signal. This is useful for screening the quality of CVD diamond films.

- Magnetic measurements on $YBa_2Cu_3O_{6+x}$ single crystals have yielded the first direct evidence in any high temperature superconductor of an effect of twin boundaries on flux pinning. Twin boundaries were shown to be weak pinning centers at low temperature (10 K). These results are important in demonstrating that twin boundaries are not effective flux pinning centers in $YBa_2Cu_3O_{6+x}$.

- A new phenomenon of twin domain matching across [001] tilt (grain) boundaries in bicrystals of $YBa_2Cu_3O_{6+x}$ has been discovered. The matching occurs due to a local coordination of the tetragonal to orthorhombic transformation strain across grain boundaries and may be beneficial with regard to electrical transport in highly-textured polycrystalline material.

- Electrical transport measurements across individual grain boundaries have yielded the first evidence that some high-angle boundaries (> 10° misorientation) can transmit significant supercurrents in high magnetic fields at 77K. These results are conceptually important in formulating approaches to develop high temperature superconductors for high-field and bulk-scale applications.

- Completion of a high resolution hard x-ray microscope, which has been tested to detect isolated 0.6 μm wide lines and resolve 1.2 μm wide lines separated by 1.2 μm wide spaces. Images are digitized to provide a basic set of two dimensional images with 1 μm resolution for 3D tomographic image reconstruction.

ELECTRONIC MATERIALS

Stephen Freiman

The Electronic Materials Group performs research in a number of different areas. A major effort is directed toward an understanding of the relationships between processing and properties of the high T_c superconducting ceramics. In this task, we are working closely with personnel throughout NIST as well as in industry and academia. One of the primary research objectives in the superconducting ceramics program is the development of phase equilibria data, leading to phase diagrams for the systems of primary interest. Phase transformations in superconducting and other materials are being investigated in various systems using X-ray diffraction techniques. In related work, there is an ongoing study on the mechanical reliability of piezoelectric components under cyclic loading including possible effects of electric fields on fracture. Preliminary work on the processing of lead niobate-lead titanate ceramics for infrared sensors and in the development of processing and characterization procedures for ferroelectric films has been conducted.

There is an ongoing effort within the Electronic Materials Group aimed toward the development of non-destructive evaluation techniques for ceramics. During this past year, this research has involved the use of thermal wave analysis for the determination of surface damage, the detection of delamination of thin films, and the observation of spatial inhomogeneities in the thermal diffusivity of electronic components.

Finally, during this past year, work was begun on the atomic modeling of ceramic materials using molecular orbital calculations. Initially directed toward a better understanding of the fundamentals of the fracture process in brittle materials, such modeling can also be used to predict properties such as thermal expansion coefficient and elastic modulus.

Molecular Orbital Calculations of Strained Si-O Bonds

G. S. White, W. Wong-Ng and S. W. Freiman

Catastrophic mechanical failure, characteristic of brittle materials, is the most important limitation in the utilization of ceramics in widespread structural applications. The failure process is seriously complicated by the presence of active environments which interact with strained bonds at crack tips, rupturing bonds at stresses below their theoretical strength. This environmentally enhanced fracture extends small cracks in ceramics until they reach critical length, at which point catastrophic failure occurs. While empirically deduced models have been developed to explain observed environmentally enhanced crack growth, no detailed understanding of the processes involved has been obtained. To that end, we have begun using molecular orbital (MO) calculations in an attempt to clarify the electronic interactions involved in bond strain both in the absence and in the presence of an environment.

Using the pyrosilicic molecule previously described (FY89) as a model for vitreous silica, we have concentrated on determining how the bridging Si-O bonds are modified by different strain geometries. Eleven different strain geometries, incorporating different symmetries and varying degrees of strain localization on the critical Si-O bond, were investigated. The strains included both bond lengthening and angle compressions. The results showed that strains highly localized on the critical Si-O bridging bond resulted in the largest positive charge on the Si ion. In addition, when the silica tetrahedra, which were linked through the bridging Si-O-Si bond to form the pyrosilicic molecule, were compressed, the charge on the silica increased substantially. In contrast, the charge on the O-ion, while increased by all of the strain geometries, was increased less when the silica tetrahedra were compressed. The electron overlap population, related to the covalent character of the Si-O bridging bond, decreased greatly with bond strain but was almost completely insensitive to the geometry in which the strain was applied. This result was particularly interesting since it showed that the decrease in electron bond overlap was not compensated by increased charge on the Si and O ions; this suggests that, during strain, electrons are removed from between the Si and O ions and may be available for interactions with an incoming environmental molecule, consistent with the empirical model proposed by Michalske and Freiman.

Cyclic Loading of PZT

G. S. White, A. S. Raynes and S. W. Freiman

Crack growth behavior during cyclic loading of polycrystalline ceramics is now recognized as a critical area of research; while some of the behavior observed during cyclic loading can be related to behavior observed in traditional mechanical properties tests, some is directly the result of the cyclic aspect of the loading. Effects of cyclic loading become more important when the material under investigation is intended to be loaded cyclically in practical applications: e.g., piezoelectric materials. One consequence of cyclic loading, particularly if the loading is at resonance frequency, is elevated temperature. We have investigated temperature effects on the fracture behavior of cyclically loaded PZT this past year to determine if crack growth behavior during cyclic loading (reported in FY89) was merely environmentally enhanced fracture or was a direct result of cyclic loading.

Specimens were driven at resonance frequency at temperatures between room temperature (RT) and 80 °C (low temperature) and between RT and 200 °C (high temperature) and crack lengths from indentation cracks were monitored as a function of cumulative excitation time. Crack growth did not occur in the low temperature specimens for times up to 20 minutes. After 20 minutes, the specimens were allowed to warm up; at ≈100 °C, catastrophic failure occurred. In contrast, high temperature specimens exhibited substantial crack growth (hundreds of micrometers) and underwent excitation times of hours before failure. These results suggest that, at low temperatures, some sort of damage accumulation was occuring that, upon elevation of the temperature, resulted in immediate failure but that, at high temperature, this damage mechanism was less important. Dynamic fatigue measurements at RT and 150 °C indicated that, at RT, environmentally enhanced fracture took place but that, at 150 °C, the specimens were no longer susceptible to environmentally enhanced crack growth. Therefore, the crack growth observed in the cyclically loaded, high temperature specimens cannot be attributed to environmentally enhanced crack growth. Presently, identification of the low temperature damage and the mechanism for high temperature crack extension in the cyclically loaded specimens remains undetermined.

Superconducting Ceramic: Crystal Chemistry and Phase Equilibria Studies

W. Wong-Ng, L. P. Cook, M. Hill, J. Stalick[1], E. R. Fuller Jr. and B. Paretzkin

[1]Reactor Radiation Division

The Ba-R-Cu-O systems

Our previous studies of the $BaO(BaCO_3)$-R_2O_3-CuO systems, where R=lanthanides and yttrium, showed two important factors, namely, the progressively decreasing size of the lanthanides, known as the lanthanide contraction, as well as the role which the stability of different oxidation states of these elements plays in governing compound formation. In the past year we continued our efforts to systematically investigate the effect of the above two factors, in particular the size factor, on the trend of phase formation and solid solution formation of selected binary and ternary compounds in the BaO-R_2O_3-CuO systems, the trend of phase diagrams, as well as the trend of the structural phase transformation between the orthorhombic and tetragonal phases of the superconductor material, $Ba_2RCu_3O_{6+x}$.

Phase Diagrams

The phase equilibrium study of the pseudoternary $BaO(BaCO_3)$-Nd_2O_3-CuO system near the Nd_2O_3 and CuO corners showed two series of solid solutions. A neutron diffraction study of the end members of this series, the 1:2:1 $BaNd_2CuO_5$ composition (the brown phase) showed that the square-planar CuO_4 groups are isolated in the structure which presumably precludes the possibility of superconductivity in this material. A study of the equilibrium between CuO and Nd_2O_3 provided the fundamental phase relationship for the characterization of the parent compound Nd_2CuO_4 of the electron superconductor $(Nd,Ce)_2CuO_4$. Due to the reduction of CuO at higher temperature, the Nd_2O_3-CuO system is more accurately represented as a ternary system of Nd_2O_3-CuO-O. Selected equilibria in this ternary system as well as the projected phase equilibria on the non-binary join Nd_2O_3-CuO have been investigated.

Solid Solution Studies

In an effort to find a processing tolerent region for synthsis of 2:1:3 superconductors, a triangular section of the Y_2O_3-Gd_2O_3-BaO-CuO system was examined to determine the single phase region and the effect of compositon upon the superconducting properties of samples made from specially selected compositions in this system. In the Gd 2:1:3 compound, a solid solution region exists where up to 20 atomic percent of Ba may be substituted with Gd. The compositional limit of solid solubility was found at $Ba_{1.8}Gd_{1.2}Cu_3O_{6+x}$. This composition, along with the composition of the stoichiometric Gd 2:1:3 compound and the stoichiometric Y 2:1:3 compound were the vertices of the triangle of compostions selected in the Y_2O_3-Gd_2O_3-BaO-CuO quaternary system. An examination of AC susceptibility and transport critical current density reveals that as the lanthanide ion is substituted for Ba, the transport current at 77 K and the T_c fall off dramatically. On the $Ba_2(Y,Gd)\ Cu_3O_{6+x}$ solid solution region the transport current is a maximum and the T_c for these samples is at 90 K.

The influence of the size of R on melting relations of $Ba_2RCu_3O_{6+x}$, where R=Y, Eu and Nd has been studied and compared with that of a high T_c superconductor mixed-lanthanide phase $Ba_2(Y_{.75}Eu_{.125}Nd_{.125})Cu_3O_{6+x}$. SEM micrographs of these samples showed the progressive features of the microstructures from sintering, grain growth through melting and then recrystallization from the melt.

Trend of Phase Formation

The investigation of the crystal chemistry and the preparation of the x-ray reference patterns of the binary series with composition, $BaO:R_2O_3$ have been completed. The compounds BaR_2O_4, where R=La, Nd, Sm, Gd, Eu, Ho, Y and Er are isostructural. Neutron diffraction analysis of $BaNd_2O_4$ indicated the structure of be the pervoskite-related $CaFe_2O_4$ type. When the size of R is small (R=Tm, Lu abnd Yb), a mixture of $Ba_3R_4O_9$ and unreacted oxides were obtained instead, indicating again, the importance of the size factor in governing the formation of BaR_2O_4. Under the same experimental conditions, the compound $BaRO_3$ was the predominant component when R=Ce, Pr and Tb.

Phase Transformation

Current efforts in the phase transformation studies have been concentrated on the $Ba_2NdCu_3O_{6+x}$ series. The orthorhombic to tetragonal transformation temperature has been found to occur at a relatively low temperature of ≈550-575°C. Again, the size factor has been found to have a marked effect on this temperature. Among the six series of superconductor materials, $Ba_2RCu_3O_{6+x}$, where R=Nd, Sm, Gd, Ho, Y, and Er we have investigated, a definite trend was observed; the smaller the size of R, the higher the tetragonal-orthorhombic transformation temperature. Also, the superconducting properties, viz. the T_c values, are less sensitive to the oxygen content for materials with smaller ionic radius.

Tl-Ca-Ba-Cu-O System

For experiments with thallium, a dedicated laboratory was essential. Previous experience with corrosive metals and salts led to the design and construction of a glovebox-enclosed high temperature apparatus utilizing MgO as the primary containment material; the apparatus has functioned well and has permitted the systematic gathering of vapor transport and quench/anneal data safely without contamination. Using this apparatus, our experiments have confirmed the existence of substantial solid solution in the 2122 phase, and an apparent correlation with variation in T_c, which has major implications for materials processing. It is essential to know if thallia materials are truly stable or simply metastable, transient phases. It appears that the 2122 has actual long term stability under oxidizing conditions, based on our experiments, meaning that processing routes can be designed to include lengthy anneals for improvement of properties, if desired.

Crack Growth in Superconducting Single Crystal YBCO

A. S. Raynes, S. W. Freiman, D. L. Kaiser and F. W. Gayle[1]

[1]Metallurgy Division

An understanding of the basic mechanical properties of superconducting YBCO ceramics is an important step towards dictating their potential uses. In this study, crack morphologies were compared for twinned crystals versus detwinned crystals, for different crystal orientations, and in the presence of moisture.

Single crystals were grown from Y-Ba-Cu-O melts. Typical crystal dimensions were 100-300 μm in the a/b directions and 80-120 μm in the c-direction. The as-grown crystals were annealed in oxygen at 420°C for 80 h., a treatment which yields sharp superconducting transitions at onset temperatures of 92-93 K. As-grown crystals exhibited characteristic {110} twin planes which formed during cooling through the tetragonal-to-orthorhombic phase transition. In an effort to determine if the twin plane structure acts to toughen the crystals, selected crystals were detwinned by applying a uniaxial pressure of 140 MPa along one of the a/b directions at 420°C for 10 h. Twinned and detwinned crystals were mounted on glass slides with a thin layer of epoxy in preparation for micro-indentation studies using applied loads of .25 to 1 Newton.

Results of past studies on $BaTiO_3$ have shown higher fracture toughness values for twinned than untwinned $BaTiO_3$. This increase has been attributed to crack interactions with the twins formed during the cubic to tetragonal phase transition. Our results indicate likewise that twinned YBCO has a higher fracture toughness than detwinned YBCO, since crack lengths in detwinned crystals were greater than those in twinned crystals.

A comparison of crack morphologies on the a/b and c faces of twinned crystals showed radial cracks with some lateral cracking evident at the surface on a majority of the a/b face indentations, but little or no lateral cracking on C-face indentations at the same applied load. In addition, crack length was not dependent upon indentation orientation on the a/b face, but was for the c-face, with cracks parallel to twin boundaries consistently shorter than those perpendicular to the twin boundaries. Finally, the YBCO single crystals were seen to exhibit moisture enhanced slow crack growth when indented in distilled water.

Phase Equilibria

R. S. Roth, C. Rawn, J. J. Ritter, J. Cline and C. Bayracki

Studies in the system Ba-Y-Cu-O on chemical preparations and high-temperature X-ray diffraction have been confined to mixed gas atmospheric conditions varying from pure N_2 to pure O_2 and including solid state synthesis in O_2 from 1-10 atmospheres. The phase $Ba_2Cu_3O_{5+x}$ was easily synthesized in 1 atm O_2 and the join Y_2O_3-$Ba_2Cu_3O_{5+x}$ was found to be the equilibrium condition at 1 atm. O_2 for the 2:1:3 composition at 700°C. The 2:1:4 and 4:3:7 phases were also synthesized establishing the subsolidus diagram for 2:1:3-CuO in 1 atm O_2. Reversible non stoichiometry in BaO_{2-x} was characterized and the transition to BaO studied by quenching and Differential Thermogravimetric Analysis methods. Several new phases in the system Ba-Au-O were also synthesized.

Phase equilibria diagrams for the relevant binary and ternary systems have been established for the four component system SrO-CaO-Bi_2O_3-CuO. Complete melting relations for CaO-Bi_2O_3, SrO-Bi_2O_5, CaO-CuO and SrO-CuO have been studied and published. Crystal structure analyses in collaboration with A.I. DuPont de Nemours scientists have been completed for $Ca_4Bi_6O_{13}$, $Ca_2Bi_2O_5$ and $Sr_2Bi_2O_5$. The ternary phase diagram for the system SrO-Bi_2O_3-CuO has been established and published, CaO-Bi_2O_3-CuO and SrO-CaO-Bi_2O_3, have been completed and await publication. Analysis of the binary phases have elucidated very strange 3, 4 and 5 coordinated Bi-O polyhedra and further analyses of other phases should be of great help in formulating theories for the proper coordination of the Bi^{+3} ions in the incommensurate Cu-containing superconductors. Ongoing studies in the four component system have shown that the ~ 80K superconductor has only a very small stoichiometry field near the 3:3:3:4 composition and is never single phase at the ideal 2:1:2:2 composition. Further studies in the four component system are proceeding.

Processing High T_c Superconductors

J. E. Blendell, M. D. Hill, E. R. Fuller, Jr., M. D. Vaudin, C. K. Chiang and S. W. Freiman

The effort in this area has centered on determining optimum processing conditions for bulk components of oxide superconductors, particulary those in the Ba-R-Cu-O system, where R is yttrium or a rare earth. The property of particular interest has been the critical current density, J_c, since the current carrying capacity of these new materials will determine their economic competitiveness in the marketplace.

This research on improved properties for bulk superconducting ceramic materials, through microstructure control involved all stages of the processing. We have found that the grain size and shape could be controlled by the atmosphere, temperature and time during sintering. At low oxygen partial pressures and low temperatures, fine grained material was produced. At higher temperatures, coarse grained material was produced and the grains were elongated. The elongation was in the a and b axis directions, with large basal facets developed. The elongation was due to the presence of liquid phases.

We have found that equiaxed fine grained materials have significantly higher J_c (factor of 2 to 3) than elongated coarse grained materials. If a liquid phase occurred, either due to impurities or the peritectic temperature being exceeded during processing, J_c was greatly reduced. It turns out this liquid phase is detrimental for two reasons: the formation of S-N-S junctions (superconducting-normal-superconducting) and the limiting of the diffusion of oxygen into the sample during low temperature oxidation.

The measured oxygen tracer diffusion coefficients in single crystals are very high for a ceramic material at low temperatures. Our preliminary measurements on bulk samples indicate that similiar values are obtained. However, many bulk samples can not be oxidized even by prolonged annealing times. Such samples have usually been processed at relativly high temperatures in order to increase the density, but this results in the formation of a liquid phase which then limits the oxygenation.

We have also studied melt processing of $Ba_2YCu_3O_{6+x}$. The formation of bulk samples by melt processing has yielded samples which have very high flux pinning. It is known that the J_c of $Ba_2YCu_3O_{6+x}$ is limited by two effects, weak links and flux creep. Understanding of the effect of microstructure on J_c involves both these effects, but the separation of these effects is difficult. Weak links, such as grain boundaries, cracks, etc are affected by the magnetic fields. For zero field (no self field/no current flow) there would be no flux creep, but there would still be weak links. As the field increases, additional weak links are formed and flux creep occurs, both of which reduce J_c.

Samples were produced by rapidly heating $Ba_2YCu_3O_{6+x}$ powders to 1450°C, where the phases present are Y_2O_3 and liquid. Due to the reactivity of the liquid, the time at temperature was very short. The sample was then quenched to room temperature. Subsequently, the sample was heated and slowly cooled through the peritectic temperature in order to grow large grains of $Ba_2YCu_3O_{6+x}$. These large grains were removed from the matrix and the properties were measured. High flux pinning was measured within these large grains.

OPTICAL MATERIALS

Albert Feldman

The objectives of the Optical Materials Group are to provide data, measurement methods, standards and reference materials, concepts, evaluated data, and other technical information on the fundamental aspects of processing, structure, properties and performance of optical and optoelectronic materials for industry, government agencies, universities, and other scientific organizations. The program supports generic technologies in crystalline, glassy, and thin film inorganic optical materials in order to foster their safe, efficient and economical use. Research in the group addresses the science base underlying new advanced optical materials technologies together with associated measurement methodology.

The effort of the Optical Materials Group has been directed into three principal areas: diamond film processing and characterization, metallorganic chemical vapor deposition (CVD) of ferroelectric oxides, and single-crystal high-temperature superconducting ceramics.

Diamond Films

Optical and optoelectronic characterization of CVD diamond films

L. H. Robins, E. N. Farabaugh, A. Feldman and L. P. Cook

Diamond is a promising material for optical and optoelectronic applications because of its optical transparency throughout a wide spectral range and its high degree of resistance to mechanical and thermal damage. The development of diamond chemical vapor deposition (CVD) at low pressure has renewed interest in diamond optics. Some proposed applications are: wear-resistant optical coatings; anti-reflection coatings for silicon or germanium infrared windows; blue-emitting electroluminescent devices; and high-speed ultraviolet and x-ray photodetectors. The goal of our research is to obtain information about the relationships between deposition process conditions, structure, and optical and optoelectronic properties of CVD diamond films. This information may then suggest ways to optimize the properties for particular applications. We are especially interested in learning how the optical and optoelectronic properties are affected by film morphology and by imperfections, such as lattice defects, chemical impurities, non-diamond phases, and grain boundaries.

The characterization techniques used in this work are: cathodoluminescence (CL) imaging and spectroscopy in an SEM; photoluminescence (PL) and photoluminescence excitation (PLE) spectroscopies; Raman scattering spectroscopy; and optical transmittance and reflectance spectrophotometry. Luminescence spectroscopy (either CL or PL) is sensitive to certain types of defects and impurities. Use of the SEM for the CL experiment allows us to map the spatial distribution of luminescence centers with sub-μm resolution and to compare CL and electron-emission images of the same sample. PL provides similar information to CL, but in PL the excitation photon energy can be tuned to selectively excite particular centers. Raman spectroscopy probes structure and chemical bonding, especially deviations from the diamond type of carbon bonding. Transmittance and reflectance are sensitive to optical absorption by imperfections and to light scattering from surfaces and interfaces.

Several interesting relationships were found in a comparative study of Raman, PL and CL spectra of a set of 48 diamond films. The films which showed the most (or least) intense Raman scattering from non-diamond forms of carbon also showed the broadest (or narrowest) diamond Raman line, the most (or least) intense luminescence under excitation by visible light, and the least (or most) intense luminescence under excitation by an electron beam or by above-bandgap ultraviolet light. The sample-to-sample variations of the visible-excited PL intensity and of the diamond Raman linewidth are compared in Figure 17a. These results suggest that an increase in non-diamond carbon content correlates with a decrease in crystalline order and with an increase in the absorption of visible light (which is indicated by the increase in visible-excited PL intensity).

Optical scatter due to surface roughness has hindered the development of diamond-film optical windows and coatings. We successfully reduced surface roughness in diamond films by increasing the initial diamond nucleation density. This was accomplished by carefully polishing the substrate with 1/8th μm diamond powder. Diamond optical coatings on silicon were characterized by reflectance spectroscopy. Diamond windows, prepared by etching away the silicon substrate, were characterized by transmittance and by reflectance from the top (free) and bottom (substrate) surfaces. Transmittance and reflectance spectra of a sub-μm thick diamond window are shown in Figure 17b. The optical measurements were correlated with stylus and scanning tunneling microscope (STM) measurements of surface roughness. It was found that the roughness of the top surface is a minimum of 0.03μm (rms value for a 0.44μm thick film) and increases with increasing film thickness; the roughness of the bottom surface is significantly lower.

A CVD diamond specimen containing large ($\approx$30μm diameter) single-crystal particles, grown at relatively low nominal substrate temperature ($\approx$600°C), was characterized by spectrally resolved CL imaging. The most intense component of the CL spectrum of this specimen, a red band attributed to nitrogen-vacancy centers, was found to be associated with {111} crystal growth sectors. The other intense component, a violet band attributed to donor-acceptor pairs, was associated with both {111} and {100} sectors. Previous observations of specimens grown at higher substrate temperature showed that both of the intense CL bands are associated with {100} growth sectors. The spatial distribution of CL centers we have observed thus shows more varied behavior than observed previously.

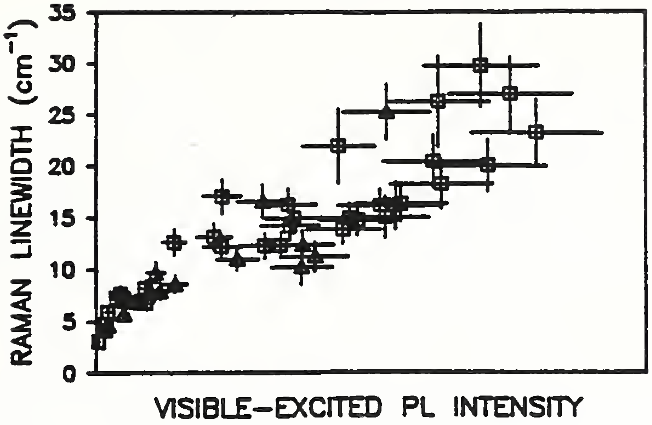

Figure 17a. Sample-to-sample variation, within a set of 48 CVD diamond films, of the visible-excited PL intensity and of the diamond Raman linewidth. Squares represent films grown by hot-filament CVD and triangles represent films grown by microwave-plasma CVD.

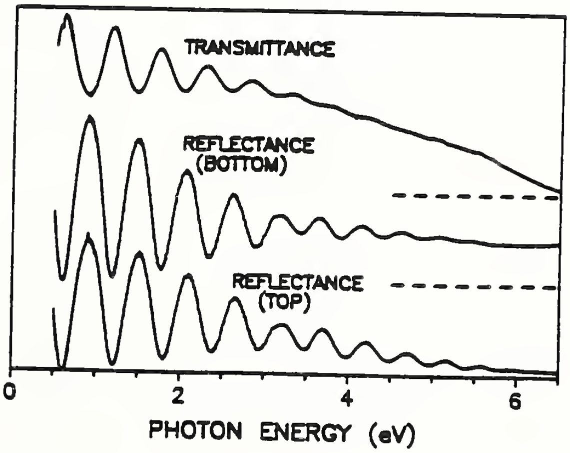

Figure 17b. Spectra of optical transmittance, reflectance from bottom (substrate) surface, and reflectance from top (free) surface, for 0.44 μm thick CVD diamond window prepared by etching of the silicon substrate. Dashed horizontal lines indicate zero offsets for upper two spectra.

Diamond Film Growth

E. N. Farabaugh, L. H. Robins and A. Feldman

Diamond films have been produced during the past year to generate samples for studies of growth rate, cathodoluminescence, thermal diffusivity, Raman spectroscopy and high resolution transmission electron microscopy. A new microwave deposition system was placed in operation this year, so that the specimens were prepared both by microwave assisted chemical vapor deposition (CVD) and hot filament CVD.

The influence of the filament geometry on growth in a hot filament CVD reactor was examined. Growth rate was determined both by weighing substrates before and after deposition and morphological data were obtained from SEM micrographs. The specimens were prepared on silicon wafer substrates in a chamber using single and dual W filaments containing 5, 10 and 15 turns and feed gas compositions ranging from 0.25% to 1.00% $CH_4:H_2$. The influence of the feed gas input position on film growth was also examined.

In a single filament process, the film growth rate increased nearly linearly with the number of turns, other deposition conditions being the same. (See Figure 18a). The films growth also increased with number of turns in a dual filament system but the increased growth rate was not as dramatic except for the case of the five turn filaments. Figure 18b displays the growth rates for a single 5 turn filament and for dual 5 turn filaments for different fractions of CH_4 in the feed gas. The maximum growth rate was 0.36 μm/hr. The explanation for the observations are as follows: Increasing the number of turns increases the reactive area of the filament which serves to increase the amount of atomic hydrogen and reactive hydrocarbon species. This results in increasing the deposition rate. However, in the case of the dual filament we believe that the increased reaction rates act to deplete the local concentrations of methane, a saturation effect which limits the growth rate, although the coverage is double that of the single filament. Evidence to support this premise is the observation of dual filament deposition morphologies typical of single filament morphologies obtained at lower methane concentrations, mentioned below.

The use of dual filaments enabled film growth on substrates areas up to 4cm^2 (double the area for single filament growth). The films showed uniform morphology and thickness. Changes in morphology related to the concentration of CH_4 in the feed gas mixture and filament geometry have also been seen. {111} faceting appears at lowest CH_4 concentrations while {100} faceting predominates at the highest CH_4 fraction (1%). From morphology and growth rate measurements, it appears that dual 15 turn filaments produce morphologies typical of the lower CH_4 concentrations even though higher concentration were used.

Growth rates did not change by changing the shape of the feed gas tube opening; however the growth rate decreased by a small amount when the feed gas entered the chamber far from the filament. Feed gas flow directed over the filament and normal to the substrate was found to give the highest growth rates.

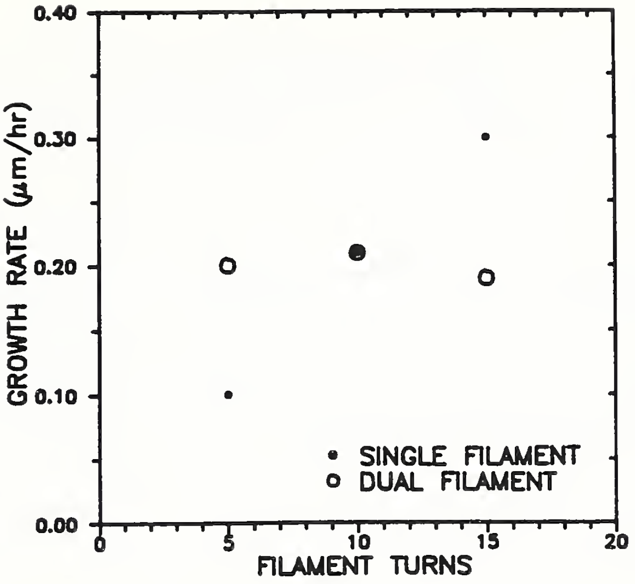

Figure 18a. Growth rate vs. number of filament turns for depositions in a hot filament reactor with single filaments and dual filaments. The nominal substrate temperature was 750°C and the methane fraction was 0.5%.

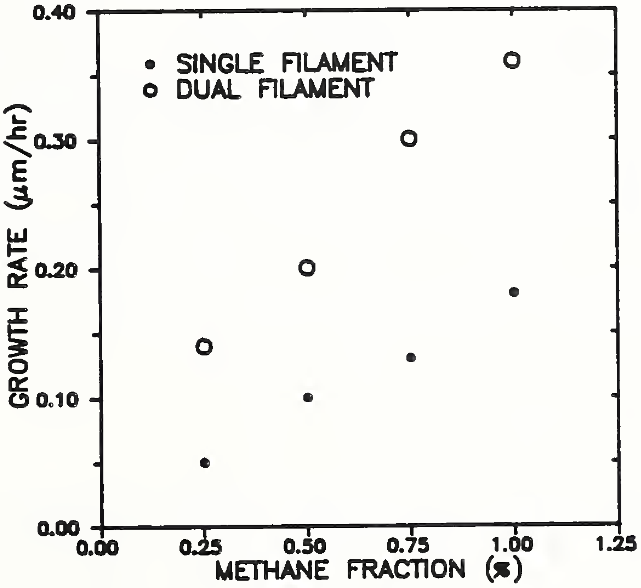

Figure 18b. Growth rate vs. % methane for depositions in a hot filament reactor containing single 5 turn filaments and containing dual 5 turn filaments. The nominal substrate temperature was 750°C.

Modelling Thermal Wave Propagation In Diamond Films

A. Feldman, H. P. R. Frederikse[1] and S. J. Norton[2]

[1] Consultant to NIST
[2] Metallurgy Division

The high thermal conductivity of diamond make it an attractive material for heat dissipation applications such as substrates for high density electronics. In order to evaluate the quality of CVD diamond for such applications convenient noncontact methods are desirable for measuring the thermal conductivity of diamond both as a thin film and as a thick coating. We have been investigating photothermal radiometry (PTR), a thermal wave technique, as a method for determining the thermal conductivity of CVD diamond. In this report, we discuss a theoretical analysis of photothermal radiometry which makes it possible to calculate the thermal diffusivities. A diagram of the PTR experiment is shown in Figure 19.

Previously, we had reported on the interpretation of PTR measurements by means of a one dimensional (1D) thermal wave analysis. In this report we present the results of a three dimensional (3D) thermal wave analysis. The analysis takes into account the finite size of the heating beam, r_0, the thickness of the film, w, the presence of air above the film, the substrate material, and the detector size.

The complex temperature, consisting of a real part T_r and an imaginary part T_i, is obtained by solving the heat diffusion equation for a coating on a substrate in air, heated at frequency, f, by a laser beam with a gaussian beam profile of 1/e radius, r_0. It is assumed that the heating occurs at the top surface of the film. The PTR signal is an average of the temperature over the region of the specimen surface that corresponds to the image of the infrared detector projected onto the specimen surface by the infrared focussing lens. We are interested in the phase of this signal, $\phi = -\tan^{-1}(T_i/T_r)$, as a function of $\sqrt{f}$.

ϕ has been obtained numerically for a variety of film configurations and the results have been compared with the results of the 1D solution. Figure 20 compares 1D and 3D solutions with different values of r_0 for a diamond film in vacuum .

The conclusions regarding use of the PTR method are:

> PTR is a noncontact method to measure the thermal diffusivity of diamond coatings; however; a black coating is needed to enhance absorptivity and emissivity at the specimen surface. A thin graphite coating ($<1\mu m$ thick) on a bulk diamond has a small effect on ϕ; however, the effect of a graphite coating on a diamond film is yet to be determined.
>
> The 1D analysis does not describe experimental data adequately especially when $w \geq r_0$. The 3D analysis must be used to analyze the experimental data. One dimensional treatment may be used at high frequencies when $w \ll r_0$. However, the 3D analysis is needed to verify the results.

In order to obtain detectable signals with reasonable signal to noise, we require a finite sized heating source necessitating the use of the 3D analysis. The heating beam diameter should be as large as possible in order to minimize effects of detector misalignment.

The experimental geometry must be experimentally defined: the heating beam dimensions must be measured, the specimen surface should be accurately focussed on the detector plane, and the magnification of the specimen image on the detector plane should be known.

Effects of air can usually be ignored for diamond films >10μm thick.

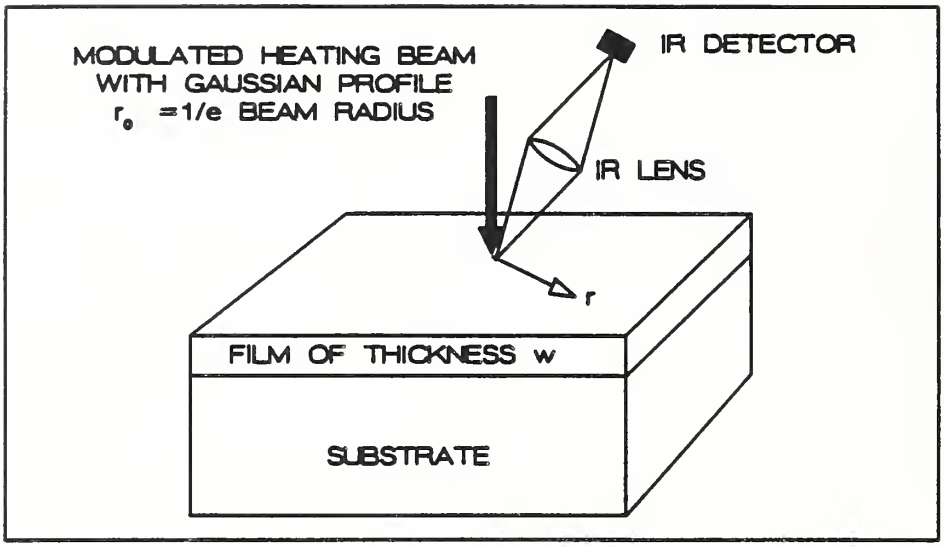

Figure 19. Schematic diagram of the photothermal radiometry experiment.

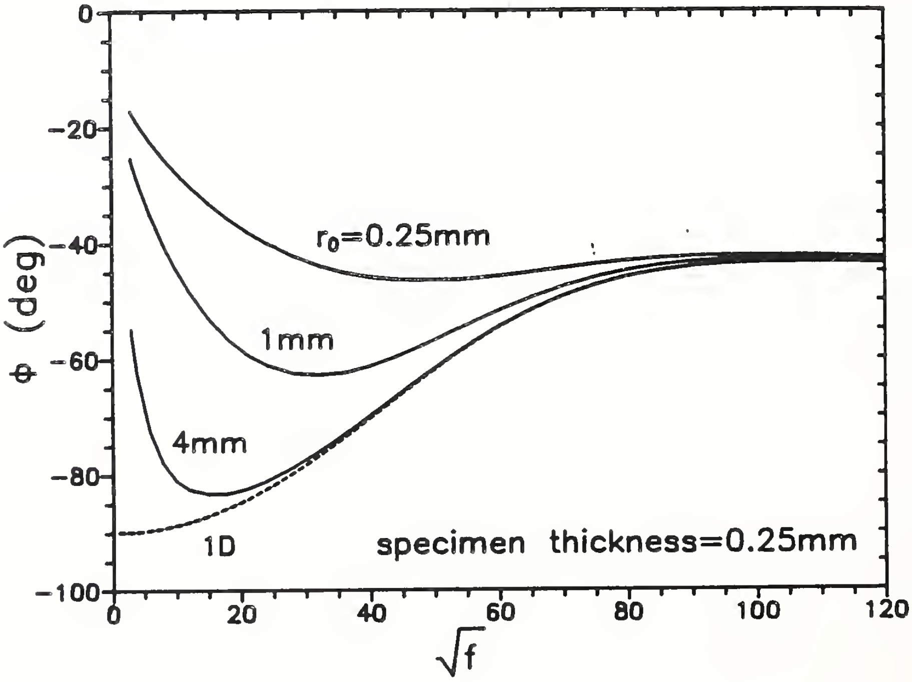

Figure 20. Plot of phase vs. square root of frequency based on 1D (dashed line) and 3D (solid lines) thermal wave calculations for a diamond film in vacuum with the a given specimen thickness, w and beam radii, r_0, shown on the figure. The detector size is assumed to be 1mm in diameter.

Superconducting $YBa_2Cu_3O_{6+x}$ Crystals

Detwinned and Twinned Single $YBa_2Cu_3O_{6+x}$ Superconductor Crystals

D. L. Kaiser, F. W. Gayle[1], L. J. Swartzendruber[1], A. Roitburd[2], L. H. Bennett[1], S. F. Watkins[3], F. R. Fronczek[3], J. S. Wallace, G. Gillen[4], A. Raynes and S. Freiman

[1]Metallurgy Division
[2]University of Maryland, College Park, MD
[3]Louisiana State University, Baton Rouge, LA
[4]Center for Analytical Chemistry

The development of a thermomechanical process for detwinning $YBa_2Cu_3O_{6+x}$ single crystals in FY89 has presented opportunities for numerous characterization studies. Comparative investigations on twinned and detwinned crystals were conducted to elucidate the effect of twin boundaries on properties and to determine anisotropy of properties. Magnetic measurements have yielded the first direct evidence in any high temperature superconductor of an effect of twin boundaries on flux pinning. Furthermore, twin boundaries were shown to be weak pinning centers at low temperature (10 K). Mechanical measurements on twinned crystals have revealed that indentation cracks propagating perpendicular to the c-axis are 1.5-2.0 times as long as those running parallel to the c-axis, suggesting a significant anisotropy in fracture toughness. Fracture toughness in twinned crystals was approximately 20% higher than in detwinned crystals, indicating that twin boundaries act as toughening defects. Oxygen diffusivity measurements on twinned crystals support the results of an earlier study (Argonne National Laboratory) which demonstrated a large anisotropy in diffusion between the a/b and c-directions. Structure determination studies on a detwinned crystal with a superconducting transition temperature (T_c) of 89 K have revealed that the oxygen atoms in the O(4) chain sites are offset from the crystallographic b-axis, leading to zig-zag rather than linear Cu-O chains. The results of these characterization studies may be useful in applications development and in understanding the mechanism of high temperature superconductivity.

$YBa_2Cu_3O_{6+x}$ Superconductor Bicrystals

D. L. Kaiser, F. W. Gayle[1], L. C. Smith[1], M. D. Vaudin, S. E. Babcock[2], X. Y. Cai[2] and D. C. Larbalestier[2]

[1]Metallurgy Division
[2]University of Wisconsin, Madison, WI

The role of grain boundaries in electrical transport in polycrystalline samples of the high temperature superconductor $YBa_2Cu_3O_{6+x}$ (YBCO) is not well defined although an understanding of this role is a key element to the application of these materials. In this program, well-defined grain boundaries in bulk-scale multi-crystals have been employed to: (1) characterize the nature of one class of grain boundaries and (2) perform electrical transport measurements across single boundaries of known orientation.

In phase I of this program, facetted grain boundary segments in multi-crystals having nearly coincident c-axes ([001] tilt boundaries) were characterized by optical microscopy techniques. Grain boundary orientations were widely distributed, with a slight favoring of {110}, {310} and {510} boundary planes. All grain boundaries, except those far from the symmetric condition and those with {110} facets, exhibited well-developed matching of the twin domains across the boundary. It is suggested that this newly-reported phenomenon of twin pattern matching occurs due to a local coordination of the tetragonal to orthorhombic transformation strain across grain boundaries and may be beneficial with regard to electrical transport in highly-textured polycrystalline material.

In phase II of this program, electrical transport measurements across single grain boundaries have yielded the first evidence that some high-angle (> 10° misorientation) boundaries do not display Josephson Junction weak-link character and can transmit significant supercurrents in high magnetic fields at 77K. These results are conceptually important in formulating approaches to develop high temperature superconductors for high-field and bulk-scale applications.

High resolution X-ray imaging with synchrotron radiation is being developed on NIST/MSEL beamline X23A3 at NSLS. The sample is illuminated by nearly parallel radiation from a double flat crystal monochromator using symmetrically cut crystals. The sample image, which may be radiographic of topographic, is magnified in two dimensions by extremely asymmetric diffraction from two flat crystals. Magnification factors over 100 have been achieved. The magnified image is detected by an X-ray sensitive charge coupled device (CCD) area detector with 20 micron square pixels. Thus, submicron sample features may conceivably be resolved.

High Resolution Hard X-Ray Microscope

R. C. Dobbyn, R. D. Spal, H. E. Burdette and M. Kuriyama

Materials failures are often attributed, for example, to residual stresses that may have been produced during fabrication processes. Residual stresses can be measured in some cases with limited precision. However, those are normally represented by an average value over the entire specimen or in a rather large volume. Materials failure happens at local catastrophic events. In microelectronic devices, where different atoms are doped into mutually coherent layers or three-dimensional quantum wells, the thickness and shape of doped regions may change so as to degrade the functional properties originally designed. What we need is a measurement technique to "see" what happens locally and pinpoint local events of significance with high spatial resolution. Once we recognize such local phenomena, we can devise methods to accurately measure physical quantities which are necessary and meaningful in relation to each local event.

One such measurement technique using x-ray imaging for detection of microstructural flaws and defects was developed this year; that is the construction of a high resolution hard x-ray microscope. The combination of a charge-coupled device (CCD) area detector and an x-ray image magnification technique has made it possible to create the high resolution x-ray microscope with less than 1 μm resolution. There are two unique concepts that are essential for the realization of the x-ray microscope: (a) x-ray sensitive direct imaging should be used, that is, the direct conversion of x-ray photons to electric charges. The direct conversion has been considered to destroy CCD detectors. However, it was found that the lifetime of detectors is not affected, as long as a monochromatic x-ray beam with limited brilliance ($\leq 10^{4-5}$ photons per mm^2 per sec) is used, and (b) the x-ray image magnification technique that was developed at NIST in 1979 and was later applied to real time experiments in materials science at Cornell High Energy Synchrotron Source in 1982 should be used before an image strikes any area detector. This technique is equivalent to an optical lens capable of magnifying images due to x-ray dynamical diffraction and circumvents the current technical problems associated with the reduction of pixel size in CCD detectors.

A photograph of the x-ray microscope is shown in Figure 21 Asymmetrically-cut x-ray optical elements, A and B, are orthogonally aligned to function as the objective lenses of the microscope. An x-ray sensitive CCD array is indicated by E. Figure 22 shows what has been achieved with the x-ray microscope to date. This is a microradiographic image of a pattern of 0.15 μm thick Pd lines of various widths, deposited on a 0.38 mm thick Si wafer. The image was obtained with the microscope operated at the magnification of 79 and a wavelength of 1.0 Å (12.25 keV). At this magnification, one CCD pixel represents 0.25 μm. The eleven evenly spaced lines are 1 μm wide and 50 μm long, with a center-to-center spacing of 5 μm. The single line above the eleven lines is 0.6 μm wide. The sub-micrometer feature is clearly visible for the first time. The image in Figure 21 has been normalized to a blank field to correct for intensity variations due to non-uniform illumination. This is another advantage of CCD cameras which store digital image data for further image processing and quantitative analyses.

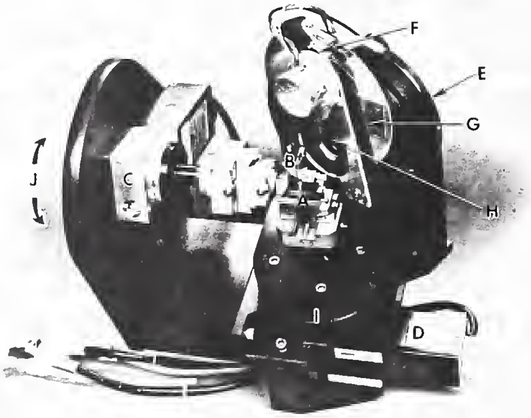

Figure 21. The high-resolution hard x-ray microscope capable of detecting submicron features. A and B: x-ray optical elements controlled by rotators C and D; E: an x-ray sensitive CCD; F: a photodiode; G. a shutter; H: an aperature and J: another rotator (not shown).

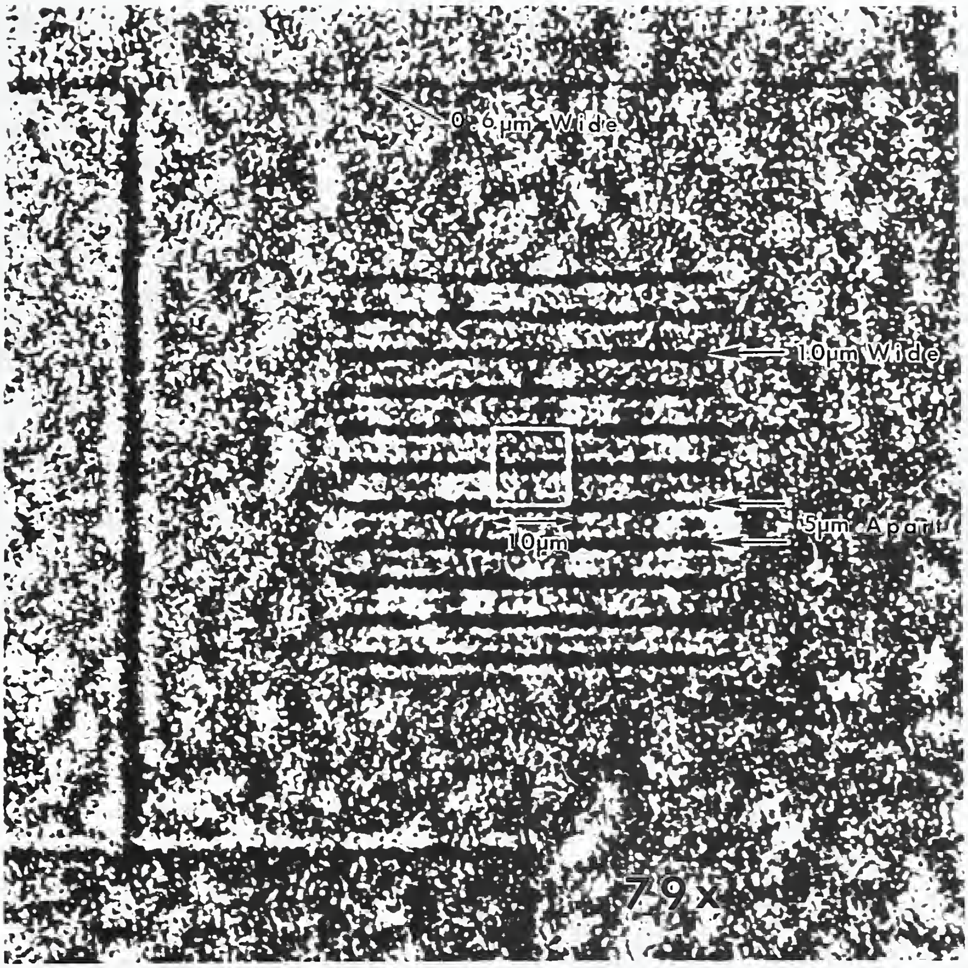

Figure 22. A microradiographic image of Pd lines on Si. The microscope is operated at a magnification of 79 X and a wavelength of 1.0 Å (12.3 keV).

For the evaluation of spatial resolution, line pairs of various widths and spacings should be used. Figures 23 a, b, c, show the images taken from Pd line pair patterns with the microscope operated at the magnification of 79. The images of line pairs, (a) 1.4 μm wide and 1.4 μm apart and (b) 1.2 μm wide and 1.2 μm apart, clearly show well-resolved patterns, while the image of line pairs, (c) 1.0 μm wide and 1.0 μm apart, is hardly discernible. Although the microscope is able to show isolated submicron features as evidenced in Figure 23, the resolution of the microscope is currently 1.2 μm limited by the present x-ray source size. The metrological Pd pattern samples were provided by I. C. Bassignana and S. Eicher, Bell-Northern Research Ltd.

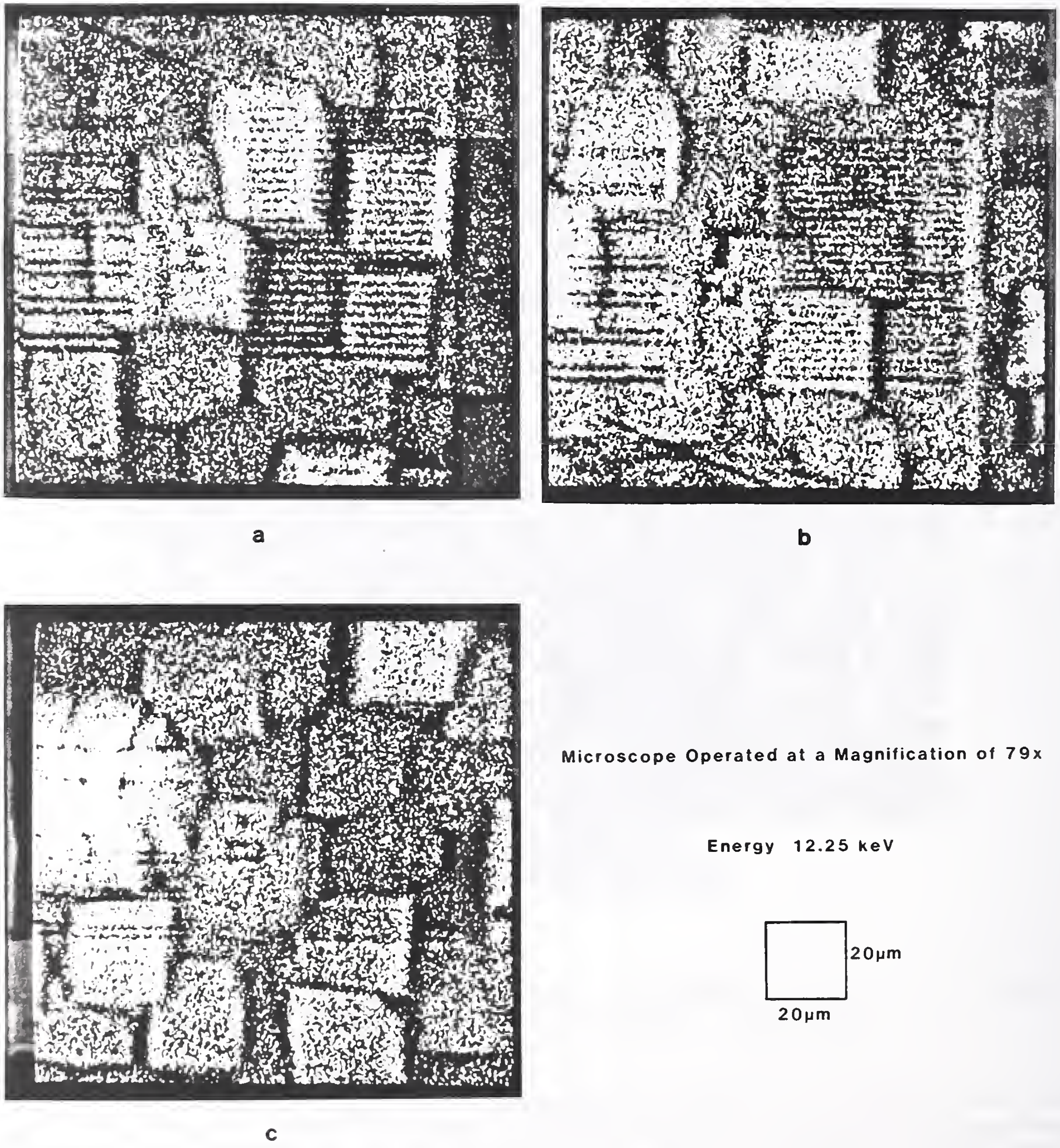

Figure 23. Microradiographic images of various line pairs with the microscope operated at a magnification of 79 X and an energy of 12.25 keV. (a) 1.4 μm wide and 1.4 μm apart, (b) 1.2 μm wide and 1.2 μm apart and (c) 1.0 μm wide and 1.0 μm apart.

Microradiographic Observation of a Single SiC Fiber in a Fiber Reinforced Metal-Matrix Composite

R. C. Dobbyn, D. R. Black, H. E. Burdette and M. Kuriyama

The newly developed high resolution hard x-ray microscope has many applications in the detection of flaws and defects in all sorts of materials. These include advanced structural and functional material components, dental, medical and biotechnological materials as well as in the development of new processing and chemical treatments for these materials (examples in the dental research area were demonstrated in 1985 and 1987 by NIST scientists). Here, a straight forward application of this microscope to microradiography is presented. A reinforced Ti_3Al Nb metal-matrix composite material is used to image a single SiC fiber with the microscope operated at the magnification of 55 X and at a photon energy of 12.15 keV. The thickness of the sample is about 1.7 mm. The x-ray beam is transmitted through the sample in a direction parallel to the fiber axis. Figure 24 shows a series of images taken with an angular increment of 0.1° inclined from the x-ray beam. Each view shows a slightly different aspect of the SiC fiber. This fiber is roughly 130 μm in diameter, surrounded by a Ti_3Al Nb matrix. A graphite core is at the center. The detailed structure of SiC appears as a bundle composed of layers with great clarity; no pixel images are registered discernibly. The CCD pixel size is equivalent to 0.45 μm at this magnification. A square in each figure indicates a 10 μm X 10 μm box. The separation of a SiC layer in the outer edge of the fiber is prominently shown. Also significant is the existence of a dense material region between the graphite core and SiC layers.

As in the operation of an optical microscope, the zooming capability of the x-ray microscope is indispensable to first locate such a small single object in a wide field of view, using a lower magnification, and then to increase a magnification to desired levels. Also necessary is the capability to manipulate the sample orientation while viewing images. As a series of high resolution images shown in Figure 24 demonstrates, a set of two-dimensional images is easily collected as a function of rotational angle with an increment less than one degree. This is an essential step before reconstruction of a three-dimensional image for high resolution microtomography. Algorithms are available for tomographic reconstruction. A working microtomographic system capable of reaching one micrometer or less spatial resolution has become a reality with this hard x-ray microscope.

Si C Fiber in Ti_3 Al Nb

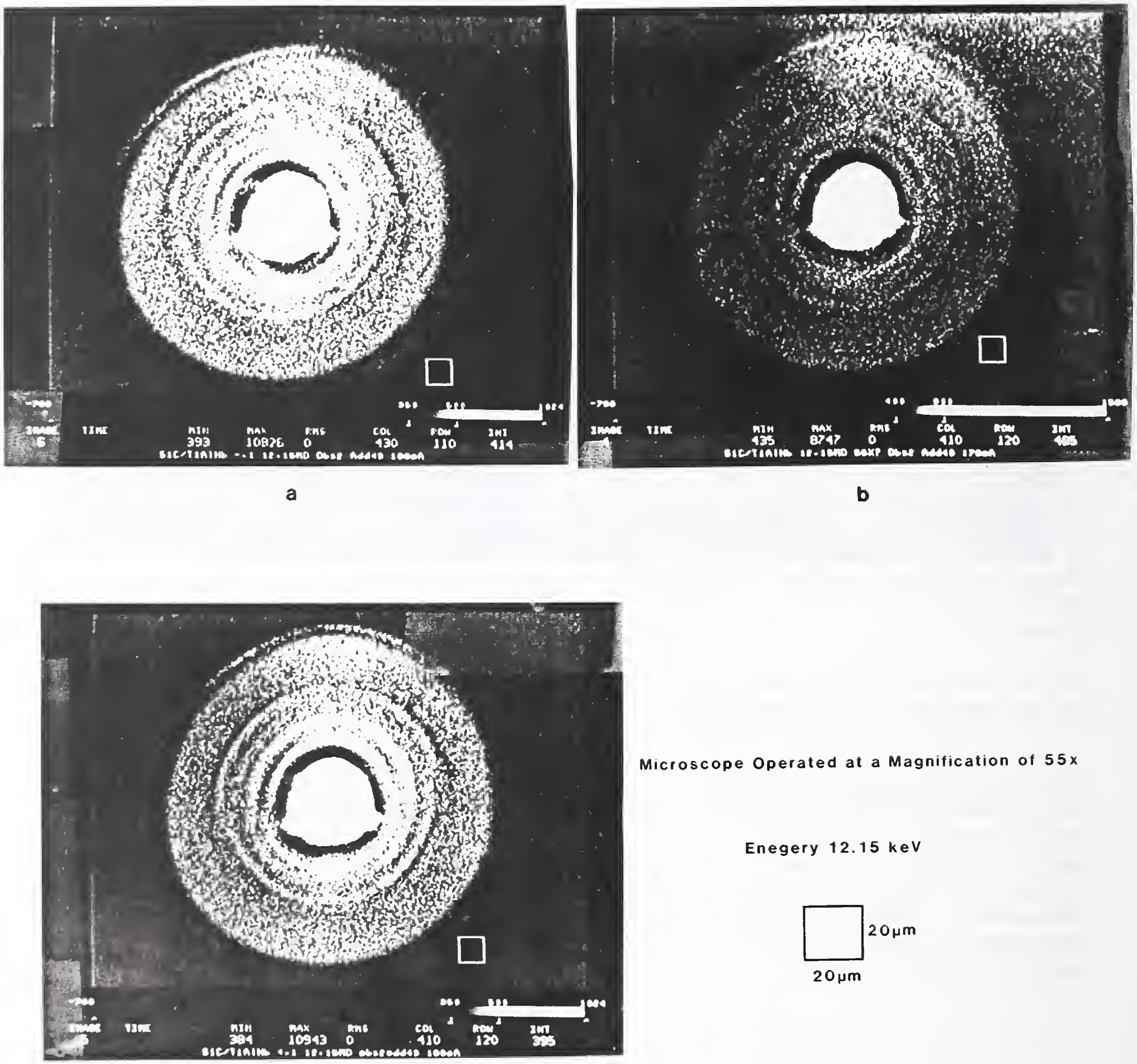

a

b

c

Microscope Operated at a Magnification of 55x

Enegery 12.15 keV

Figure 24. Three images of a single SiC fiber in a reinforced Ti_3Al Nb composite. The microscope is operated at a magnification of 55 X and an energy of 12.15 keV. The sample is about 1.7 μm thick, and the diameter of the fiber is about 130 μm.

X-Ray Phase Contrast Microscopy of Coherent Layers in Laser Diodes

R. C. Dobbyn, H. E. Burdette, R. D. Spal and M. Kuriyama

The application of the new high-resolution hard x-ray microscope is not limited to microradiography. One of the useful examples is presented here. Device features in microelectronics and photonics are prepared by a sequence of depositions of a few atoms at a time and doping in appropriate time intervals. These features are almost perfectly lattice-matched to each other and to the substrate. It is difficult to create images with good contrast from mutually coherent features consisting of similar materials. Electron microscopy suffers the same problem. The physical shape of these features, if visible in microradiography, may not give clues for the understanding of phenomena actually taking place.

Most advanced electronic and photonic materials are often highly perfect single crystals, which can diffract x-rays under Bragg conditions. When single crystal substrates or expitaxially coherent regions are brought into a Bragg condition in transmission, two diffracted images appear: one in the forward direction of the incident beam is called the O-beam image, and the other in the Bragg diffracted direction is called the H-beam image. These images are essentially identical in dynamical diffraction. X-rays can pass through more than one-half millimeter thick samples consisting of high Z elements due to the anomalous transmission (or Borrmann) effect in dynamical diffraction.

With the x-ray microscope set in the forward diffraction direction or in the anticipated Bragg diffraction direction, the O-beam or the H-beam image can be viewed on the monitor screen merely by rotating the sample. Further aided by micro-manipulation of angles and positions of the sample and by the zooming capability, the microscope can view the diffraction image of particular layers or layer sections. Figure 25 shows a 220 diffraction image in transmission in the Bragg diffracted direction (H-beam image) with the microscope operated at the magnification of 100 X and 12.3 keV, precisely tuned to local features of two 0.5 ~ 1.0 μm thick layers near the surface of this device. These are indicated by A's and B's. Also normally there are 2 ~ 3 μm thick layers located 20 - 50 μm below the surface (these images are not included in Figure 25). These thicker images are considered to be related to "striations" caused by growth conditions when the substrate material was produced. Being magnified by the x-ray microscope, the striations appear in the shape of bands.

Two thin layer images, A and B, are made x-ray-visible by either local strains or lattice parameter changes, representing the 0.5 ~ 1.0 μm layers, which may be AlGaAs or InP doped differently on the InP substrate. These layers are part of the device mechanism. Note that the diffraction vector, (220), is contained in the layers, thus making the diffraction condition most sensitive to the interfacial strains. Figure 25 shows that layer A looks like a discontinuous layer and layer B looks like a collection of segments. The discontinuous and segmented images of these layers are indicative of the local variations of the precise Bragg angle for these layers. When the sample is rotated by less than 1 arcsec, new segments of the layers replace the existing images. This type of operation requires precise manipulation while magnified images are under view. The layers were confirmed to be continuous by the images obtained by diffracting planes which are rotated by 90° from the [220] direction and are less sensitive to interfacial strains.

In this mode of phase contrast imaging, the dynamical diffraction effect guarantees that those transmitted images in diffraction represent true transverse cross sectional images of the layers. This work was performed in collaboration with H. Kuwamoto and A. Applebaum, Rockwell International Corporation.

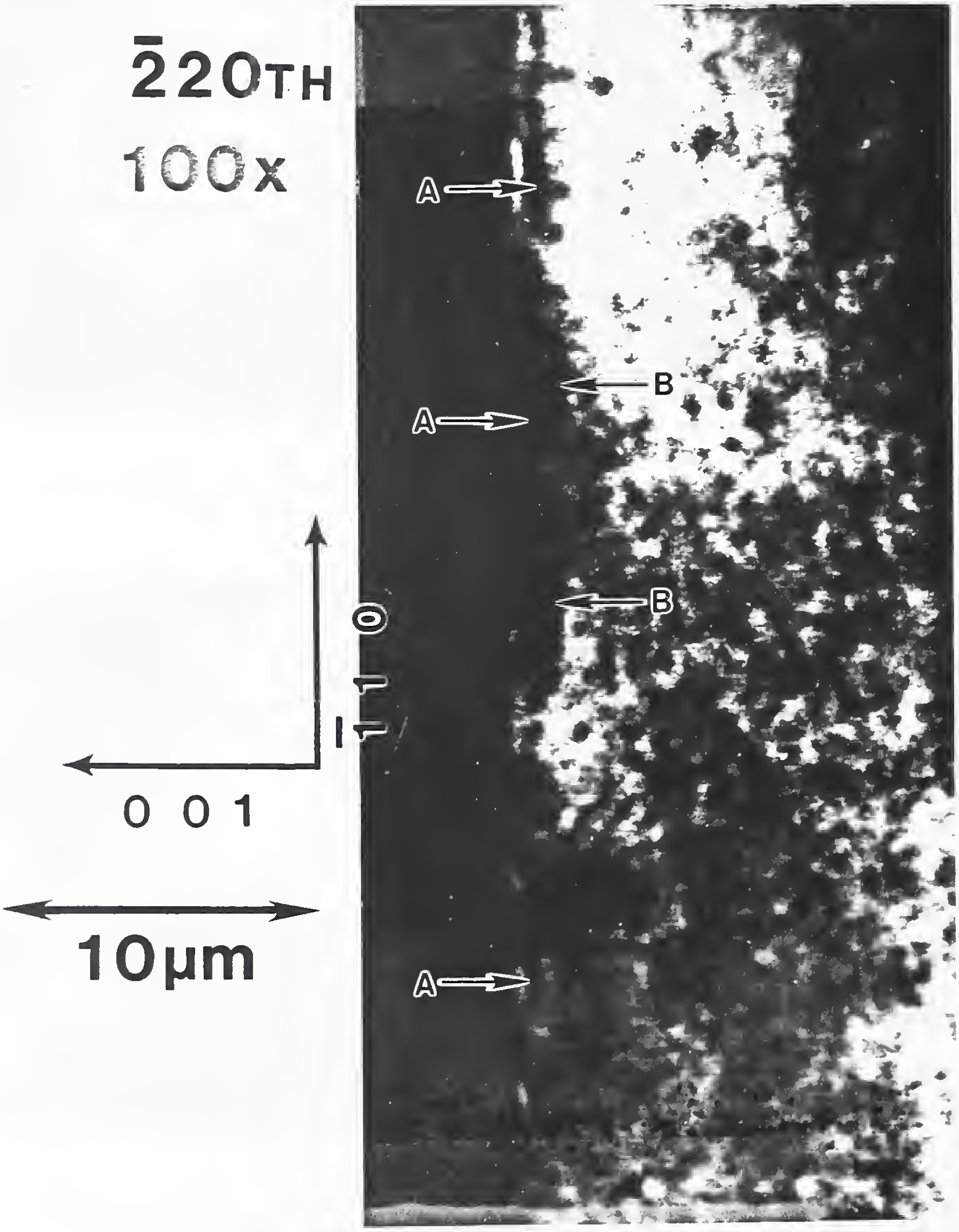

Figure 25. The H-beam image of the GaAs layers in an In(GaAs)P laser diode for the 220 diffraction in transmission with the microscope operated at a magnification of 100 X and an energy of 12.3 keV – phase contrast microscopy. A's are the discontinuous images of the first 0.5 ~ 1.0 μm thick layer and B's are the segmented images of the second 0.5 ~ 1.0 μm thick layer.

Diffraction Imaging of Synthetic and Natural Diamond

D. R. Black, H. E. Burdette and M. Kuriyama

To exploit the practical applicability of the high resolution imaging technique developed at the NIST/MSEL materials science beam line, X23A3, at National Synchrotron Light Source to solve problems relating to the quality and yield of materials, a preliminary examination of synthetic and natural diamond was made in collaboration with Edge Technologies, Inc. A natural diamond was chosen for comparison, and also was used to demonstrate the x-ray optical quality of the present diffraction imaging technique in a routine operation. Figure 26a shows images taken using different diffracting planes. These images appear to reveal what the jewelers term "grain" in natural diamond. Grain in a diamond can be thought of as similar to the grain in a piece of wood. As when cutting or shaping wood, the grain in a diamond produces very subtle changes in the way that the stone will polish in different directions. These changes are in addition to the usual differences observed between different crystallographic directions.

Synthetic diamonds are used to make high precision cutting tools, the quality and yield of which depend critically on the processes of producing high quality synthetic diamonds. Figure 26b shows images from a synthetic diamond which contains a large amount of nitrogen in processing. Figure 26c shows images taken from a different synthetic diamond which contains much less nitrogen identified as "ultra pure nitrogen" diamond. The diffraction images from both diamonds indicate that the crystal growth is kinetic driven, presumably in phase transformation processes under high pressures at elevated temperatures, resulting in facet growth. Also present are interfaces, or layers extending over a large portion of the crystals. These layers are {111} planes, probably created by higher concentration of nitrogen in the phase transition process. The "ultra pure nitrogen" diamond has much less layer formation; each layer is clearly visible, while the other synthetic diamond has layers overlapped with each other throughout the crystal. These layers as well as the facet fronts are considered to be chronological traces of the crystal growth.

Scientists in industry have indicated that the cross section of these layers may be related to an optically observed flaw in failed tools. Also, a non-faceted growth region which forms irregular boundaries seen in the left top corner of all images in Figure 26c is recognized as a trouble region for grinding out the edge of machine tools. To resolve the problems that industry is facing, further systematic studies of diamonds with different levels of nitrogen are obviously required in a close collaboration with the diamond supplier, Sumitomo Electric Industries, Ltd as well as Edge Technologies, Inc. and General Electric.

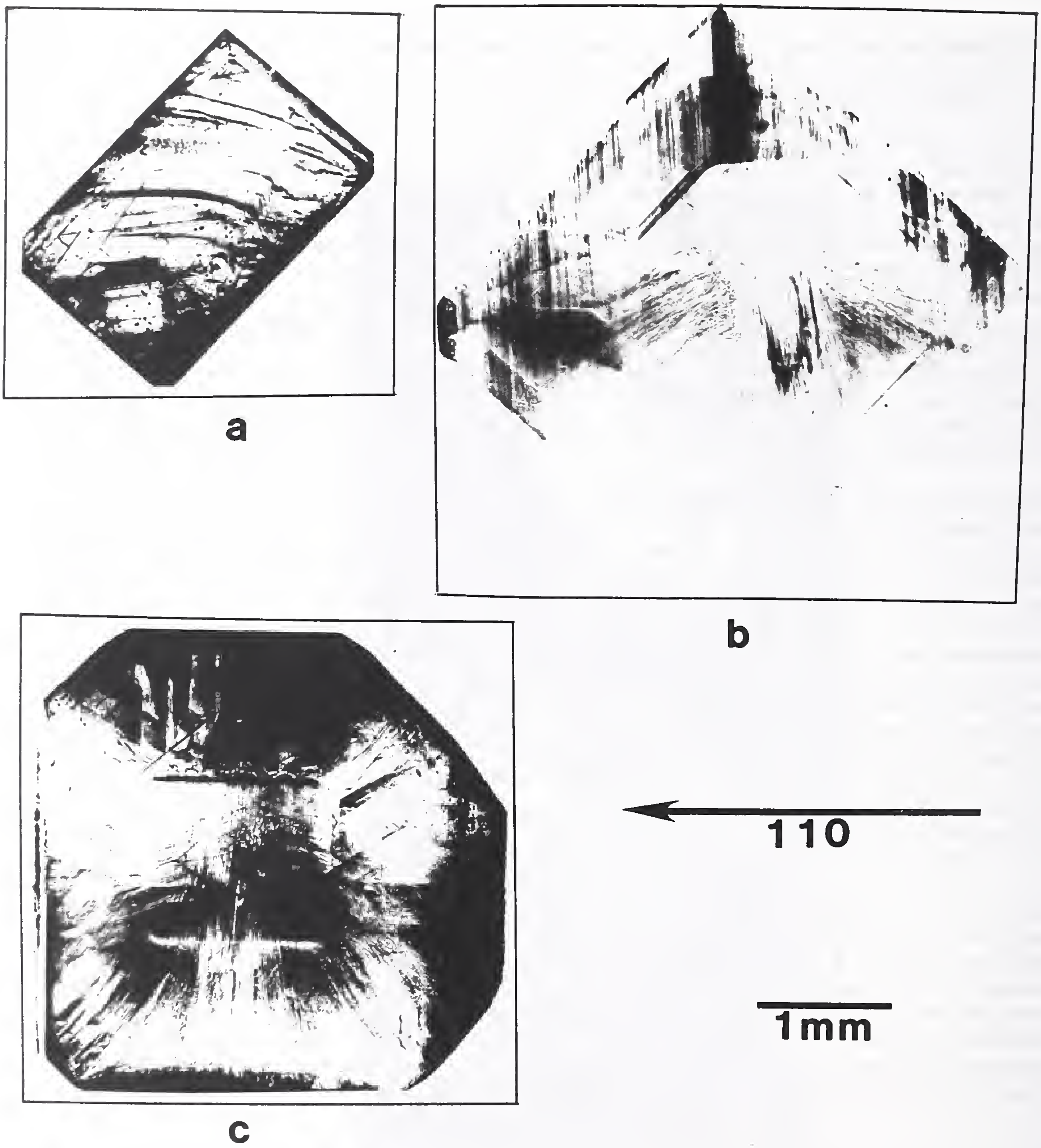

Figure 26. $1\bar{1}1$ asymmetric transmission diffraction images of (a) natural diamond, (b) synthetic diamond used for making cutting tools, and (c) "ultra pure nitrogen" synthetic diamond.

Polycrystalline Materials Characterization: Independent Measurements of Grain Orientation and Residual Strain

D. R. Black, H. E. Burdette and M. Kuriyama

In normal x-ray diffractometry where line profile analyses are applied to "measure" residual strains (stresses), the effect of the distribution of individual grain orientations is buried under the line broadening caused by local lattice variations, part of which corresponds to "residual strains". No local information is usually obtained with desired levels of accuracy. This fact could be overlooked in the days of solid state physics but not in contemporary material science. Recent advances in materials science and high performances applications of advanced materials demand more accurate measurements of local "residual strains" based on microstructural details.

As a continuing effort started two years ago, a new measurement technique has now been completed. This is called "q-vector scan", which measures independently both misorientation angles of individual subgrains or grains and variations in lattice parameter in these individual grains, whose size can be about 1 μm.

This technique challenges one of the fundamental problems which x-ray diffraction measurements have had to contend with in the past fifty years: A continuous spread of diffraction lines does not provide an immediate clue to the question of whether the spread is caused by any of three possibilities; (a) a continuous change in orientation of neighboring subgrains, (b) actual lattice parameter changes (residual strains) in individual subgrains which can be undiscernibly small or (c) inhomogeneous strain within the elastic limit throughout the material. Certainly the last possibility complicates the situation further. The new technique was developed based on the following idea. If an ideally parallel and monochromatic beam can be prepared, a given scattering angle 2θ corresponds uniquely to a single lattice parameter $d_{hkl} = \lambda/2\sin\theta$. With this fixed scattering angle, all diffraction images (spots) appearing while the sample is rotated must have the same lattice parameter d_{hkl}. Furthermore, the sample angle at which a diffraction spot appears gives the relative orientation of this particular grain or subgrain under the Bragg condition. By changing the scattering vector, typically called a q-vector given by $|q| = 2\pi/d_{hkl}$, one can select a particular lattice parameter while the sample is being rotated, and thereby discriminate between misorientation and lattice parameter change.

The sample diffracts a parallel synchrotron radiation beam, and a symmetric Si 111 diffraction analyzer was placed after the sample to select a particular q-vector. This arrangement guarantees $\Delta q/q = \Delta d_{hkl}/d_{hkl} \sim 10^{-4}$. With a fixed q-value, the sample rotation yields the true misorientation distribution of grains with the same lattice parameter as shown in Figure 27. With varying q-values, the integrated intensity of each q-value can be plotted to give the distribution of lattice parameters as shown in Figure 28. This q-vector scan shows that the α Al_2O_3 sample contains two populations of grains with a slightly different lattice spacing.

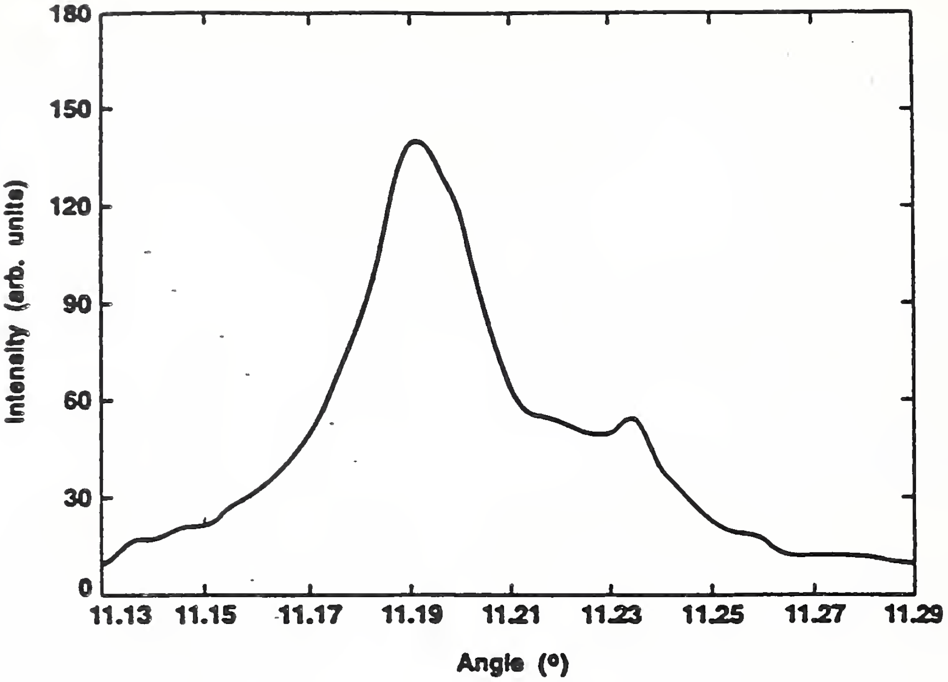

Figure 27. The true misorientation distribution of grains with the same lattice parameter in a α Al_2O_3 sample.

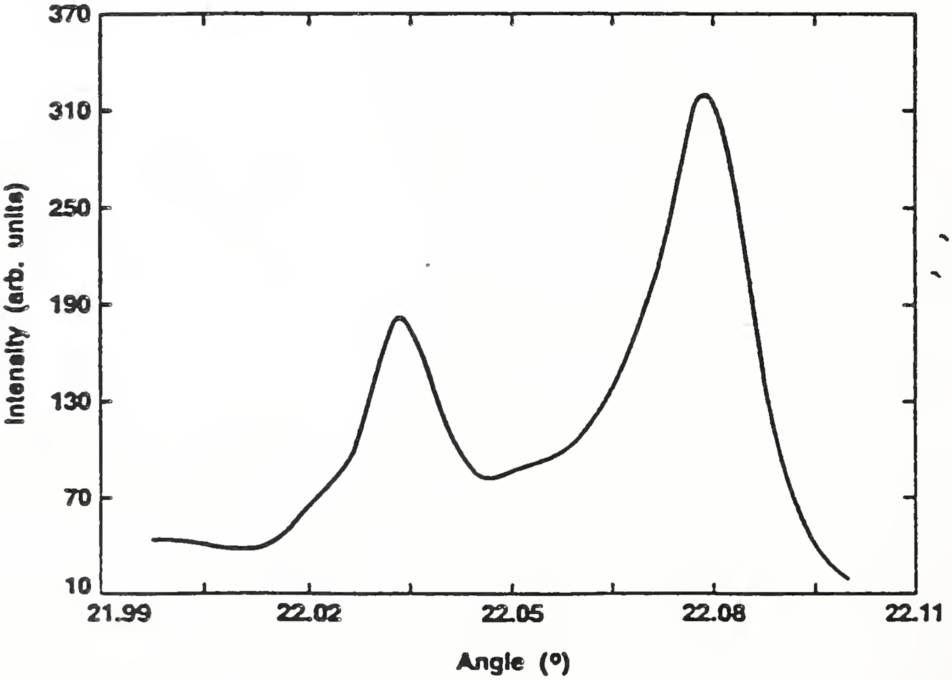

Figure 28. A plot of the distribution of lattice parameters measured by a q-vector scan showing two populations of grains within the α Al_2O_3 sample with a slightly different lattice spacing.

STANDARDS AND DATA ACTIVITIES

STANDARDS AND DATA ACTIVITIES

Overview

The ceramics industry requires the availability of carefully determined standard materials, techniques, and data. Division activities address these needs through the development of standard reference materials and the dissemination of evaluated data. Transfer to industry is implemented through the ASTM in the case of test methodologies, and through the American Ceramic Society and the NIST Offices of Standard Reference Data and Standard Reference Materials for data and materials.

Our continuing efforts in data evaluation are exemplified by the publication of Volumes 7 and 8 of Phase Diagrams for Ceramists and the Computerized Structural Ceramics Database, Version 1.0.

Increasing international competition in the advanced ceramics field necessitates participation in multinational standards development activities. Techniques of measurement have been evaluated and developed through our powder characterization program conducted under the auspices of the International Energy Agency (described under Powder Characterization and Processing), and the Versailles Agent on Materials and Standards for future and wear evaluation. We plan to continue our participation in these programs, serving as the domestic focal point.

Structural Ceramics Database

R. G. Munro and E. F. Begley

The U. S. efforts to develop applications with structural ceramics have been hampered by the general inaccessibility of critical property data. Published data have tended to be widely dispersed in a very large number of journals and reports, making information retrieval very cumbersome, costly, and time comsuming. A large portion of the published reports have also been found to suffer from a chronic lack of data in materials specification and measurement method details. The lack of this information often makes the interpretation of the data difficult or impossible. Design engineers who are not experts in ceramics have especially indicated a need to have the data reviewed or evaluated.

The Structural Ceramics Database (SCD) was developed to resolve these problems. From the beginning, this system was designed not only to collect and evaluate data, but also to help the non-expert to make use of the newest advances in high temperature ceramics. As such, the SCD project was designed to accelerate the development cycle of ceramics technology by forming a critical link between materials research and industrial applications of ceramics.

The needs for well defined, evaluated data and for a computer program that would be easy to use were given equal emphasis.

Data for the first version of the SCD, SCSN 1.0, were collected from published reports. Over a thousand papers from more than thirty journals were examined. Focusing on potential applications such as heat exchangers and engine components, these papers were reduced to only those containing thermal or mechanical property data for silicon carbides and silicon nitrides. Acceptance criteria were established, and the property data were reviewed by experts in ceramics. The resulting evaluated data were placed in the unique, user-friendly SCD database program. Field tests of the system were conducted at a research facility (NASA Lewis Research Center), a ceramics manufacturer (Coors Ceramics), and an applications manufacturer (Babcock & Wilcox).

Designed for DOS-based personal computers, the SCD uses a menu-driven interface with unique computer-assisted user entries. Searches for property data or materials are conducted in a query-by-example format that allows users to search the database without being an expert in computers, databases, or materials. Property values are recorded with measures of quality, methods and procedures information, and significant cautions, along with materials specification information. All sources of data are fully documented.

A Computerized Tribology Information System

S. Jahanmir and A. W. Ruff

A computerized tribology information system, named "ACTIS", is under development at NIST. The ACTIS system consists of six components: numeric databases, design calculation codes, a newsletter, bibliographic searching, a research-in-progress database, and a product and services directory. The anticipated users will be researchers, material engineers, application engineers, and design engineers. The Tribomaterials Database I has been completed and delivered to the NIST Standard Reference Data Office for release. This first ACTIS product, designed for personal computers, contains evaluated data on friction and wear of common tribomaterials along with data on their physical and mechanical properties. Agreement has been reached with a private company, ACTIS Inc. to market the database and initial versions of several design calculation codes, all for use in PC's.

As a continuing effort, a Tribology Data Center has been established at NIST with support from the Ceramics Division and the Standard Reference Data Office to continue to obtain, evaluate, and disseminate critical data on ceramic tribomaterials. It is important to provide such data to assist in the introduction of ceramic materials into commercial technology. Other database modules, presently under development, include programs for design of bearings and gears; and computer codes for calculation of contact stress, temperature, and lubricant film thickness.

Standards and Measurement Activities

A. W. Ruff

Activities in ASTM Committee G-2 on Wear and Erosion continued in several areas. A new standard for Wear Testing with a Pin-on-Disk apparatus, written at NIST, was approved and issued as ASTM Standard G-99. Data and information obtained in the process of carrying out the latest VAMAS wear test activity were included in the standard. This is the first U.S. standard covering this readily available wear test system design.

In view of the growing role of computers in tribology, a new sub-committee on Computerization in Wear and Erosion was formed at the last G-2 meeting. The sub-committee is chaired by an NIST staff member. As a result of ideas developed at a recent G-2 Workshop on Computer Utilization in Tribology, organized with NIST leadership, preliminary work on standards development has begun in areas such as computer control of wear test systems, databases of tribology information, statistical analysis of wear data, and expert systems for material selection.

A new task group has been formed in G-2 to develop a standard for reciprocating pin-on-disk testing of materials. The standard will build upon the new G-99 document, and will attempt to include existing commercial designs. NIST will have a prominent role in writing the standard and will participate in round-robin test series utilizing our three reciprocating sliding test systems.

Ceramic Phase Equilibria Program

H. M. Ondik, S. W. Freiman, M. A. Clevinger, T. R. Green[1], K. M. Kessell[1], C. D. Pryor[1], N. M. Cure[1] and C. G. Messina[1]

[1]American Ceramic Society Industrial Research Associates

The continuing purpose of the Ceramic Phase Equilibria Program is to provide the ceramics user community with evaluated phase equilibria data covering all non-alloy, inorganic systems. This past year has been the fifth full year of operation of the Ceramics Phase Diagram Data Center under the expansion plan sponsored cooperatively by NIST and the American Ceramic Society (ACerS). Over $2,500,000 has been raised by the ACerS from industry and universities for the support of the program.

Volume 7 on salts and Volume 8 on high-pressure aqueous systems were published, Volume 7 in late 1989 and Volume 8 in early 1990. Volume 7 contains 1057 diagrams discussed in 934 commentaries. Volume 8 contains 915 diagrams discussed in 295 commentaries.

A 500-page publication, Bibliographic Update through January 1, 1989 and Cumulative Indexes for Volumes I-VIII, was also completed and printed in March 1990. The update portion provided chemical system and author indexes and bibliographic references for over 12,000 diagrams in the Data Center computer files which have not yet appeared in any volume of Phase Diagrams for Ceramists. The number of references involved is about 7,000 since a number of papers contain more than one phase diagram.

Since the completion of the Bibliographic Update, information for almost 2000 new diagrams have been entered in the Data Center computer files. These new data files cover all chemical systems currently being included in the search, for oxide and salt systems, boride, carbide, and nitride systems, systems containing elements of Groups IVa, Va, and VIa of the Periodic Table, and aqueous systems. It is planned that the ACerS will publish bibliographic updates regularly as a portion of Ceramic Abstracts and data transfer procedures are currently being tested.

The chemical system sort program has been revised and now provides for a sort covering all the chemistries. Some modifications were necessary to accommodate the inclusion of the non-oxide, non-salt systems.

Examination, evaluation, and digitization of diagrams for inclusion in Volume 9 of Phase Diagrams for Ceramists is well underway. This next volume will contain systems of interest to the semiconductor community (systems containing Groups IVa, Va, and VIa elements). It is expected to be completed and available for distribution in the autumn of 1991. Also well underway is an annual volume which is expected to be available for the ACerS Annual Meeting in April of 1991. This volume will not cover chemistries topically but will include a variety. Although the diagrams will be properly evaluated, they will not have the cross-referencing and comparison of similar diagrams which occurs in the regular topically-oriented volumes. The annual volumes are intended to help catch up with the backlog of diagrams currently in the Data Center files.

A database system for use on DOS-based personal computers (PC) is expected to be ready for marketing by NIST and the ACerS in the autumn of 1990. The system includes the bibliographic and chemical system information for Volumes 1 through 8 permitting the user to search for specific diagrams in these volumes. This portion of the system is contained in and operated by a customized commercial database system. A graphics program, written by NIST staff, operates within the system to permit diagrams to be plotted and manipulated on screen. The manipulation includes such features as cursor position readout, magnification, reversal of binary end-members, diagram overlay, curve follow with cursor position readout, and application of the lever rule. The database will include the diagrams of Volumes 6, 7, and 8, the only volumes which have been produced using digitized diagrams.

Versailles Advanced Materials and Standards (VAMAS)

Mechanical Properties of Ceramics

E. R. Fuller and S. W. Freiman

Over the past few years, Drs. E. R. Fuller, Jr. and S. W. Freiman have led a VAMAS effort aimed at defining test procedures to determine the moisture sensitivity of crack growth in ceramics. Sixteen laboratories from five countries participated in the interlaboratory tests to establish "dynamic fatigue" test procedures. The material used in the tests was aluminum oxide supplied by Demarquest in France in the form of 2000 machined test bars. This study has been completed, and the results presented at an ASTM sponsored symposium and an international ceramics meeting. A paper describing the study will be published in the near future.

Work is now underway on an interlaboratory test series whose purpose is to identify reliable techniques for measuring the critical fracture toughness, K_{Ic}, of ceramic materials. Specimens of silicon nitride and zirconia have been supplied by the Japan Fine Ceramics Center. The critical fracture toughness of these materials will be determined in laboratories in the U.S. and abroad using three different test procedures. The work in the U.S. is being coordinated through two different committees of ASTM.

Wear Testing

S. Jahanmir

Two international round robin tests have been completed by the Wear Test Methods Technical Working Area of VAMAS. The purpose of these tests were to identify the important variables and technical issues related to wear testing of advanced materials. These tests were conducted on alumina and silicon nitride, and the results were compared with a bearing steel. the final results were published in VAMAS Reports and in two articles in the International Journal of Wear. The results of these tests have been used to develop ASTM and DIN standard test methods of wear. Thirty-eight laboratories, including thirteen from the U.S.A., participated in this activity. Presently, the Wear Test Methods Committee is developing plans for the next round of activities under the chairmanship of Dr. S. Jahanmir, of NIST. Activities under consideration include coatings, computerized databases, and a different set of test procedures.

STANDARD REFERENCE MATERIALS

The Division provides science, industries, and government a central source of well characterized materials certified for chemical composition of physical or chemical properties. These materials are issued with a certificate and are used to calibrate instruments, to evaluate analytical methods, or to produce scientific data which can be referred to a common base.

DESCRIPTION	SRM NUMBER
Alumina Elasticity	718
Alumina Glass Anneal Point	714
Alumina Glass Anneal Point	715
Alumina Melting Point	742
Aluminum Magnetic Susceptibility	763-1
Aluminum Magnetic Susceptibility	763-2
Aluminum Magnetic Susceptibility	763-3
Barium Glass Anneal Point	713
Borosilicate Glass Composition	93(A)
Borosilicate Glass Thermal Expansion	731L1
Borosilicate Glass Thermal Expansion	731L2
Borosilicate Glass Thermal Expansion	731L3
Cadmium Vapor Pressure	746
Chlorine in Base Oil	1818
Container Glass Composition	621
Container Glass Leaching	622
Container Glass Leaching	623
Copper Thermal Expansion	736L1
Fused Silica Thermal Expansion	739L1
Fused Silica Thermal Expansion	739L2
Fused Silica Thermal Expansion	739L3
Glass Analytical Standard	1835
Glass Dielectric Constant	774
Glass Electrical Resistance	624
Glass Fluorescence Source	477
Glass Liquidus Temperature	773
Glass Refractive Index	1820
Glass Sand (High Iron)	81A
Glass Sand (Low Iron)	165A
Glass Stress Optical Coefficient	708
Glass Stress Optical Coefficient	709
Glass Viscosity Standard Renewal	717
Gold Vapor Pressure	745
High Boron Glass Viscosity	717
Intensity XRD Set	674
Lead Barium Glass Composition	89
Lead Glass Anneal Point	712
Lead Glass Viscosity	711
Line Profile	660
Liquids Refractive Index	1823
Low Boron Glass Composition	92
Lube Oil Oxidation Test Kit	1817
Lube Oil Oxidation Test Kit	1817b

Lube Oxidation Catalysts	8500
Lubricant Oxidation Research Test Kit	8500a
MNF_2 Magnetic Susceptibility	766-1
Mica X-Ray Diffraction	675
Neutral Glass Anneal Point	716
Nickel Magnetic Susceptibility	772
Opal Glass Composition	91
Palladium Magnetic Susceptibility	765-1
Palladium Magnetic Susceptibility	765-2
Palladium Magnetic Susceptibility	765-3
Platinum Magnetic Susceptibility	764-1
Platinum Magnetic Susceptibility	764-2
Platinum Magnetic Susceptibility	764-3
Refractive Index Glass	1822
Respirable Cristobalite	1879
Respirable Quartz	1878
Ruby EPR Absorption	2601
Sapphire Thermal Expansion	732
Silicon X-Ray Diffraction	640(b)
Silver Vapor Pressure	748
Soda Lime Flat Glass Composition	S620
Soda Lime Float Composition	1830
Soda Lime Glass Viscosity	710
Soda Lime Sheet Composition	1831
Sulfur in Base Oil	1819
Toluene 5 ML	211C
Total Nitrogen in Lubricating Base Oil	1836
Tungsten Thermal Expansion	737
Total Nitrogen in Base Oils	1836
X-Ray Diffraction Intensity Set	674a
Wear Metals in Oil	1084a
Wear Metals in Oil	1085a

RESEARCH STAFF

POWDER CHARACTERIZATION AND PROCESSING

Cline, James P.	• Standard reference materials • High-temperature X-ray diffraction • Microstructural effects in X-ray diffraction • Rietveld Refinement of XRD data
Kelly, James F.	• Quantitative scanning electron microscopy • Image analysis • Microstructure analysis • In-situ crack propagation studies
Long, Gabrielle G.	• Multiple small angle neutron scattering • High Resolution Small angle X-ray scattering
Lum, Lin-Sien H.	• Powder characterization • Instrumental analysis
Malghan, Subhas G.	• Powder and dense slurry characterization • Colloidal processing and forming • Interfacial and surface chemical studies on powders
Minor, Dennis B.	• Analytical SEM of ceramics and particulates • Powder test sample preparation • Powder characterization
Pei, Patrick T.	• Spectroscopic and thermal characterization • Chemical coating • Bulk chemical properties
Ritter, Joseph J.	• Chemistry of powders synthesis • Specialty powders synthesis • Powder preparation and compositional evaluation
Pechenik, Alexander	• Novel powder processing • High pressure, low temperature powder compaction • Powder processing science
Wallace, Jay S.	• Processing and microstructure • Silicon nitride densification • Thermal analysis
Wang, Pu Sen	• Solid state NMR • Surface characterization by X-ray photoelectron and Auger electron spectroscopy

MECHANICAL PROPERTIES

Chuang, Tze-Jer	• Creep/Creep Rupture • Mechanics
Cranmer, David C.	• Ceramic and glass composite fabrication • Composite test development • Ceramic composite properties • Glass viscosity • Properties of glass
Grabbe, Alexis	• Surface forces • Surface and interfacial chemistry • Colloidal processing
Hockey, Bernard J.	• Electron microscopy
Horn, Roger G.	• Surface forces • Fracture mechanics • Colloidal processing • Tribology • Adhesion
Kauffman, Dale A.	• Glass melting
Lawn, Brian R.	• Microstructure/strength relations • Fracture mechanics • Contact phenomena • Surface forces in fracture
Ostertag, Claudia P.	• Influence of heterogeneities on sintering • Processing and sintering of reinforced ceramics • Investigation of toughening mechanisms in pressureless sintered composites • Measurement of residual stresses by cathodoluminescence and in situ high temperature X-ray diffraction
Smith, Douglas T.	• Surface forces • Charge transfer at interfaces • Adhesion

TRIBOLOGY

Ives, Lewis K.	• Wear of materials • Transmission electron microscopy • Mechanical properties

Jahanmir, Said	• Wear mechanisms • Boundary lubrication • Mechanical behavior of materials
Ku, Chia-Soon	• Lubrication of ceramics • Oxidation, thermal stability and volatility • Lubricant degradation mechanisms
Perez, Joseph M.	• Additive chemistry, deposits and engine emissions • Thermal and oxidation stability of fluids • Fuels, lubricants and diesel engines
Peterson, Marshall B.	• Wear of materials • Solid film lubricants • Mechanical behavior
Ruff, Arthur W.	• Wear of materials • Microstructure effects • Mechanical behavior
Whitenton, Eric P.	• Surface profilometry • Data processing • Computer interfaces

ELECTRONIC MATERIALS

Blendell, John E.	• Ceramic processing and clean-room processing • Sintering and diffusion controlled processes • Processing high T_c ceramic superconductors • Activation chemical analysis
Block, Stanley	• Ceramic processing and high pressure sintering • Pressure-induced transformation toughening • High pressure physical properties and structures • High pressure x-ray diffraction and spectroscopy
Chiang, C. K.	• Electronic ceramics • Superconductivity • Electrical Measurements
Clevinger, Mary, A.	• Phase diagrams for ceramists • Computerized data

Cook, Lawrence P.	• High temperature chemistry • Phase equilibria • Electronic ceramic films
Freiman, Stephen W.	• Electronic ceramics • Mechanical properties • Superconductivity
Hill, Michael D.	• Superconducting materials • Ceramic processing
Ondik, Helen M.	• Phase diagrams for ceramists • Database management systems
Piermarini, Gasper J.	• Ceramic processing and high pressure sintering • Pressure-induced transformation toughening • High pressure physical properties and structures • High pressure X-ray diffraction and spectroscopy
Rawn, Claudia J.	• Phase diagrams • X-ray diffraction
Raynes, Alan S.	• Fracture • Microstructure
Roth, Robert S.	• Crystal chemistry • Phase diagrams • Phase equilibria
Vaudin, Mark	• Electron microscopy of ceramic superconductors and of ceramic-ceramic and ceramic-metal composites • Microscopy and diffraction studies of interfaces • Computer modelling of grain boundary phenomena
White, Grady S.	• Thin films • Nondestructive evaluation • Subcritical crack growth
Wong-Ng, Winnie	• X-ray analysis • X-ray standards • Molecular orbital calculations

OPTICAL MATERIALS

Farabaugh, Edward N.	• Chemical vapor deposition of diamond • Structure and morphology analysis • Scanning electron microscopy • X-ray diffraction • Thin film deposition • Surface analysis
Feldman, Albert	• Chemical vapor deposition of diamond • Thermal properties • Modelling thermal wave propagation • Thin film optical properties
Kaiser, Debra L.	• Bulk single crystal growth • Phase equilibria • Physical properties and structures of high temperature superconductors • Interfaces in high temperature superconductors • Chemical vapor deposition of ferroelectric oxide thin films
Robins, Lawrence H.	• Defect identification and distribution in CVD diamond • Stress in ceramics • Cathodoluminescence imaging and spectroscopy • Photoluminescence spectroscopy • Optical properties • Raman spectroscopy • Scanning electron microscopy

SYNCHROTRON RADIATION

Black, David R.	• Inelastic x-ray scattering • Energy dispersive diffraction • Fluorescence and absorption • Polycrystalline diffraction imaging
Burdette, Harold E.	• X-ray optics engineering • Crystal growth • Instrumentation
Dobbyn, Ronald C.	• X-ray imaging • X-ray optics • Microradiography • Diffraction imaging
Kuriyama, Masao	• Scattering Physics • Condensed matter physics • Crystallography

Spal, Richard D.	• X-ray optics • X-ray image detectors • Condensed matter physics • Diffraction Physics

DATA BASE ACTIVITIES

Begley, E. F.	• Database management for scientific and engineering data • User-friendly interfaces Materials property databases
Munro, R. G.	• Material properties of advanced structural ceramics • Wear of ceramics under harsh tribological conditions • Analysis of complex and multivariate data relations

DIVISION OFFICE

Carpenter, J. A., Jr.,	• Functional ceramics applications • Technical assessments • Industrial liaisons
Carter, W. Craig	• Microstructural evolution of ceramics and other materials • Micromechanics of composites and relationships of processing to fracture • Computer simulations of materials-related phenomena. • First principles calculation of phase diagrams • Studies capillary forces in ceramics processing
Dapkunas, S. J.	• Structural ceramics applications • Technical assessments
Hsu, S. M.	• Tribology of ceramics materials • Advanced high temperature lubrication concepts • Wear maps concepts and methodology
Fuller, Edwin R. Jr.	• Influence of microstructure on fracture and other physical properties of materials • Toughening mechanisms in ceramics and ceramic composites, and their relations to processing • Interfacial fracture and toughening mechanisms in reinforced ceramic composites • Processing/property relations and phase equilibria of high T_c ceramic superconductors

GUEST SCIENTISTS AND GRADUATE STUDENTS

Alexandropoulos, Nikos	University of Ioannina
Balasubramanian, Raghuraman	Clarkson University
Bender, Gerald	University of Groningen
Bennison, Stephen	Lehigh University
Blackburn, Douglas	Consultant
Braun, Linda	Lehigh University
Butler, Elizabeth	Lehigh University
Chang, Luke	University of Maryland
Chen, Yung-Mien	University of Maryland
Cheng, Herbert	Northwestern University
Coyle, Thomas	GPR Systems
Craig, Charles	Defense Tech Security
Cure, Nicole	American Ceramics Society
Czubarow, Pawel	American University
Dally, James	University of Maryland
Domingues, Louis	Trans-Tech, Inc.
Dong, Xiaoyuan	University of Maryland
Dragoo, Alan	Department of Energy
Frederikske, Hans	Consultant
Green, Thomas	American Ceramic Society
Haller, Wolfgang	Abbott Laboratories
Harmer, Martin	Lehigh University
He, Chuan	University of Maryland
Hong, William	Institute for Defense Analysis
Hu, Zu-Shao	East China University
Hwang, Nong-Moon	Korea Science and Engineering Institute

Inglehart, Lorretta	Johns Hopkins University
Ito, Osamu	Hitachi Research Lab
Jiang, Si-Juan	Tsinghua University
Kessell, Kimberly	American Ceramic Society
Kim, Seock-Sam	Korea Science and Engineering Institute
Klaus, Elmer	Pennsylvania State University
Kruger, Jerome	Johns Hopkins University
Kuwamoto, Hidehiko	Rockwell International
Lacey, Paul	University of Maryland
Larsen-Basse, Jorn	National Science Foundation
Lathabai, Srinivasarao	Lehigh University
Lee, Soo Wohn	University of Illinois
Martin, Curtis	Naval Surface Warfare Center
McMurdie, Howard	Joint Center for Powder Diffraction Studies
Messina, Carla	American Ceramic Society
Messina, Theresa	American Ceramic Society
O'Neil, Peggy	American Ceramic Society
Padture, Nitin	Lehigh University
Parekzkin, Boris	Joint Center for Powder Diffraction Studies
Paulik, Steven	Northwestern University
Pryor, Caroline	American Ceramic Society
Ranade, Madhav	Particle Technology
Rigdon, Michael	Institute for Defense Analysis
Ritter, Andrew	Martin Marietta
Roedel, Juergen	Lehigh University
Russell, Thomas	Naval Surface Warfare Center
Sater, Janet	Institute for Defense Analysis

Schioler, Liselotte	Air Force Office of Scientific Research
Shechtman, Dan	Johns Hopkins University
Shen, Ming	University of Illinois
Sivakumar, Ananthasubramanian	Columbia University
Smith, Wallace	Office of Naval Research
Sun, Jian-Xia	Shanghai University of Science and Technology
Swanson, Nils	American Ceramic Society
Thanomkul, Srinuan	Chulalongkorn University
Trivedi, Sudhir	Brimrose Corporation
Vandiver, Pamela	Smithsonian Institute
Wachtman, John	Rutgers University
Wan, Kai-Tak	University of Maryland
Wang, Yushu	University of Maryland
Wilcox, William	Clarkson University
Wu, Dong-Di	East China University
Ying, Tsi-Neng	University of Maryland
Zhang, Yuming	University of Maryland
Zutshi, Ajoy	Rutgers University

AWARDS

First Place Annual Photo Contest Award awarded to D. Kaiser by the American Conference on Crystal Growth for entry entitled "Twin Structure in an $YBa_2Cu_3O_{6+x}$ Single Crystal", July 19, 1990.

Honorary Fellow of ASTM for Dedicated Service awarded to Arthur W. Ruff, December 15, 1989.

Society of Tribologists and Lubrication Engineers for a National Award for Significant Scientific Contributions to the Field of Tribology awarded to Marshall Peterson.

Internal Awards

Bronze Medal	Debra Kaiser For research on Detwinning of YBaCuO Single Crystals.
Crittendon Medal	Dale Kaufman For Sustained Technical Support in the Production of Standard Reference Materials.
Silver Medal	Stephen Hsu, Subhas Malghan and Alan Dragoo For Leadership in the IEA Round Robin on Ceramic Powder Characterization.
Silver Medal	Roger Horn and Douglas Smith For Development of Techniques of Measurement of Surface Forces between Dissimilar Materials.

OUTPUTS AND INTERACTIONS

TECHNICAL PUBLICATIONS

POWDER CHARACTERIZATION AND PROCESSING

Kelly, J. F. and Ritter, J. J. "Compositional Homogeneity in Processing Precursor Powders to the $YBa_2Cu_3O_{7-x}$ High T_c Superconductor", submitted J. Mater. Sci.

Malghan, S. G. and Pujari, V. "Critical Evaluation of Silicon Nitride Powder Characterization and its Effect on Injection Molding", In "Advanced Materials Processing", V. Lakshmanan and J. D. Miller, Eds., SME, Feb. 1990.

Malghan, S. G. and Lum, L.-S. "Factor Affecting Interface Properties of Silicon Nitride Powders in Aqueous Environment", In "Powder Processing Science III", G. L. Messing et.al., Eds., ACerS, July 1990.

Malghan, S. G., Dragoo, A. L., and Hsu, S. M. "Physical and Chemical Characterization of Ceramic Powders in an International Interlaboratory Comparison Program", Proceedings of World Congress CIMTEC, Vincenzini, Ed., June 1990.

Ritter, J. J. "Optimization of Some Oxides for Use As Supports in Alkaline Fuel Cell Electrocatalysis", Final Report to NASA for the period February 12, 1989 to February 12, 1990.

Ritter, J. J., Kelly, J. F., Newbury, D. E., and Minor, D B. "Molecular Chemistry and the Synthesis of Precursors to Electronic Ceramic Materials", Proc. Int'l Conf. on: The Chemistry of Electronic Materials, Jackson, WY, August 17-22, 1990.

Wang, P. S., Hsu, S. M., Malghan, S. G., and Wittberg, T. N. "Surface Oxidation Kinetics of Si_3N_4 - 4% Y_2O_3 Powders Studied by Bremsstrahlung-Excited Auger Spectroscopy", in press, Journal of Materials Science (London).

Wang, P. S., Malghan, S. G., Wittberg, T. N., and Hsu, S. M. "Surface Oxidation Kinetics of SiC Platelets Studied by X-Ray Photoelectron and X-Ray Induced Auger Electron Spectroscopy", submitted to the Society of Material Research.

Powder Processing

Kelly, J. F., Rodel, J., Stoudt, M., and Bennison, S. "A Loading Device for Fracture Testing of Compact Tension Specimens in the SEM", submitted to Scanning Microscopy.

Long, G. G., Krueger, S., Jemian, P., Black, D., Burdette, H., Cline, J. C., and Gerhardt, R. "Small Angle Scattering Determination of the Microstructure Morphology of Porous Silica Precursor Bodies", J. Appl. Cryst. (1990) to be published.

Long, G. G. "Small Angle Neutron Scattering and Small Angle X-Ray Scattering from Bulk Microporous Silica", in Neutron Scattering for Materials Science, Mat. Res. Soc., Pittsburgh (1990) 421-426.

Long, G. G., Mendoza, E. A., Wolkow, E., Gafney, H. D., Sunil, D., Rafailovich, M., Sokolov, J., and Jemain, P. R. "The Effect of Photodeposited Iron Oxide and Tin Oxide on the Consolidation of Porous Vycor Glass", Appl. Phys. Lett. (1990) to be published.

Long, G. G., Jemian, P. R., Weertman, J. R., Black, D. R., Burdette, H. E., and Spal, R. "High Resolution Small Angle X-Ray Scattering Camera for Anomalous Scattering", J. Appl. Cryst. (1990) to be published.

Long, G. G., Krueger, S., and Page, R. A. "The Effect of Green Body Density and the Role of MgO Additive on the Densification of Alumina Measured by Small-Angle Neutron Scattering", J. Am. Ceram. Soc. (1991).

Long, G. G., Krueger, S., Gerhardt, R. A., and Page, R. A. "Small Angel Neutron Scattering Characterization of Processing/Microstructure Relationships in the Sintering of Crystalline and Glassy Ceramics", J. Materials Research (1991).

Long, G. G. and Jemian, P. R. "Silicon Photodiode Detector for Small Angle X-ray Scattering", J. Appl. Cryst. (1990) to be published.

Long, G. G., Krueger, S., and Page, R. A. "Characterization of the Densification of Alumina by Multiple Small-Angle Neutron Scattering", Acta Cryst. A. (1991).

Long, G. G., Krueger, S., and Page R. A. "Multiple Small Angle Neutron Scattering Characterization of the Densification of Alumina", in Neutron Scattering for Materials Sciences, Mat. Res. Soc., Pittsburgh (1990) 61-66.

Malghan, S. G., Minor, D. B., Wang, P. S., and Ostertag, C. "Coating of Fibers by a Colloidal Technique in Ceramic Composites Pressing", Ceramic Eng. Sci., 10 (7-8), 1990.

Pechenik, A. and Matthews, M. D. "Rapid Hot Pressing of Ultra-Fine PSZ Powders", submitted to J. Am. Ceramic Society.

MECHANICAL PROPERTIES

Ceramic Matrix Composites

Cranmer, D. C. "An Assessment of Testing Methodology for Glass, Glass-Ceramic, and Ceramic Matrix Composites", submitted to J. Research (NIST), 1990.

Cranmer, D. C., Deshmukh, U. V., and Coyle, T. W. "Comparison of Methods for Determining Fiber/Matrix Interface Frictional Stresses in Ceramic Matrix Composites", in Thermal and Mechanical Behavior of Metal Matrix and Ceramic Matrix Composites, ASTM STP 1080, J. M. Kennedy, H. H. Moeller, and W. S. Johnson, Eds., ASTM, Philadelphia, 1990, pp. 124-135.

Cranmer, D. C., Freiman, S., Fuller, E., Haller, W., Koczak, M., Barsoum, M., and Chou, J. "Mechanical Property Enhancement in Ceramic Matrix Composites", NIST IR in process, 1990.

Fuller, E. R., Jr., Butler, E. P., Krause, R. F., Jr., and Vaudin, M. D. "Structural Reliability and Damage Tolerance of Ceramic Composites for High Temperature Applications", NIST IR in process, 1990.

Handwerker, C. A., Deshmukh, U. V., and Cranmer, D. C. "Fabrication and Interface Debonding of Al_2O_3-Cr_2O_3-Cr Composites", in Metal & Ceramic Matrix Composites: Processing, Modeling, and Mechanical Behavior, R. B. Bhagat, A. H. Clauer, P. Kumar, and A. M. Ritter, Eds., TMS, Warrendale, 1990, pp. 457-465.

Monteiro, P. and Ostertag, C. "Analysis of the Aggregate-Cement Paste Interface Using Grazing Incidence X-ray Scattering", J. Cement and Concrete Research (International), 19, 929 (1989).

Ostertag, C. "Reduction in Sintering Damage of Fiber Reinforced Composites", in Sintering of Advanced Ceramics, C. A. Handwerker, J. E. Blendell, and W. A. Kaysser, Eds., Ceramic Transactions Volume 7, Amer. Ceram. Soc., Westerville, 1990, pp. 745-766, (1989).

Ostertag, C. and Malghan, S. "Stress Relaxation in Sintering of Fiber Reinforced Composites Through Fiber Coating", Cer. Eng. Sci. Proc., 10 [7-8] 730-734 (1989).

Ostertag, C. P., Charalambides, P. G., and Evans, A. G. "Observations and Analysis of Sintering Damage", in Sintering of Advanced Ceramics, C. A. Handwerker, J. E. Blendell, and W. A. Kaysser, Eds., Ceramic Transactions Volume 7, Amer. Ceram. Soc., Westerville, 1990, pp. 710-732.

Ostertag, C. P. "Differential Sintering", in Advances in Sintering, (1990), in press.

Ostertag, C. P., Charalambides, P. G., and Evans, A. G. "Analyses of Sintering Damage", Acta Matall, 37, [7], 2077, (1989).

Ostertag, C. P., Robins, L. H., and Cook, L. P. "Cathodoluminescence Measurements of Strained Alumina Single Crystals", submitted to Journal of the European Ceramic Society, 1990.

Creep and Creep Rupture

Chen, C.-F. and Chuang, T.-J. "Improved Analysis for Flexural Creep with Application to Sialon Ceramics", J. Am. Ceram. Soc., 73 [8], 2366-2373 (1990).

Chen, C.-F., Wiederhorn, S. M., and Chuang, T.-J. "Cavitation Damage During Flexural Creep of Sialon-Yag Ceramics", submitted to J. Am. Ceram. Soc., 1990.

Chuang, T.-J., Liu, W., and Wiederhorn, S. M. "Steady-State Creep Behavior of Si-SiC C-rings", submitted to J. Euro. Ceram. Soc., 1990.

Chuang, T.-J. and Mai, Y.-W. "Flexural Behavior of Strain-softening Solids", Int. J. Solid Structures, Vol 25, no. 12, 1427-1443 (1989).

Hockey, B. J. and Wiederhorn, S. M. "Effect of Creep on the Microstructure of Reaction Bonded Silicon Carbide", accepted for publication in J. Amer. Ceram. Soc., 1990.

Hockey, B. J., Wiederhorn, S. M., Liu, W., Baldoni, J. G., and Buljian, S.-T. "Tensile Creep of SiC Whisker Reinforced Silicon Nitride", in Proceedings of the 27th Automobile Technology Development Contractors' Coordination Meeting (ATD/CCM), October, 1989.

Krause, R. F., Jr. and Chuang, T.-J. "A Test Method for Tensile Creep of Structural Ceramics Using Flexure Beams", to be published in the Proceedings of the 7th CIMTEC World Ceramics Congress, P. Vincenzi, Ed., Elsevier, Amsterdam, 1990, in press.

Wiederhorn, S. M. and Hockey, B. J. "Tensile Creep of SiC Whisker Reinforced Silicon Nitride", submitted to J. Matl. Res., 1990.

Wiederhorn, S. M. and Hockey, B. J. "High Temperature Degradation of Structural Composites", to be published in the Proceedings of the 7th CIMTEC World Ceramics Congress, P. Vincenzi, Ed., Elsevier, Amsterdam, 1990, in press.

Wiederhorn, S., Hockey, B., and Carroll, D. "Creep of Two Phase Ceramics", in Sintering of Advanced Ceramics, C. A. Handwerker, J. E. Blendell, and W. A. Kaysser, Eds., Ceramic Transactions Volume 7, Amer. Ceram. Soc., Westerville, 1990, pp. 492-505.

Wiederhorn, S., Hockey, B., and Chuang, T.-J. "Crack Growth, Creep, and Creep Rupture at High Temperatures", to be published in the Proceedings of the NATO Advanced Research Workshop on Toughening Mechanisms in Quasi-Brittle Materials, 1990.

Wiederhorn, S. M., Hockey, B. J., Liu, W., Baldoni, J. G., and Buljian, S.-T. "Tensile Creep of Whisker Reinforced Silicon Nitride", accepted for publication in J. Mater. Sci., 1990.

Fracture and Microstructural Design

Bennison, S. J. and Lawn, B. R. "Role of Interfacial Grain-Bridging Sliding Friction in the Crack-Resistance and Strength Properties of Nontransforming Ceramics", Acta Metall, 37, 2659 (1989).

Bennsion, S. J. and Lawn, B. R. "Flaw Tolerance in Ceramics with Rising Crack-Resistance Characteristics", J. Mater. Sci., 24, 3169 (1989).

Bennison, S. J., Rodel, J., Lathabai, S., Chantikul, P., and Lawn, B. R. "Microstructure, Toughness Curves and Mechanical Properties of Alumina Ceramics", in Toughening Mechanisms in Quasi-Brittle Materials, Kluwer Academic Publishers, Dordrecht, The Netherlands, in press, 1990.

Chantikul, P., Bennsion, S., and Lawn, B. "Role of Grain Size in the Strength and R-Curve Properties of Alumina", J. Amer. Ceram. Soc., 73 2419 (1990).

Cho, S.-J., Hockey, B., Lawn, B., and Bennison, S. "Grain-Size Dependence of Brittle Wear of Ceramics with R-curve Behavior", J. Amer. Ceram. Soc., 72, 1249, (1989).

Chuang, T.-J., Shiue, S.-T., and Lee, S. "Asymmetric Tip Morphology of Creep Microcracks Growing Along Bi-material Interfaces", submitted to Phil Mag., 1990.

Lathabai, S. and Lawn, B. "Fatigue Limits in Noncyclic Loading of Ceramics with Crack Resistance Curves", J. Mater. Sci., 24, 4298 (1989).

Lathabai, S., Mai, Y., and Lawn, B. "Cyclic Fatigue Behavior of an Alumina Ceramic with Crack Resistance Curves", J. Amer. Ceram. Soc.,72, 1760 (1989).

Lathabai, S., Rodel, J., Dabbs, T., and Lawn, B. "Fracture Mechanics Model for Subthreshold Indentation Flaws I. Equilibrium Fracture", accepted for publication in J. Mater. Sci., 1990.

Lathabai, S., Rodel, J., Dabbs, T., and Lawn, B. "Fracture Mechanics Model for Subthreshold Indentation Flaws II. Nonequilibrium Fracture", accepted for publication in J. Mater. Sci., 1990.

Lathabai, S., Rodel, J., and Lawn, B. R. "Cyclic Fatigue from Frictional Degradation at Bridging Grains in Alumina", accepted for publication in J. Amer. Ceram. Soc., 1990.

Lawn, B. R. "Fundamental Condition for Existence of Microcrack Clouds in Monophase Ceramics", accepted for publication in J. Euro. Ceram. Soc., 1990.

Padture, N. P., Chan, H. M., Lawn, B. R., and Readey, M. J. "The Role of Crystallization of an Intergranular Glassy Phase in Determining Grain Boundary Residual Stresses in Debased Aluminas", Mater. Res. Soc. Sympos. Proc., 170, 245 (1990).

Rodel, J., Kelly, J., and Lawn, B. "In Situ Measurements of Bridged Crack Interfaces in the SEM", accepted for publication in J. Amer. Ceram. Soc., 1990.

Rodel, J., Kelly, J., Stoudt, M., and Bennsion, S. "A Loading Device for Fracture Testing of Compact Tension Specimens in the SEM", submitted to Scanning Microscopy, 1990.

Runyan, J. and Bennsion, S. "Fabrication of Flaw-Tolerant Aluminum Titanate-Reinforced Alumina", submitted to J. Mater. Sci., 1990.

Wan, K. T., Lathabai, S., and Lawn, B. R. "Crack Velocity Functions and Thresholds in Brittle Solids", accepted for publication in J. Euro. Ceram. Soc., 1990.

Glass Science and Technology

Behrens, E. G., Powell, R. C., and Blackburn, D. H. "Optical Applications of Laser-Induced Gratings in Eu-Doped Glasses", Applied Optics, 29 [11] 1619-1624 (1990).

Chuang, T.-J. and Fuller, E. R. "An Extended Charles-Hillig Theory for Stress Corrosion Cracking of Glass", submitted to J. Am. Ceram. Soc., 1990.

Chuang, T.-J., Tang, J., and Fong, J. "An Application of a Simple Technique for Estimating Errors of Finite Element Solutions Using a General Purpose Code", ASME PVP Vol. 185, 1990, pp. 105-115.

Cranmer, D. C., Freiman, S. W., Chuang, T.-J., Raynes, A. S., Siahatgar, S., and Aggarwal, I. "Design Diagrams For Heavy Metal Fluoride Glasses", to be published in High Power Laser Optical Components III, 1990.

Cranmer, D. C., Freiman, S. W., White, G. S., and Raynes, A. S. "Moisture- and Water-Induced Crack Growth in Optical Materials", in SPIE Proceedings of Symposium on Optical Surfaces Resistant to Severe Environments, 1990.

French, V. A., Powell, R. C., Blackburn, D. H., and Cranmer, D. C. "Refractive Index Gratings in Rare Earth-Doped Glasses", submitted to Journal of Applied Physics, 1990.

Hicho, G. E., Smith, L. C., Handwerker, C. A., and Kauffman, D. A. "Determination of the Prior-Austenitic Grain Size of Selected Steels Using a Molten Glass Etch", submitted to ASM Journal of Heat Treating, 1990.

Surface Forces

Finkelstein, Y., Wiederhorn, S. M., Hockey, B. J., Handwerker, C. A., and Blendell, J. E. "Migration of Sapphire Interfaces into Vitreous Bonded Aluminum Oxide", in Sintering of Advanced Ceramics, C. A. Handwerker, J. E. Blendell, and W. A. Kaysser, Eds., Ceramic Transactions Volume 7, Amer. Ceram. Soc., Westerville, 1990, pp. 258-279.

Horn, R. G., Smith, D. T., and Haller, W. "Surface Forces and Viscosity of Water Measured Between Silica Sheets", Chem. Phys. Letters, 162 (1989) 404-408.

Horn, R. G. and Smith, D. T. "Measuring Surface Forces to Explore Surface Chemistry: Mica, Sapphire and Silica", J. Non-Cryst. Solids, 120 (1990) 72-81.

Horn, R. G. "Surface Forces and their Action in Ceramic Materials", J. Amer. Ceram. Soc., 73, 1117-1135 (1990).

Horn, R. G. and Smith, D. T. "Surface Forces and Adhesion between Dissimilar Materials Measured in Various Environments", in Interfaces in Composites, C. G. Pantano and E. J. H. Chen, Eds., MRS Symposia Series, 170 (1990) pp. 3-9.

Horn, R. G. and Ninham, B. W. "Experimental Study of Solvation Forces", in Micellar Solutions and Microemulsions, S.-H. Chen and R. Rajagopalan, Eds., Springer-Verlag, New York (1990) pp. 81-97.

Horn, R. G. and Smith, D. T. "Analytic Solution for the General Three-Layer Interferometer", Applied Optics, in press (1990).

Smith, D. T. "Measuring Contact Charge Transfer at Interfaces: A New Experimental Technique", submitted to J. Electrostatics, 1990.

Wan, K. T. and Lawn, B. R. "Surface Forces at Crack Interfaces in Mica in the Presence of Capillary Condensation", accepted for publication in Acta Mater., 1990.

Wan, K. T., Aimard, N., Lathabai, S., Horn, R. G., and Lawn, B. R. "Interfacial Energy States of Moisture-Exposed Cracks in Mica", J. Mater. Res., 5 (1990) 172-182.

Super Conductivity

Choi, C. S., Prask, H. J., and Ostertag, C. P. "Texture Study of the Magnetically Aligned $YBa_2Cu_3O_7$ Type Materials by Neutron Diffraction", Of Crystal Growth, 22, 465-469 (1989).

TRIBOLOGY

Ceramic Wear Maps

Hsu, S. M., Lacey, P. I., and Lee, S. W. "Wear Mechanism Maps of Ceramics," Presented at the 1990 International Symposium on Industrial Tribology, Northwestern University, August 29-31, Chicago, IL, 1990. Submitted for STLE for publication.

Hsu, S., "Tribology of Advanced Ceramics," Proceedings of the NBS/BAM 1986 Symposium on Advanced Ceramics, NIST SP766, pp. 144-163, May 1989.

Hsu, S. M., Lim, D. S., and Munro, R. G., "Ceramic Wear Maps," Proceedings of the 3rd International Symposium, "Ceramic Materials and Components for Engines," ACerS, pp. 1236-1245. 1989.

Hsu, S. M., Wang, Y. S., Munro, R. G., "Quantitative Wear Maps as a Visualization of Wear Mechanism Transitions in Ceramic Materials," Wear, 134, 1-11, 1989.

Hsu, S. M., Lim, D. S., Wang, Y. S., and Munro, R. G., "Ceramic Wear Maps; Concepts and Method Development, accepted for publication in Tribology Trans.

Wang, Y. S., Hsu, S. M., and Munro, R. G., "Ceramic Wear Maps: Alumina Under Various Conditions, accepted for publication in Tribology Trans.

Lim, D. S., Ye, B. W., Hsu, S. M., "Brittle Ductile Transition in Frictional Sliding of Single Crystal silicon and Alumina, submitted to the J. of Cermaic Science.

Lee, S. W., Hsu, S. M., and Munro, R. G., "Ceramic Wear Maps: SiC Whisker Reinforced Alumina, proceedings of the ASM Tribology of Composites Materials, Oak Ridge, TE, May 1-3, 1990.

Cho, S. J., H. Moon, Hockey, B. J., and Hsu, S. M., "Wear Transition Mechanism in Alumina during Sliding, submitted to Metallurgica Ecta.

Zhang, P. Y., and Hsu, S. M., "The Mechanisms of Some Antioxidants on Lubricant Oxidation Using Chemiluminescence Techniques," to be published in Tribology Trans., of STLE.

Hsu, S. M., Klaus, E. E., Chang, H. S., Lacey, P., Shen, M. C., Ying, T., and Chao, K. K., "A Mechano-chemical Model: Reaction Temperatures in a Concentrated Contact," submitted to the J. of Tribology.

Wear Mechanisms of Advanced Ceramics

Deckman, D. E., Jahanmir, S. and Hsu, S. M. "Wear Mechanisms of Alpha-Alumina Lubricated with a Paraffin Oil", submitted for International Conference on Wear of Materials, 1991.

Dong, X., Jahanmir, S., and Hsu, S. M. "Tribological Characteristics of Alpha-Alumina at Elevated Temperatures", submitted to J. Am. Cer. Soc.

Gates, R. S. and Hsu, S. M. "Tribochemical Mechanism of Alumina with Water", Tribology Trans., 32, 3, 357-363, 1989.

Hsu, S. M., Lim, D. S., Wang, Y. S., and Munro, R. G. "Ceramic Wear Maps: Concepts and Method Development", STLE, in press.

Jahanmir, S., Deckman, D. E., Ives, L. K., Feldman, A., and Farabaugh, E. "Tribological Characteristics of Synthesized Diamond Films on Silicon Carbide", Wear, 133, 73-81, 1989.

Wang, Y. S., Hsu, S. M., and Munro, R. G. "Ceramic Wear Maps: Alumina", STLE, in press.

Whitenton, E. P. and Deckman, D. E. "Measuring Matching Wear Scars on Balls and Flats", Surface Topography, 2, 205-222, 1989.

Tribology of Self-Lubricating Composites

Gangopadhyay, A. and Jahanmir, S. "Control of Friction and Wear of Alpha-Alumina with a Composite Solid-Lubricant Coating", ASM Symposium on Composites, April 1990.

Gangopadhyay, A. and Jahanmir, S. "Friction and Wear Characteristics of Silicon-Nitride-Graphite and Alumina-Graphite Composites", to be published in Tribology Trans. 1990.

Gangopadhyay, A., Jahanmir, S., and Hegemann, B. E. "Reduction in Friction Coefficient in Sliding Ceramic Surfaces by In-Situ Formation of Solid Lubricant Coatings", Mechanics of Coatings Conference, 1990.

Ruff, A. W. and Peterson, M. B. "Wear Mechanisms in Self-Lubricating Metal Matrix Composites", Proceedings of ASM Conference on Tribology of Composite Materials, Oak Ridge, TN, May 1990, in press.

Tribological Films and Coatings

Ruff, A. W. "Considerations on Data Requirements for Tribological Modeling", Proceedings of ASTM Symposium on Wear Modeling, San Francisco, CA, May 1990, in press.

Ruff, A. W. "Modified Surface Layers and Coatings", Tribology: Soviet and American Approaches in Research and Application, Allerton Press, New York, NY, 1990, in press.

Ruff, A. W. and Wang, Z. X. "Sliding Wear Studies of Nickel-Copper Composition-Modulated Coatings on Steel", Wear, 131, 259-272, 1989.

Fracture Mechanics Analysis of Near-Surface Cracks

Dally, J. W., Cheng, Y.-M., and Jahanmir, S. "Analysis of Subsurface Crack Propagation and Implications on Wear of Elastically Deforming Materials", to be published in Wear, 1990.

Jahanmir, S., Dally, J. W., and Chen, Y.-M. "Fracture Mechanics Analysis of Near-Surface Cracks", Proceedings of Japan International Tribology Conference, Nagoya, 1990.

Advanced Liquid Lubricants

Gates, R. S., Jewett, K. L., and Hsu, S. M. "A Study on the Nature of Boundary Lubricating Film: Analytical Method Development", STLE Tribology Trans., 32, 4, 423-430, 1989.

Perez, J. M., Ku, C. S., Pei, P., Hegemann, B. E., and Hsu, S. M. "Characterization of Tricresylphosphate Lubricating Films by Micro-Fourier Transform Infrared Spectroscopy", Tribology Trans., 33, 1, 131-139, 1990.

Zhang, Y., Pei, P., Perez, J. M., and Hsu, S. M. "A New Method to Evaluate Deposit Forming Tendencies of Liquid Lubricants by Differential Scanning Calorimetry", submitted to STLE for publication.

Zhang, Y., Perez, J. M., Pei, P., and Hsu, S. M. "The Deposit Forming Tendencies of Diesel Engine Oils -- Correlation Between The Two-Peak Method and Engine Tests", submitted to STLE for publication.

Hsu, S. M., Pei, P., Ku, C. S., Lin, R. S., and Hsu, S. T., "Mechanisms of Additive Effectiveness," Lub. Sci., 1, 2, 165-184, 1989.

A Computerized Tribology Information System

Jahanmir, J., Hsu, S. M., and Munro, R. G. "ACTIS: Towards A Comprehensive Tribology Database", *Computerization and networking of Materials Data Bases*, ASTM STP 1017, J. S. Glazman and J. R. Rumble, Eds., 1989.

Jahanmir, S. and Peterson, M. B. "Development and Use of a Tribology Research-in-Progress Database", Lubrication Engineering, March 1990.

Ruff, A. W. "Tribomaterials I Database - Technical Manual", NSRDS Special Publication, Database 22, November 1989.

Ruff, A. W., Rumble, J., and Jahanmir, S. "A Numeric Database for Tribology: Format and Application Issues", Proceedings of the Second International Symposium on Computerization of Materials Property Data, ASTM E-49, Orlando, FL, November 30, 1989, in press.

Standards and Measurement Activities

Ruff, A. W. "Comparison of Standard Test Methods for Non-Lubricated Sliding Wear", Wear, *134*, 49-57, 1989.

ELECTRONIC MATERIALS GROUP

Molecular Orbital Calculations of Strained Si-O Bonds

Wong-Ng, W. W., White, G. S., and Freiman, S. W. "Molecular Orbital Calculations of Strained Silica", submitted to WERB 8/90.

Wong-Ng, W. W., White, G. S., and Freiman, S. W. "Molecular Orbital Calculations of Bond Rupture in Brittle Solids", Proceedings at the Frontiers of Chemistry: Materials by Design, November 1990.

Wong-Ng, W. W., White, G. S., and Freiman, S. W. "Molecular Orbital Study of Water Enhanced Crack Growth Process", MRS Proceedings.

Cyclic Loading of PZT

Raynes, A., White, G., and Freiman, S. "Electric Field Effects on Crack Growth in a PMN Ceramic", Proceeding of the American Ceramic Soc., Anaheim, CA, November 1989.

Superconducting Ceramics: Crystal Chemistry and Phase Equilibria Studies

Wong-Ng, W., Cook, L., Hill, D., Paretzkin, B., and Fuller, E. "Crystal Chemistry and Phase Equilibrium Studies of the BaO ($BaCO_3$)-R_2O_3)-R_2O_3-CuO Systems. V. Melting Relations in the $Ba_2RCU_3O_{6+x}$ (R=Nd, Eu, Y) and Ba_2 (Y, Nd, Eu)Cu_3O_{6+x} Systems", Proceedings of meeting, Boston, MA (1989).

Cook, L., Chiang, C., Wong-Ng, W., Swartzendruber, L., and Bennett, L. "Phase Equilibria in the System Tl-Ca-Ba-Cu-O. I. Stability of the 2122 Phase Under Conditions of Oxygen Annealing", submitted to Mat. Research Soc., Annual Meeting, Boston, MA (1989).

Wong-Ng, W. W., Gayle, F., Kaiser, D., Watkins, S. F., and Franzek, F. "X-ray Crystallographic Studies of a Thermomechanically Detwinned Single Crystal of $Ba_2YCu_3O_{6+x}$", Phys Rev B, Vol. 41, p. 4220 (1990).

Wong-Ng, W. W., Paretzkin, B., and Fuller, E. R., Jr. "Crystal Chemistry and Phase Equilibria Studies of the BaO-R_2O_3-CuO systems. V. Crystal chemistry and sub-solidus phase relationship studies of the CuO-rich region of the ternary diagrams, R=lanthanides", J. Solid State Chemistry, Vol. 85, p. 117-132 (1990).

Chiang, C. K., Freiman, S. W., Wong-Ng, W. W., Cook, L. P., Shull, R. D., and Shapiro "Preparation of Bi-Pb-Sr-Ca-Cu-O superconducting composites using glass technology", Physica C Vol. 162-164, p. 901-902 (1989).

Wong-Ng, W. W., Paretzkin, B., and Fuller, E. R., Jr. "Crystal Chemistry and Phase Equilibria Studies of the BaO-R_2O_3-CuO systems", Advances in X-ray Analysis, Vol. 33, p. 453 (1990).

Wong-Ng, W. W., Paretzkin, B., and Fuller, E. R., Jr. "Crystal Chemistry and Phase Equilibria Studies of the BaO-R_2O_3-CuO systems. III. X-ray Powder Characterization and diffraction patterns of $BaR_3Cu_6O_{14+x}$, R=lanthanides", Powder Diffraction, Vol. 5, (No. 1) p. 26 (1990).

Kaiser, D., Gayle, F., Swartzendruber, L., Wong-Ng, W. W., Watkins, S. F., and Franzek, F. "Structural and magnetic properties of untwinned $YBa_2Cu_3O_{6+x}$ single crystals", in MRS symposium Proceedings: HIGH-TEMPERATURE SUPERCONDUCTORS: FUNDAMENTAL PROPERTIES AND NOVEL MATERIALS PROCESSING, Vol. 169, p. 793-796 (1990).

Wong-Ng, W. W., Cook, L. P., Paretzkin, and B., Fuller, E. R., Jr. "Crystal Chemistry and Phase equilibrium studies of the BaO($BaCO_3$)-R_2O_3-CuO systems. V. Melting relations in $Ba_2(Y,Nd,Eu)Cu_3O_{6+x}$", in MRS symposium Proceedings: HIGH-TEMPERATURE SUPERCONDUCTORS: FUNDAMENTAL PROPERTIES AND NOVEL MATERIALS PROCESSING, Vol. 169, p.81-86 (1990).

Wong-Ng, W. W., Chiang, C. K., Hwang, N. M., Freiman, S. W., Hill, M. D., and Cook, L. P. "X-ray Characterization of the crystallization process of high-T_c Superconducting oxides in the Sr-Bi-Pb-Ca-Cu-O system", in MRS symposium Proceedings: HIGH-TEMPERATURE SUPERCONDUCTORS: FUNDAMENTAL PROPERTIES AND NOVEL MATERIALS PROCESSING, Vol. 169, p. 123-128 (1990).

Stalick, J. and Wong-Ng, W. W. "Neutron diffraction study of the "brown phase" $BaNd_2CuO_5$", Materials Letters, Vol. 9, No. 10, p. 401 (1990).

Cook, L. P., Wong-Ng, W. W., Chiang, C. K., and Bennett, L. H. "Effects of synthesis conditions on the formation of the 2122 (Tl:Ca:Ba:Cu) high T_c phase", Ceramic Transactions, "Superconductivity and Ceramic Superconductors," Vol. 13, p. 329, K. M. Nair and E. A. Giess, Eds., The American Ceramic Society, Inc., (1990).

Wong-Ng, W. W., Chiang, C. K., Freiman, S. W., Cook, L. P., Hwang, N. M., and Hill, M. D. "Phase formation in the Pb-doped Bi-Sr-Ca-Cu-O glass ceramics", Ceramic Transactions, "Superconductivity and Ceramic Superconductors," Vol. 13, p. 115, K. M. Nair and E. A. Giess, Eds., The American Ceramic Society, Inc., (1990).

Cook, L. P., Chiang, C. K., Wong-Ng, W. W., and Bennett, L. H. "Phase equilibria in the system Tl-Ca-Ba-Cu-O. I. Stability of the 2122 phase under conditions of oxygen annealing", in MRS symposium Proceedings: HIGH-TEMPERATURE SUPERCONDUCTORS: FUNDAMENTAL PROPERTIES AND NOVEL MATERIALS PROCESSING, Vol. 169, (1990), in press.

Phase Equilibria

Roth, R., Rawn, C., Burton, B., and Beech, F. "Phase Equilibria and Crystal Chemistry in Portions of the System SrO-CaO-Bi_2O_3-CuO, Part II- The System SrO-Bi_2O_3-CuO", NIST, Journal Research 95, [3], 291-335, (1990).

Roth, R., Rawn, C., and Ritter, J. "$Ca_{1-x}CuO_2$, a $NaCuO_2$ - typed related structure", submitted to Chem. of Mat. 2, [2], 192-194 (1990).

Roth, R. S., Rawn, C. J., and Burton, B. "Phase Equilibria and Crystal in Portions of the System SrO-CaO-Bi_2O_3-CuO, Part III - Preliminary Phase Diagrams for the Ternary Systems SrO-Bi_2O_3-CuO, CaO-Bi_2O_3-CuO and SrO-CaO-Bi_2O_3", Proceedings of the First International Ceramic Science and Technology Congress, Anaheim, CA. Ceramic Transactions, Vol. 13 "Superconductivity and Ceramic Superconductors", Am. Ceram. Soc., Westerville, OH, p. 23-34 (1990).

Hwang, N. M., Roth, R. S., and Rawn, C. J. "Phase Equilibria in the Systems SrO-CuO and SrO-½Bi_2O_3", J. Am. Ceram. Soc. Vol. 72 [8] p. 2531-33 (1990).

Siegrist, T., Roth, R. S., Rawn, C. J., and Ritter, J. "$Ca_{1-x}CuO_2$, a $NaCuO_2$-type Related Structure", Chem. of Mater. Vol 2 [2], p. 192-194 (1990).

Rawn, C. J., Roth, R. S., and McMurdie, H. "Improved Crystallographic Data on $AlNbO_4$", accepted by Powder Diffraction, JCPDS PDF, Set 41, (1990).

Parise, J., Torardi, C., Whangbo, M., Rawn, C. J., Roth, R. S., and Burton, B. "$Ca_4Bi_6O_{13}$, A Compound Containing Unusual Bi - Coordination and Short Bi---Bi Contacts", Chem. of Mat., Vol. 2 [4], p. 454-458 (1990).

Hwang, N. M., Roth, R. S., Rawn, C. J., and Ritter, J. "Phase Equilibria in the Systems CaO-CuO and CaO-½Bi_2O_3", Werb Approved.

Roth, R. S., Rawn, C. J., and Hill, M. D. "Synthesis and Characterization of Phases in the System Ba-Au-Ag-O", to be published in proceedings of the conference, Chemistry of Electronic Ceramic Materials, Jackson, WY, Aug. 17-23, 1990, R. S. Roth, P. K. Davies and R. J. Cava, Eds., to be published as NIST-SP (1990).

Roth, R. S., Rawn, C. J., and Bendersky, L. A. "Crystal Chemistry of the Compound $Sr_2Bi_2CuO_6$", J. Mater. Res., Vol 5, [1], p. 46-52 (1990).

Roth, R. S. "User Aspects of Phase Equilibria in High T_c Ceramic Superconductors", accepted for publ. in Proceedings of the Conference User Aspects of Phase Diagrams, June 25-27, 1990., JRC Petten, Netherlands, to be published by The Institute of Metal, London, G.B. (1990).

Bendersky, L. A., Roth, R. S., Ramon, J. T., and Shechtman, D. "Crystallographic Characterization of Some Intermatallic Compounds in the Al-Cr System", submitted to Met. Trans. A. April 5, (1990).

Ceramic Phase Equilibria Program

Mysen, B., McMurdie, H., and Ondik, H. "Phase Diagrams for Ceramists-Volume VIII", published, American Ceramic Society (1990).

Clevinger, M., Russell, K., Messina, C., and Ondik, H. "Phase Diagrams for Ceramists-Bibliographic Undate through January 1, 1988 and Cumulative Indexes for Volumes I-VIII", submitted to American Ceramic Society, (1990).

Cook, L. P. and McMurdie, H. F., Eds., "Phase Diagrams for Ceramists, Volume VII", Amer. Ceram. Soc., Westerville, Ohio, 591 p. (1989).

Processing High T_c Superconductors

Chiang, C., Freiman, S., Wong-Ng, W., Cook, L., and Shull, R. "A Glass Ceramic Containing High T_c Superconductors", submitted to Phys. and Chem. of Glass, 1989.

Turchinskaya, M., Bennett, L. H., Swartzendruber, L. J., Roitburd, A., Chiang, C. K., Hill, M. D., Blendell, J. E., and Sawano, K. "Comparison of Dynamics in Two Samples of $YBa_2Cu_3O_7$ with Different Pinning", MRS Proceedings (1990).

Johnson, W., Kahn, A. H., Chiang, C. K., and Wadley, H. N. G. "Eddy Current Sensing of Oxygen Content in High T_c Superconductors", Progress in Quantative NDE Conference, Vol. 9B, in Plenum Press, p. 2085-2090 (1990).

Chiang, C. K., Turchinskaya, M., Swartzendruber, L. J., Shull, R. D., and Bennett, L. H. "Levitation of Superconducting Composites", Adv. in Materials Sci. Appl. of High Temp. Superconductors, (1990).

Chiang, C. K., Freiman, S. W., Wong-Ng, W. W., Hwang, N. M., Hill, M. D., Cook, L. P., Shull, R. D., Shapiro, A. J., Shapiro, L. J., Swartzendruber, L. J., and Bennett, L. H. "Bi-Pb-Sr-Ca-Cu-O Superconductors Processed from the Amorphous State", Adv. in Materials Sci., Appl. of High Temp. Superconductors, (1990).

Wong-Ng, W. W., Chiang, C. K., Freiman, S. W., Cook, L. P., Hwang, N. M., and Hill, M. D. "Phase Formation in the Pb-Doped Bi-Sr-Ca-Cu-O Glass Ceramics", K. M. Nair and E. A. Geiss, Eds., Ceramic Transactions, Vol. 13, Superconductivity and Ceramic Superconductor, p. 115 (1990).

Mechanical Reliability

Block, S., Piermarini, G. J., Bean, V., and Raynes, A. "Pressure Sintering and Transformation of Zinc Sulfide", Mat. Sci. and Eng., Vol. A127 p. 99.104 (1990).

Raynes, A. S., White, G. S., Freiman, S. W., and Rawal, B. S. "Electric Field Effects on Crack Growth in a Lead Magnesium Niobate Ceramic", Proceedings of Anaheim Meeting of Am. Cer. Soc. 1989.

Cranmer, D. C., Freiman, S. W., White, G. S., and Raynes, A. S. "Moisture- and Water-Induced Crack Growth in Optical Materials", Proceedings of SPIE 1990 International, Symposium on Optical & Optoelectronic, Applied Science and Engineering

High Temperature Chemistry

Cook, L., Bonnell, D., and Rathnamma, D. "Model for Molton Salt Corrosion of Ceramics", Proceedings of International Sym. on Corrosion and Corrosive Degradation of Ceramics, Nov. 1-2, Anaheim, CA (1989).

Cook, L. P., Bonnell, D. W., and Rathnamma, D. "Model for Molten Salt Corrosion of Ceramics", p. 251-275 in M. McNallan and R. Tresslen, Eds., Corrosion and Corrosive Degradation of Ceramics, Ceram. Trans. Vol. 10, Amer. Ceram. Soc., Westerville, OH (1990).

Cook, L. P., Plante, E. R., Bonnell, D. W., and Hastie, J. W. "Reaction of Liquid Al with Gaseous ClO_3F", High Temp. Sci. 28, p. 293-312 (1990).

Plante, E. R. and Cook, L. P. "Vapor Pressure and Thermodynamics of Lithium Aluminates", p. 129-145 in G. W. Hollenberg and I. J. Hastings, Eds., Fabrication and Properties of Lithium Ceramics II, Adv. in Ceram. Vol. 27, Amer. Ceram. Soc., Westerville, OH (1990).

Cook, L. P. "Phase Equilibria of Alumina", p . 49-71 in L. D. Hart, Ed., Alumina Chemicals; Science and Technology Handbook, Amer. Ceram. Soc., Westerville, OH, p. 611 (1990).

Thin Film Ferroelectrics

Chiang, C., Cook, L., Schenck, P., Brody, P., and Benedetto, J. "Lead Zirconate-Titanate Thin Films Prepared by The Laser Ablation Technique", Proceedings of Mat. Research Soc., (1990).

Cook, L., Schecnk, P., Chiang, C., Wong-Ng, W., Brody, P., Benedetto, J., Rod, B., and Bennett, K. "Microstructure and Ferroelectric Properties of Lead Zirconate-Titanate Films Produced by Laser Evaporation", Proceedings of the IEEE International Sym. on Ferroelectric (1990).

Cook, L. P., Schenck, P. K., Zhao, J., Farabaugh, E., and Vaudin, M. "Ceramic Thin Films by Laser Deposition", p. 99-117 in B. V. Hiremath, Ed., Ceramic Thin and Thick Films, Ceram. Trans. Vol. 11, Amer. Ceram. Soc., Westerville, OH, p. 464 (1990).

Schenck, P. K., Cook, L. P., Zhao, J., Hastie, J. W., Farabaugh, E. W., Chiang, C. K., Vaudin, M., and Brody, P. S. "Laser Vaporization and Deposition of Lead Zirconate Titante", p. 587-592 in J. A. Knapp, P. Borgesen, and R. A. Zuhr, Eds., Beam-Solid Interactions: Physical Phenomena, Mat. Res. Soc., Symp. Proc. Vol. 157, Pittsburgh, PA, p. 872 (1990).

Energetic Materials

Piermarini, G. J., Block, S., and Miller, P. J. "Chemistry and Physics of Energetic Materials", NATO ASI SERIES, Surya N. Bulusu, Ed., Kluwer Academic Publishers, Dordrecht, The Netherlands, Vol. 309, p. 369-89 (1990).

Piermarini, G. J., Block, S., and Miller, P. J. "Chemistry and Physics of Energetic Materials", NATO ASI SERIES, Surya N. Bulusu, Ed., Kluwer Academic Publishers, Dordrecht, The Netherlands, Vol. 309 p. 391-412 (1990).

Ceramic Processing

(Book edited): Blendell, J. E., Handwerker, C., and Kaysser "Ceramic Transaction", Vol. 7, Sintering of Advanced Ceramics (1990).

(Article in Book edited): Finkelstein, Wiederhorn, Hockey, Handwerker, and Blendell "Migration of Sapphire Interfaces into Vitreous Bonded Aluminum Oxide", in Ceramic Transaction, Vol. 7. (1990). Not yet submitted.

OPTICAL MATERIALS

Feldman, A. Status and Applications of Diamond and Diamond-Like Materials: An Emerging Technology, chapter on "Applications", National Materials Advisory Board, Commission on Engineering and Technical Systems, National Research Council, MNAB-445, National Academy Press, 1990.

Jahanmir, S., Deckman, D. E., Ives, L. K., Feldman, A., and Farabaugh, E. "Tribological Characteristics of Synthesized Diamond Films on Silicon Carbide", Wear, 133, 73-81 (1989).

Feldman, A., Robins, L. H., Frederikse, H. P. R., Farabaugh, E. N., and Etz, E. "Physical and Chemical Properties of Chemical Vapor Deposited (CVD) Diamond", in Proceedings of the First International Symposium on Diamond and Diamond-Like Films, J. P. Dismukes et al, Eds. (The Electrochemical Society, Inc., Pennington, NJ, 1989) pp.162-72.

Farabaugh, E. N. and Feldman, A. "Effects of Different CH_4-H_2 Gas Compositions on the Morphology and Growth of Diamond Grown by Hot Filament CVD", Mat. Res. Soc. Proc. 162, 127 (1990).

Etz, E. S., Schrolder, T., Farabaugh, E. N., Robins, L. H., and Feldman, A. "Laser-induced Optical Emissions of CVD Diamond Studies In The Raman Microprobe", in Diamond Optics II, A. Feldman and S. Holly, Eds., SPIE Vol. 1146 (1989).

Feldman, A., Frederikse, H. P. R., and Ying, X. T. "Thermal Wave Measurements of the Thermal Properties of CVD Diamond", in Diamond Optics II, A. Feldman and S. Holly, Eds., SPIE Vol. 1146, 78-84 (1989).

Robins, L. H., Cook, L. P., Farabaugh, E. N., and Feldman, A. "Cathodoluminescence Imaging and Spectroscopy of CVD Diamond in a Scanning Electron Microscope", in Diamond Optics II, A. Feldman and S. Holly, Eds., SPIE Vol. 1146, 166 (1989)

Frederikse, H. P. R., Ying, X. T., and Feldman, A. "Thermal Diffusivity of Thin Diamond Films", Proceedings of the 6th International Topical Meeting on Photoacoustic and Photothermal Phenomena, in press.

Feldman, A., Frederikse, H. P. R., and Norton, S. J. "Analysis of Thermal Wave Propagation in Diamond Films", in SPIE Vol. 1325 - Diamond Optics III, in press.

Robins, L. H., Farabaugh, E. N., and Feldman, A. "Lineshape analysis of the Raman Spectrum of Diamond Films grown by Hot-Filament and Microwave-Plasma Chemical Vapor Deposition", Journal of Materials Research (1990), in press.

Robins, L. H., Farabaugh, E. N., and Feldman, A. "Studies of Defects in Diamond Films and Particles by Raman and Luminescence Spectroscopies", in Diamond Optics III, A. Feldman and S. Holly, Eds., Proceedings of the SPIE, in press.

Robins, L. H., Farabaugh, E. N., Feldman, A., and Cook, L. P. "Inverse Correlation between the Intensity of Luminescence excited by Electrons and by visible light in CVD Diamond Films", to be submitted to Journal of Applied Physics.

Robins, L. H., Tjossem, P. J. H., Smyth, K. C., Barnes, Y., Farabaugh, E. N., and Feldman, A. "Photoluminescence excitation in CVD Diamond Films by Bandgap Optical Absorption", to be submitted to Physical Review B.

Robins, L. H., Farabaugh, E. N., Feldman, A., and Whitenton, E. P. "Structure and Optical Properties of Diamond Films grown on Substrates with a High Density of Nucleation Sites", to Proceedings of the Second International Conference on New Diamond Science and Technology; also to Journal of Material Research (in an expanded version).

Robins, L. H., Cook, L. P., Farabaugh, E. N., and Feldman, A. "Cathodoluminescence Image contrast in Monocrystalline Diamond Particles grown by Hot-Filament CVD", to Journal of Materials Research.

Ostertag, C. P., Robins, L. H., and Cook, L. P. "Cathodoluminescence measurements of Strained Alumina Single Crystals", to Journal of the European Ceramics Society.

Farabaugh, E. N., Feldman, A., and Robins, L. H. "Influence of Filament Geometry on the CVD Hot Filament Growth of Diamond Films", (completion projected Sept. 1990).

Robins, L. H., Whitenton, E. P., Farabaugh, E. N., and Feldman, A. "Structure and Optical Properties of Diamond Films grown on Substrates with High Density of Nucleation Sites", (completion projected Sept. 1990).

Feldman, A., Frederikse, H. P. R., and Norton, S. J. "Thermal Wave Propagation in Diamond Films", (completion projected Sept. 1990).

Superconducting $YBa_2Cu_3O_{6+x}$ Crystals

Swartzendruber, L. J., Roitburd, A., Kaiser, D. L., Gayle, F. W., and Bennett, L. H. "Direct Evidence for an Effect of Twin Boundaries on Flux Pinning in Single-Crystal $YBa_2Cu_3O_{6+x}$", Phys. Rev. Lett 64, 483 (1990).

Roitburd, A., Swartzendruber, L. J., Kaiser, D. L., Gayle, F. W., and Bennett, L. H. "Temperature Dependence of Vortex-Twin Boundary Interaction in $YBa_2Cu_3O_{6+x}$", Phys. Rev. Lett. 64, 2962 (1990).

Bennett, L. H., Swartzendruber, L. J., Kaiser, D., Bohandy, J., Kim, B. F., Adrian, F. J., and Moorjani, K. "SQUID and MAMMA Observations of the Superconducting Transition in Single Crystals of $YBa_2Cu_3O_{7-x}$", J. Appl. Phys. 67 (9), 5044 (1990).

Wong-Ng, W., Gayle, F. W., Kaiser, D. L., Watkins, S. F., and Fronczek, F. R. "X-ray Diffraction Study of a Thermomechanically Detwinned Single Crystal of $YBa_2Cu_3O_{6+x}$", Phys. Rev. B 41, 4220 (1990).

Kaiser, D. L., Gayle, F. W., Swartzendruber, L. J., Wong-Ng, W., Watkins, S. F., and Fronczek, F. R. "Structural and Magnetic Properties of Untwinned $YBa_2Cu_3O_{6+x}$ Single Crystals", High Temperature Superconductors: Fundamental Properties and Novel Materials Processing, Vol. 92 (Materials Research Society, Pittsburgh, PA, 1990), in press.

Kaiser, D. L., Swartzendruber, L. J., Gayle, F. W., and Bennett, L. H. "Lower Critical Field Measurements in $YBa_2Cu_3O_{6+x}$ Single Crystals", Proceedings of the AMSAHTS (Advances in Materials Science and Applications of High Temperature Superconductors) 1990 Meeting, NASA Publication, in press.
Gillen, G., Kaiser, D. L., and Wallace, J. S. "Image Depth Profiling SIMS: An Evaluation for the Analysis of ^{18}O Diffusion in $YBa_2Cu_3O_{7-x}$ Single Crystal Superconductors", Surface and Interface Analysis, in press.

Babcock, S. E., Cai, X. Y., Kaiser, D. L., and Larbalestier, D. C. "Weak-link-free Behavior of High-Angle $YBa_2Cu_3O_{7-x}$ Grain Boundaries at High Fields", Nature, in press.

Gayle, F. W. and Kaiser, D. L. "The Nature of [001] Tilt Boundaries in $YBa_2Cu_3O_{6+x}$", F. W. Gayle and D. L. Kaiser, to be submitted to Journal of Materials Research.

Optical Properties Measurement and Thin Films

Feldman, A., Ying, X. T., and Farabaugh, E. N. "Optical Properties of Mixed Yttria-Silica Films", Appl. Opt. 28, 5229 (1989).

Ying, X. T., Feldman, A., and Farabaugh, E. N. "Fitting of Transmission Data for Determining the Optical Constants and Thicknesses of Optical Films", J. Appl. Phys. 67, 2056-9 (1990).

Schenck, P. K., Cook, L. P., Zhao, J., Hastie, J. W., Farabaugh, E. N., Chiang, C. K., Vaudin, M. D., and Brody, P. S. "Laser Vaporization and Deposition of Lead Zirconate Titanate", Mat. Res. Soc. Symp. Proc. 157, 587 (1990).

Cook, L. P., Schenck, P. K., Zhao, J., Farabaugh, E. N., and Chiang, C. K. "Ceramic Thin Films By Laser Deposition", Proceedings of Thick and Thin Films Symposium, American Ceramic Society 1989, in press.

McClain, M., Feldman, A., Kahaner, D., and Ying, X. T. "An Algorithm and Computer Program for the Calculation of Envelope Curves", Computers in Physics, in press.

SYNCHROTRON RADIATION

Kuriyama, M., Black, D., Burdette, H., and Spal, R. "Diffraction Imaging of Polycrystalline Materials", J. Mat. Res. (1990).

Kuriyama, M. "Materials Science With SR Using X-ray Imaging -- Spatial Resolution/Source Size", Nuclear Instr. and Methods, Dec. (1990).

Kuriyama, M., Dobbyn, R., and Spal, R. "High Resolution Hard X-ray Microscope", The Rigaku Journal, 19 (1990).

Kuriyama, M., Dobbyn, R., Burdette, H., Spal, R., and Black, D. "Hard X-ray Microscope with Submicron Spatial Resolution", J. Res. NIST, 95 (1990).

Steiner, B., Kuriyama, M., and Dobbyn, R. "Insight Into the Genesis of Irregularity During Crystal Growth Achieved Through High Sensitivity Monochromatic Synchrotron X-Radiation Diffraction Imaging (Topography)", Prog. in Crystal Growth and Charact. (1989).

STRUCTURAL CERAMICS DATABASE

System Development

Munro, R. G. and Hubbard, C. R. "Property Database for Gas-Fired Applications of Ceramics", Ceramic Bulletin, Vol. 68, No. 12 (1989).

Munro, R. G., Begley, E. F., and Baker, T. L. "Strengths and Deficiencies in Published Advanced Ceramics Data", Ceramic Bulletin, Vol. 69, No. 9 (1990).

Begley, E. F. and Munro, R. G. "An Overview of the Structural Ceramics Database", NIST SP 787 (1990).

Begley, E. F. and Munro, R. G. "User's Guide to the Structural Ceramics Database", NISTIR 90-4366 (1990).

Begley, E. F. and Munro, R. G. "The Structural Ceramics Database Version SCSN 1.0", Standard Reference Database Number 30 (1990).

Munro, R. G. and Begley, E. F. "Materials Property Database Requirements for Gas-Fueled Ceramic Heat Exchangers", ASTM STP 1106 (1990).

Munro, R. G. and Begley, E. F. "Computerization of Materials Property Data for Composite Ceramics", NASA-ITAR Report (1990).

Munro, R. G. and Begley, E. F. "The Structural Ceramics Database: Data Acquisition Format for Monolithic Ceramics".

Begley, E. F. and Munro, R. G. "The Structural Ceramics Database: Design and Implementation"

CERAMICS DIVISION PATENTS

1990

Novel Synergistic Additive Packages Containing High Molecular Weight Antioxidants for High Temperature Lubricants	S. Hsu J. Perez C. Ku Y. Zhang
Low Energy (Thermal) Neutron Absorbing Glass	D. Blackburn (Retired) C. Stone D. Cranmer
Phosphorous Containing Boundary Lubrication Antiwear Additives for Silicon Nitride Ceramic Materials	R. Gates S. Hsu
Process for Elimination of Twins in Perovskite-Type Superconducting Single Crystals	D. Kaiser F. Gayle
A Method for Fabrication of Materials from Nano-Sized Particles Using High Pressure and Cryogenic Temperatures	A. Pechenik G. Piermarini
Method to Make Transparent Si_3N_4 at Low Temperature Without Additives	A. Pechenik G. Piermarini S. Block

1989

Ultraviolet Transmitting Glass for 308mm Ring Dye Laser	D. Blackburn D. Cranmer D. Kauffman
Buffered Cell for Sintering of High T_c Thallium Containing Ceramics	L. Cook
Polished Plates of Chemical Vapor Deposited Diamond	A. Feldman E. Farabaugh
Diamond Coated Infrared Transmitting Optics	A. Feldman
Additive Packages Containing High Molecular Weight Antioxidants for High Temp Lubricant	S. Hsu J. Perez C. Ku
Fluid to Solubilize High Temperature Liquid Lubricant Antioxidants	J. Perez C. Ku S. Hsu

A Process for the Fabrication of Ceramic Monoliths	J. Ritter
Preparation of a Composite of Ultra-Fine Particles	J. Ritter R. Shull
Optical Sensor: Molecular Orientation and Viscosity of Polymeric Materials	A. Bur R. Lowry R. Roth
Elimination of Twins in Perovskite-Type Superconducting Single Crystals	F. Gayle D. Kaiser

1988

Stress-Free Sintering of Fiber-Reinforced Ceramic Composites	C. Ostertag
Electrode Array for Analysis of Particles in Slurries	A. Dragoo
Aluminum Hydroxides as Solid Lubricants	R. Gates S. Hsu
Quantitative & Qualitative Technique for Assessing Stresses During Densification	C. Ostertag
Fiber-Reinforced Ceramic and Process for Its Manufacture	W. Haller U. Deshmukh
A Process for the Chemical Synthesis & Forming of BiPbSrCaCuO and BiSrCaCuO High Temperature Superconductors	J. Ritter
Co-Precipitation Synthesis of Precursors to Bismuth Containing Superconductors	J. Ritter
High Pressure Process for Producing Transformation Toughened Ceramics	S. Block G. Piermarini
Superconductor-Polymer Composite	A. DeReggi C. Chiang G. David

CONFERENCES AND WORKSHOPS SPONSORED

NIST Testing Methodology for Glass, Glass-ceramic, and Ceramic Matrix Composites Workshop, February 8, 1990. David Cranmer, 35 attendees.
To review test methodologies and data requirements for composite property determination.

NIST/ASM Symposium on Intelligent Processing of Materials, March 1, 1990, Gaithersburg, MD, J. A. Carpenter, 30 attendees.
To review the state-of-the-art intelligent processing.

Workshop on Measurements of Properties of Materials in Microelectronic Packaging, May 1-3, 1990, Gaithersburg, MD, J.A. Carpenter, 70 attendees.
To determine a research agenda for measurements and properties of microelectronic packaging.

Interagency Coordinating Committee on Structural Ceramics, Gaithersburg, MD, May 10-11, 1990, S. J. Dapkunas, 30 attendees.
To coordinate federal agencies research programs in structural ceramics research.

NIST Surface Forces Workshop, May 31-June 1, 1990. Roger Horn and Douglas Smith, 15 attendees.
To exchange results from experimental programs on surface forces research.

Diamond Optics III, at the 34th Annual International Technical Symposium on Optical and Optoelectronic Applied Science and Engineering, San Diego, CA, July 8-10, 1990, A. Feldman, 120 attendees.
To review research in diamond film research.

American Ceramic Society/American Society of Nondestructive Testing Conference NDE of Modern Ceramics, G. White, July 9-12, 1990, Columbus, OH, 130 attendees.
To review research on NDE of Ceramics.

Eighth American Conference on Crystal Growth, Vail, CO, July 15-20, 1990, D. Kaiser, 350 attendees.
To review research on crystal growth and analysis.

NIST Mechanical Testing Methodology for Ceramic Design and Reliability Workshop, September 5-7, 1990, 50 attendees.
To identify data and experimental methodologies required for ceramic design and reliability.

U. S. Assessment of the New Diamond Technology in Japan, Arlington, VA, September 13, 1990, A. Feldman, 50 attendees.
To exchange information gained in assessments of Japanese diamond film technology.

NIST Workshop on Ceramic Machining, Gaithersburg, MD, September 19, 1990, S. J. Dapkunas, 35 attendees.
To identify research needs in ceramic machining.

SELECTED TECHNICAL/PROFESSIONAL COMMITTEE LEADERSHIP

American Ceramic Society
Program and Meetings Committee
        S. Freiman, Incoming Chairman
    Glass Division
        Committee on Glass Standards Classification and Nomenclature
            M. Cellarosi, Chairman
        Editorial Committee
            S. Wiederhorn, Subchairman
    Basic Science Division
        Editorial Committee
            B. Lawn, Chairman
        Program Committee
            E. Fuller, Jr., Chairman
    Communication of the American Ceramic Society
            E. Fuller, Jr., Contributing Editor
    Baltimore-Washington Section
            J. Wallace, Vice Chairman
    Engineering Ceramics Division
            D. Cranmer, Secretary

ASM International
    Energy Division
            S. Dapkunas, Chairman
    Journal of Engineering Materials
            S. Dapkunas, Associate Editor

American Society for Testing and Materials
    C14: Glass and Glass Product
            M. Cellarosi, Chairman
    C14.01: Nomenclature of Glass and Glass Products
            M. Cellarosi, Chairman
    C28.05: Task Group on Powder Characterization
                S. Malghan, Working Group Chairman
    D2: Petroleum Products and Lubricants
    D2.09G: Response of Base Oils to Oxidation Inhibitors
            J. Perez, Chairman
            C. Ku, Secretary
    E29.01: Advanced Ceramics, Organizational Meeting
            M. Cellarosi
    E42: Surface Science, G. G. Long
    F1: Electronics
    F1:02: Lasers
                A. Feldman, Subcommittee Editor
    G2: Erosion and Wear
    G2.2.02: Solid Particle Erosion
                A. Ruff, Task Group Leader
    G2.4.04: Pin-on-Disk
            A. Ruff, Chairman

American Society of Mechanical Engineers
    Tribology Division Executive Committee
        S. Jahanmir, Member
    Research Committee on Tribology
        S. Jahanmir, Chairman
        S. Hsu, Member
    Wear of Materials Conference Steering Committee
        A. Ruff, Member

COMAT Subcommittee on Structural Ceramics
        S. Hsu, Member
COMAT Subcommittee on Superconductivity
        S. Dapkunas, Member

International Energy Agency
    Task II - International Standards
        S. Hsu, Overall Task Leader on Powder Characterization
        Subtask 6 Powder Characterization Subgroup
            S. Malghan, U. S. Task Leader
        Assignment II-0-3 Ceramic Characterization
            E. Fuller, Jr., Member

International Union of Crystallography (IUCr)
    Commission on Crystallographic Studies at Controlled
    Pressures and Temperatures
        G. Piermarini, Chairman

Minerals and Metallurgical Processing Journal
    Editorial Board
        S. G. Malghan, Member

National Materials Advisory Board, National Academy of Sciences
    Committee on Ceramic Tribology
        S. Hsu, Member
        S. Jahanmir, Member
    Committee on superhard Materials
        A. Feldman, Member

Oak Ridge National Laboratory
    High Temperature Materials Laboratory Advisory Committee
        S. Wiederhorn, Chairman

Powder and Bulk Engineering Journal
        S. Malghan, Member Editorial Advisory Board

Society of Automotive Engineers
    Task Group on Recommended Practices for the Measurement of Unregulated
    Diesel Emissions
        J. Perez, Chairman

Society of Mining and Metallurgical Engineers
    Mining Processing Division
        Concentration Committee
            S. Malghan, Chairman
    Mining and Metallurgical Processing Journal
        Editorial Board
            S. Malghan, Member

Society of Tribologists and Lubrication Engineers
    Annual Meeting Program Committee
            S. Jahanmir, Member
    Board of Directors
            S. Hsu, Director
    Ceramics and Composite Committee
            S. Jahanmir, Chairman

Superconductor Applications Association
            E. Fuller, Jr., Member of Advisory Board

Versailles Project on Advanced Materials and Standards (VAMAS)
    International Round-Robin in Ceramic Working Area
            S. Freiman, Co-chairman
            E. Fuller, Jr., Co-chairman
    Subcommittee on Wear
            S. Jahanmir, U. S. Representative

INDUSTRIAL AND ACADEMIC INTERACTIONS

INDUSTRIAL

ACTIS, Inc.

An agreement has been signed between NIST and ACTIS, Inc. for a joint research and development activity related to comprehensive computerized tribology databases. These databases will be evaluated by NIST and marketed by ACTIS, Inc. Other participants in the program are DOE, U.S. Army, U.S. Air Force, ASME and STLE.

Adiabatics, Inc.

As part of the Gas Research Institute joint study, research on valve materials selection and wear mechanisms in gas-fired engines was conducted (L. K. Ives and E. P. Whitenton, NIST; R. Kamo, Adiabatics).

Advanced Technology Materials (ATM)

A collaboration between NIST (L. H. Robins) was begun with Advanced Technology Materials (C. Beetz) to characterize chemically doped diamond specimens from ATM by cathodoluminescence imaging and spectroscopy.

Akzo Chemical Co.

A Cooperative Research and Development Program is in progress to utilize the NIST technology (J. M. Perez and C. S. Ku, NIST; T. Marolewski, AKZO) in development of a high temperature liquid lubricant for evaluation in low heat rejection engines.

Allied Signal Aerospace Company

The Tribology Group (S. Jahanmir) is participating in a joint program with Allied in research aimed at using silicon nitride in diesel engine applications. The purpose of this program is to define the role of surface condition and finishing methods on tribological performance. The samples are prepared and characterized by Allied Signal Aerospace Company (M. Meiser), and subsequently tested and analyzed by NIST.

Allied Signal Corporation

A joint research program is underway to determine the role of impurities in superconducting ceramic powders on limiting the critical current density in the final product. Allied (A. Trivedi) is supplying superconducting powders containing various quantities of carbon and other impurities. NIST (S. Freiman) is processing these powders and determining critical current densities. The work will be published as a joint paper.

AT&T Bell Labs

This is a joint research program on the phase relations in superconducting ceramics between AT&T Bell Laboratories (S. Sunshine) and NIST (R. Roth). Specimens are exchanged and x-ray diffraction data analyzed to determine crystal structure. Several joint papers have resulted from the ongoing interaction between NIST and AT&T.

AVX Corporation

A joint effort is ongoing aimed at an understanding of the mechanical reliability of multilayer ceramic capacitors. AVX (B. Rawal) prepares specimens of differing composition and properties. These specimens are subsequently tested at NIST (S. Freiman). This work has resulted in three joint publications, as well as leading to improved AVX products.

Babcock and Wilcox, Inc.
Coors Ceramics, Inc.
NASA Lewis Research Center

The performance of the Structural Ceramics Database developed at NIST by R. Munro and E. Begley, was reviewed at selected sites, including a research laboratory (NASA Lewis Research Center), a ceramics manufacturer (Coors Ceramics, Inc.), and an applications manufacturer (Babcock and Wilcox, Inc.).

Battelle Columbus Laboratories

A joint activity is underway to prepare a wear atlas from selected literature and research findings at Battelle Columbus Laboratories, NIST, and the West German Bundesanstalt fur Materialprufung. Battelle (W. Glaeser) and NIST (A. W. Ruff) are evaluating publications in wear and friction to select authoritative findings that relate wear and friction with materials properties and surface morphology.

Carborundum Company

Dr. Divakar is a Research Associate in the Tribology Group, participating in a joint research program with NIST (S. Jahanmir) on the wear mechanisms of advanced ceramics and composites at elevated temperatures. The aim of this program is to define the controlling effect of microstructure on friction and wear behavior of silicon carbide.

Catalyst Research Corp.

D. Schrodt (CRC) has obtained laboratory procedures from J. Ritter for designing tests for Li-batteries.

Caterpillar Corporation

Discussions and an exchange of visits has taken place with technical staff from Caterpillar Corporation (F. A. Kelley) in connection with wear of certain types of equipment bearings. The company is considering establishing a Research Associate at NIST (A. W. Ruff) in the area of wear-resistant coatings and galling wear.

CPS Superconductor

A joint research program has been established to determine the link between melt processing procedures and phase equilibria in superconducting ceramics, as well as to determine the strength of superconducting ceramic fibers. CPS Superconductor (J. Hodge) is supplying materials, while NIST (S. Freiman) will develop the necessary test procedures and phase diagrams. The work will result in joint publications.

E. I. DuPont de Nemours & Co.

DuPont (D. Roach) has provided alumina and alumina-zirconia fibers to C. Ostertag for incorporation into ceramic, ceramic-metal, and glass matrix composites.

E/M Corporation

A joint research program was conducted to determine the tribological characteristics of high temperature solid lubricant coatings on ceramic surfaces. E/M Corporation (R. Gresham) prepared several solid lubricant coatings on alumina. These samples were subsequently tested and characterized at NIST (S. Jahanmir).

Electric Power Research Institute

EPRI (W. Bakker) is funding a program in the Ceramics Division (S. Freiman) to develop superconducting ceramics for conductor applications. The program involves determining the effects on critical current density of substituting other rare earth ions for yttrium in Ba-Y-Cu-O superconducting ceramics. Phase equilibria and processing data relevant to the production of these materials are being obtained.

Ford Motor Company

Ford Motor Company (K. Carduner and M. Rokosz) has been active in the applications of NMR spectroscopy and imaging to characterize ceramic materials. The first stage of collaborative effort with P. S. Wang involves data exchange of Si-27 CP/MAS NMR for phase composition determination of silicon nitride and carbide powders. In the future, we will provide imaging capability for Ford's applications.

Garrett Ceramic Components

In this project, the Garrett Ceramic Components has assisted S. Malghan by providing a design for a pressure slip casting system. This system is being used in our studies on densification of colloidal suspensions.

In addition, NIST is conducting collaborative studies with B. Busovne and J. Pollinger on the interactions of powder-binder-sintering aid in the processing of silicon nitride powders.

Gas Research Institute and Center for Advanced Materials, Pennsylvania State University

The Structural Ceramics Database project was funded in part by the Gas Research Institute through the Center for Advanced Materials at Pennsylvania State Unversity, as an important step towards the use of advanced ceramics in heat exchangers and gas-fueled engines.

GTE Laboratories, Inc.

GTE (J. Baldoni) has provided whisker-reinforced and whisker-free silicon nitrides to S. Wiederhorn and D. Cranmer for evaluation of creep and creep rupture, and changes in microstructure as a result of creep.

Johns Hopkins University

The magnetic properties of superconducting $YBa_2Cu_3O_{6+x}$ single crystals fabricated at NIST (D. Kaiser) are being measured at Johns Hopkins (K. Moorjani, J. Bohandy) using the recently-developed magnetically modulated microwave absorption (MAMMA) technique. The crystals have produced the cleanest, sharpest spectra of any superconducting sample measured by this technique. The objective of this effort is to study the details of the superconducting transition in twinned and detwinned crystals in order to further the understanding of the mechanism of high temperature superconductivity.

Johns Hopkins (D. Shechtman) is collaborating with NIST (A. Feldman and E. Farabaugh) in the high resolution TEM analysis of CVD diamond nucleation and growth.

Louisiana State University

Crystal structure determinations on a detwinned single crystal of $YBa_2Cu_3O_{6+x}$ ($T_c = 89$ K) were performed in this joint activity between Louisiana State University (S. Watkins, F. Fronczek) and NIST (D. Kaiser, F. Gayle). The results indicated that the oxygen atoms in the O(4) chain sites are offset from the crystallographic b-axis, leading to zig-zag rather than linear Cu-O chains. Weak superlattice reflections were observed, indicating a possible superstructure linked to three-dimensional ordering of oxygen and/or gold atoms.

Naval Research Laboratory

S. Lawrence and B. Bender (NRL) are collaborating with J. Wallace on the thermochemical treatment of polymer-derived SiC fibers and the degradation mechanisms of these fibers during high temperature heat treatments. A joint publication is planned.

Norton Company

In this collaborative project with V. Pujari, C. Willkens, Norton Company, S. Malghan is studying the characteristics of agitation milled silicon nitride powders in aqueous environment. Norton Company has provided silicon nitride powder samples with an intent to actively get involved if the results are applicable to their processing studies. The active involvement may be possible if our studies demonstrate that particle size reduction can be achieved without contamination.

Thermal conductivity measurements are important for characterizing diamond films. Interaction with Norton (K. Grey) involved learning to use the NIST (A. Feldman and H.P.R. Frederikse) photothermal radiometry facility for the purpose of setting up such a facility at Norton. We plan to collaborate in the analysis of the data generated at Norton.

Norton/TRW Co.

Norton/TRW (R. Yeckley) has provided a Y_2O_3-containing silicon nitride to S. Wiederhorn and D. Cranmer for evaluation of creep and creep rupture, and changes in microstructure as a result of creep.

3M Corporation

3M (A. Holtz) has provided mullite and other fibers to D. Cranmer which have been specially treated to change interface properties. These fibers have been incorporated into composites for testing.

Ube Industries, Japan

Ube Industries (T. Yamada) has collaborated with S. Malghan by providing powder samples for studying the high energy agitation milling of silicon nitride powders. The specific interest lies in the development of an understanding of morphological and surface chemical changes taking place to the milled powders.

Uniroyal/Ciba Geigy/R. T. Vanderbilt/Shell Ltd.

Development of high temperature liquid lubricants involves cooperative efforts with several additive manufacturers. This cooperative research (C. S. Ku and J. M. Perez) has resulted in several candidate lubricants for evaluation in low heat rejection engines.

U.S. Assessment of the New Diamond Technology in Japan

This was an interaction involving selection of a delegation from government, academia, and industry to participate in an assessment of the status of diamond technology in Japan. The assessment was organized by NIST (A. Feldman) under the auspices of Office of Science and Technology Policy. The assessment consisted of a planning workshop, a visit to companies, universities and government laboratories deemed leaders in diamond technology, preparation of an assessment report, and holding a debriefing seminar. Academic and industrial participants were:

AT&T Bell Laboratories (J. Mitchell)
BDM International/University of Central Florida (M. Stickley)
Case Western Reserve University (J. C. Angus)
Ford Motor Company (M. A. Tamor)
IBM (J. J. Cuomo)
North Carolina State University (J. T. Glass)
Pennsylvania State University (W. A. Yarbrough)
Research Triangle Institute (R. A. Rudder)
Rockwell International (S. Holly)
Johns Hopkins University

USSR Academy of Science

Cooperative activities under the NIST-USSR Academy of Science Agreement have continued in the areas of tribology and materials science. Current emphasis is on a joint US-USSR book on tribology (A. W. Ruff and S. Jahanmir). Future benefits to NIST and the Division include exchange of tribology data, exchange of computer software for surface analysis, and future exchange of technical staff.

ACADEMIA

Columbia University

P. Somasundaran has been collaborating with S. Malghan on a research project to study basic parameters affecting the preparation of dense suspensions of silicon nitride powder containing sintering aids.

Drexel University

This is a joint program between Drexal University (M. Barsoum) and NIST (D. Cranmer) to investigate and control the fracture behavior of ceramic and glass matrix composites.

East China University of Chemical Technology

This is a joint effort to use finite-element techniques to analyze creep behavior of ceramic c-rings at elevated temperatures. ECUCT (D. Wu and Z-D Wang) is developing the finite element model for C-rings and a computational algorithm for creep and NIST (T.-J. Chuang) is providing a theoretical framework and experimental data to support the program.

Lehigh University

This is a collaboration to determine the effect of microstructure on the fracture resistance of monolithic ceramic materials. The materials under study have been manufactured at Lehigh University (H. Chan, M. Harmer) and are being characterized at NIST (B. Lawn).

National Tsing Hua University

This joint effort is to investigate crack growth behavior along a bi-material interface. NTHU (S. B. Lee and J.-L. Chu) is developing a computer algorithm for solving an integral equation system involving crack.

Northwestern University

J. Weertman and P. Jemian are collaborating with G. G. Long, NIST, on anomalous small angle x-ray scattering to separate contributions from various scattering species in a complex material.

Northwestern University/Pennsylvania State University

Joint research involves lubrication modeling between NIST, E. E. Klaus (PSU) and H. S. Cheng (NWU). The research focuses on the microelastohydrodynamic theories under wearing conditions. This is the first attempt at combining surface chemistry with surface mechanics to create a predictive wear model.

Oklahoma State University

Collaborative research between OSU and NIST (R. Powell and D. Cranmer) is being conducted to investigate the properties of permanent, laser-induced refractive index gratings based on Eu-containing glasses. The end result of this effort will be a device for processing optical signals.

Pennsylvania State University

The Tribology Group has several joint research projects with the Department of Chemical Engineering and the materials Research Laboratory at PSU. The research projects include fundamental studies on the vapor phase lubrication of ceramic materials at high temperature; microstructural effects in ceramic wear processes; high temperature friction and wear tribometer design; and ceramic wear modeling which seeks to establish a theoretical understanding of ceramic wear processes.

Rutgers University

S. C. Danforth (Rutgers) has provided A. Pechenik (NIST) with nano-sized Si_3N_4 powder. The powder is processed at NIST using our diamond cell.

Southwest Research Institute

R. A. Page, Southwest Research Institute and S. Krueger, Reactor Division, NIST, are collaborating with G. G. Long on multiple angle small angle neutron scattering (MSANS) studies of pore evolution in alumina.

University of California at Santa Barbara

Joint experiments between University of California (J. N. Israelachvili, P. McGuiggan) and NIST (R. Horn and D. Smith) are being conducted to investigate frictional properties of silica surfaces under dry conditions and with a variety of thin (< 10nm) intervening liquid films.

University of Dayton Research Institute

Using UDRI's x-ray photoelectron spectrometer (XPS) and Auger electron spectrometer (AES), T. Wittberg, UDRI, is conducting studies on surface structures and reactivities with P. S. Wang, NIST. A variety of powders and ceramic materials have been investigated and the results have been published.

University of Florida

B. Moudgil is studying the characterization techniques and structure of flocs in dense slurries with G. G. Long and S. G. Malghan. Primary emphasis is placed on interfacial, rheological, and scattering (neutron and x-ray) techniques.

University of Illinois

Soo Wohn Lee of the Department of Civil Engineering, Mechanics, and Metallurgy are conducting joint research with NIST. The project centers on an investigation of the fundamental mechanisms of friction, wear, and surface damage in tribological applications of advanced ceramics.

University of Maryland

A collaborative study between the University of Maryland (A. Roitburd) and NIST (D. Kaiser, F. Gayle, L. Swartzendruber, L. Bennett) involves theoretical aspects of twin boundary migration under an applied stress and flux pinning by twin boundaries in $YBa_2Cu_3O_{6+x}$. A model has been developed to calculate the velocity of boundary migration as a function of temperature and applied stress. Magnetization measurements demonstrating an effect of twin boundaries on flux pinning have been understood in terms of vortex/twin boundary interactions.

Three projects are underway; on wear models of ceramics, on the determination of residual stresses in ceramics by x-ray techniques, and on modeling of indentation of a solid surface. The project on wear models (S. Jahanmir, NIST; J. Dally, U. MD) deals with the application of photoelastic techniques for analysis near surface cracks. The results of this research are used to develop a wear model for ceramics. The project on indentation modeling will compare results with NIST nanoindentation measurements of selected materials and tribological films (A. W. Ruff, NIST; J. Stewart, U. MD).

L. Chang and Y. Zhang, U. MD, are collaborating with P. S. Wang on a project to investigate ceramic surface reactivities with surface lubricants at high temperature by TGA/DSC as well as surface film formations. The lubricant oxidation is studied through free radical formation and recombinations by the electron spin resonance (ESR) method.

University of Michigan

J. Schwank is carrying out specialized characterization of conductive ceramic powders by ESCA and Auger spectroscopy in collaboration with J. Ritter, NIST. These powders are synthesized at NIST for NASA.

University of Utah

A collaboration was begun between NIST (L. Robins) and the University of Utah (J. Viner) to measure the optical absorptance of CVD diamond films by the method of photothermal deflection spectroscopy (PTDS), using the PTDS apparatus developed at the University. Initial results for one sample show that PTDS is a promising technique.

University of Houston

In this joint effort between the University of Houston (S. Moss) and NIST (D. Kaiser, F. Gayle), detwinned single crystals of $YBa_2Cu_3O_{6+x}$ are being measured by high-resolution x-ray diffraction techniques at temperatures in the range 10 - 298 K to search for a structural transition associated with the onset of superconductivity. Fully detwinned crystals are required for these measurements to eliminate ambiguities associated with the presence of twin boundaries which are present in all as-grown crystals.

University of Wisconsin

An joint activity is underway between the University of Wisconsin (S. Babcock, X. Cai, D. Larbalestier) and NIST (D. Kaiser) to characterize the magnetic and electrical transport properties of single crystals and bicrystals of superconducting $YBa_2Cu_3O_{6+x}$. Transport measurements on bicrystals with individual, bulk-scale grain boundaries of known orientation have provided the first evidence that some high-angle boundaries (> 10° misorientation) can transmit significant supercurrents in high magnetic fields at 77K.

FACILITIES

FACILITIES

POWDER CHARACTERIZATION AND PROCESSING

High Temperature X-ray Diffraction - J. P. Cline

The X-ray diffraction facility at NIST consists of a high temperature machine of theta-two theta geometry equipped with an incident beam monochrometer and a position sensitive proportional counter. The incident beam monochrometer removes the $K\alpha 2$ radiation and results in diffraction profiles that are more sensitive to effects of sample character. The position sensitive detector allows for data collection at a rate two orders of magnitude faster than conventional detectors. The furnace is an enclosed high vacuum chamber capable of reaching 3000K, it is equipped with a mass flow controller for atmospheric control. This equipment is used for the study of high temperature phase equilibria, high temperature reaction kinetics, sintering of monolithic ceramics, and strain development during sintering of ceramic composites. Additional equipment consists of four automated and updated Philips diffractometers which are used for certification of standard reference materials (SRMs), studies on the effects of microabsorption and extinction, and the development of the Rietveld method for a conventional, sealed tube, X-ray diffraction equipment.

SANS - Ceramics Furnace - G. G. Long

The SANS-Ceramic furnace is a unique facility that is now coming together. This system will allow in-situ densification studies of ceramic powders and SANS application. The experimental system has been designed to carry out densification studies of oxide powders at temperatures up to 2000°C. In addition, the furnace will be equipped with a dilatometer.

Electrokinetic Sonic Amplitude Measurement - L.-S. Lum and S. G. Malghan

The Matec ESA-8000 system has the unique capability for measuring colloidal properties in dense slurries. The analytical capabilities of the ESA system include performance in the following modes: potentiometric titration, conductometric titration, time-series titration, and concentration series titration. In the selected mode, the equipment can monitor: electrokinetic sonic amplitude, zeta-potential, electrophoretic mobility, electrical conductivity, isoelectric point, surface charge density, and phase angle of the material with the specified experimental conditions.

Slurry Rheology - S. G. Malghan

The RTI rheometer allows for viscosity as well as rheology characterization of ceramic slurries. Rheological measurements are more informative and flexible with respect to the various slurry properties: Newtonian, pseudoplastic, plastic, dilatant, and thixotropic. The modeling of these rheological properties as a function of sample treatment, surface chemical properties is paramount in developing and improving the slurry processing technology.

Physical Properties Characterization Laboratory - L. Lum, D. Minor, P. Pei and S. Malghan

The physical properties characterization laboratory is equipped with state-of-the-art techniques for the measurement of particle size distribution, specific surface area, specific gravity, tap density, and porosity. The particle size distribution is measured by three techniques -- gravity sedimentation by Sedigraph, centrifugal sedimentation by Joyce-Loeble, laser diffraction by Horiba LA-500. The range of particle size distribution covered by these techniques is 0.01 micron to 200 microns. The specific surface area determination is carried out by nitrogen adsorption and the BET method. The porosity of powders and ceramics is measured by mercury intrusion.

Agitation Milling of Powders - D. Minor, S. Malghan

High energy agitation milling of silicon nitride powders is carried out with a minimum contamination by the use of a specially designed milling system. This milling device allows for the size reduction of silicon nitride powder by milling at high slurry densities in approximately 1/6th to 1/10th of the time required by the conventional tumbling ball mill. The mill is lined with silicon nitride and the media are made of silicon nitride materials. Hence, external sources of contamination can be minimized.

Nuclear Magnetic Resonance (NMR) - P. S. Wang

The solid state NMR facility includes a Bruker MSL-400 NMR system capable of studying almost all NMR active nuclei in the periodic table in both solid and liquid states as well as performing NMR imaging in proton and carbon-13 frequencies. Currently, the operation parameters for both states at proton, deuterium, carbon-13, and aluminum-27 have been defined and proved by documented NMR spectra of organic and inorganic molecules. The equipment has been tuned to Si-29, Cu-63, and Y-89.

Scanning Electron Microscopy/Image Analysis (SEM) - J. F. Kelly

The scanning electron microscopy is used to characterize ceramic powders for their true size and shape. The capacity for characterizing thousands of individual features has been developed through the installation of a computer controlled Amray 1830 scanning electron microscope with a Kevex Quantum V EDS X-ray and image analysis system.

An in-situ fracture stage has been developed for the SEM to enable real time observation of crack propagation in ceramic wafers. This capability provides greater detail of the role of grain morphology in the mechanism of bridging behind the advancing crack tip.

The SEM is now modified to obtain single grain electron backscatter diffraction patterns from bulk specimens. This permits the measurement of crystallographic orientation in ceramic specimens.

Time-Resolved Micro-Raman - P. S. Wang

This versatile facility consists of a pulsed Nd-YAG laser, a CW Ar-ion laser, a triple monochrometer, and a gated intensified diode array detector. This facility, therefore, provides a wide variety of Raman analysis techniques in both time-resolved and continuous operation modes, using either visible or ultra-violet excitation sources for either operation mode. In addition, either bulk macro-Raman or 5 μm resolution micro-Raman analysis is available.

Thermal Analysis Facility - J. Wallace and J. Blendell

A thermal analysis facility has been set up for measurement of behavior of ceramic materials in a wide range of atmospheric conditions and temperatures. The equipment is comprised of a computer controlled differential pushrod dilatometer capable of measurement of thermal expansion or sintering shrinkage in vacuum or inert, oxidizing or reducing atmospheres with temperatures from room temperature to 1600°C. The atmosphere can be monitored using either a zirconia oxygen cell, which is connected to the dilatometer data acquisition system, or an external mass spectrometer with it's own associated computerized data acquisition system.

The second major piece of equipment is a simultaneous thermal analysis (STA) system which is capable of performing simultaneous thermogravimetric and differential thermal analysis from room temperature to 1700°C. Atmospheres can be varied from vacuum to single and mixtures of gases using a four channel mass flow controller. The STA is also connected to the mass spectrometer system and it's associated data acquisition system. The quadrapole mass spectrometer system has a capability of analyzing to 512 AMU.

Chemical Laboratory Facilities - J. J. Ritter

Chemical synthesis of powders is carried out in a well-equipped laboratory, which consists of controlled atmosphere glove boxes, preparative chemical vacuum systems, and a chemical flow reactor. A range of powders can be synthesized for exploratory purposes.

MECHANICAL PROPERTIES

Instrumented Indenter - D. Cranmer

This apparatus is designed to enhance our ability to measure the properties of the fiber/matrix interface in ceramic matrix composites. The instrumented indenter permits us to measure the force on and displacement of a fiber directly during loading and unloading. Previous methods for examining these properties could only measure the maximum applied load and inelastic displacement.

High Temperature Creep Apparatus - D. Cranmer, S. Wiederhorn

A series of four high temperature creep rigs ($T_{max} = 1550°C$) equipped with laser displacement sensors are available to determine the behavior of materials at elevated temperatures. Additionally, a rig capable of 1800°C in air equipped with the same laser displacement sensor is available.

Surface Forces Laboratory - R. Horn

The surface forces laboratory consist of a semi-clean room preparation facility and a crossed cylinders surface forces apparatus. The crossed cylinder apparatus permits measurements of the forces associated with surfaces brought to within ~2 nm of one another through contact. It can be operated with a variety of liquid or gaseous environments, thus allowing investigations of the effects of chemical changes on forces between two surfaces.

Analytical Electron Microscopy - B. Hockey

Several transmission and scanning electron microscopes are available for analysis of the changes in microstructure as a result of creep.

Glass Melting - D. Cranmer, D. Kauffman

Extensive glass melting and annealing facilities for production of melts up to 1600°C are available. Batch sizes up to about 2.5 -3 kg can be produced using this equipment. Special facilities for melts containing heavy metals such as thallium and lead are also available.

Viscometers - D. Cranmer

Rotating bob, fiber elongation, and bending beam apparatuses for determining the complete range of viscosity from about 10^{14} to 10^{1} poise over the temperature range from room temperature to 1600°C are available.

Microsphere Fabrication - D. Cranmer

This special facility is available to make relatively uniform diameter spheres of about 1 - 10 micrometers. Virtually any glass composition which can be melted below 1600°C can be made into spheres with this apparatus.

TRIBOLOGY

Friction and Wear Testing - S. Jahanmir

More than twenty different tribometers are available for the measurement of friction and wear of materials under different test conditions and environments. Examples include: high temperature unidirectional reciprocating tribometer, modified four ball wear tester with a special ball-on-three-flats adaptation, computer controlled pin-on-disk and single stroke pin-on-flat, high temperature erosion system, cross-cylinder standard test machine, dry sand and wet sand rubber wheel abrasion tester, and ferrograph for wear particle analysis. These tribometers can be used to simulate and analyze almost any desired test condition and environment.

Surface Analysis - J. Perez

Many analytical instruments are available for the chemical and morphological characterization of surfaces. These include: time resolved micro-Raman laser system for in-situ analysis of tribochemical reactions, room temperature and high temperature microindentation apparatus, computer controlled 3-D surface profilometer, computer controlled nanoindentation and scratch hardness tester, optical microscopes for surface analysis, unique liquid chromatography refractive index/UV atomic absorption surface film analyzer for organo-metallic compound identification and quantification, surface analyzer with Fourier transformed infrared and multi-photodiode ultra-violet spectroscopy, and other analytical instruments such as HPLC, LC, GC, GC-MS.

Tribo-System Simulation/Degradation Mechanisms - J. Perez

Various special lubricant simulation devices include: hot-tube, panel coker, oxidation, free radical titration, bearing corrosion, thin film oxidation test apparatus, thin film micro-oxidation apparatus for interface chemistry investigation, NIST modified thermal analyzer with high pressure differential scanning calorimeter (DSC) and thermogravimetric analyzer (TGA) for surface reaction products analysis, and NIST designed chemiluminescence apparatus to relate molecular structures to oxidation and surface reactions.

ELECTRONIC MATERIALS

Thermal Analysis Facility - J. Wallace and J. Blendell

A thermal analysis facility has been set up for measurement of behavior of ceramic materials in a wide range of atmospheric conditions and temperatures. The equipment is comprised of a computer-controlled differential pushrod dilatometer capable of measurement of thermal expansion or sintering shrinkage in vacuum or inert, oxidizing or reducing atmospheres with temperatures from room temperature to 1600°C. The atmosphere can be monitored using either a zirconia oxygen cell, which is connected to the dilatometer data acquisition system, or an external mass spectrometer with its own associated computerized data acquisition system.

The second major piece of equipment is a simultaneous thermal analysis (STA) system capable of performing simultaneous thermogravimetric and differential thermal analysis from room temperature to 1700°C. Atmospheres can be varied from vacuum to single and mixtures of gases using a four-channel mass flow controller. The STA is also connected to the mass spectrometer system and its associated data acquisition system. The quadrapole mass spectrometer system has a capability of analyzing to 512 AMU.

Ceramics Processing Laboratory - J. Blendell, J. Wallace, S. Malghan

A processing laboratory for the synthesis and production of well controlled ceramics has been assembled. Equipment includes: cold isostatic process, hot presses, furnaces, milling equipment, a sinter forge and tape caster.

Level 10 Clean Room - J. Blendell

A Level 10 Clean Room has been constructed for the processing of ceramics in a controlled environment where the presence of air low contaminants can seriously affect the final products properties. The room is provided with separated work stations to allow simultaneous conduct of experiments.

Thermal Wave Analysis Facility - A. Feldman, G. White

This facility is used for characterizations based on variations of thermal diffusivities. Equipped with both an Ar-ion and CO_2 laser, the facility permits analyses by infrared and Mirage methods. It is especially useful as a nondestructive method of detecting flaws in ceramics especially in near-surface regions.

OPTICAL MATERIALS

Diamond Film Deposition - E. Farabaugh, A. Feldman

Facilities consist of two hot filament CVD reactors, a microwave enhanced CVD reactor. The hot filament reactors can deposit diamond onto substrates up to 2.5cm x 2.5cm. The microwave reactor can accommodate substrates up to 10cm in diameter. The reactant gases are hydrogen and methane. Growth rates typically range from 0.1 to 0.6μm/hr.

Optical Characterization - L. Robins, A. Feldman

Facilities include an Cary spectrophotometer for measuring optical transmittance in the spectral range 0.2 μm to 2.5 μm, optical spectrometers for measuring photoluminescence and Raman spectra, and an argon ion laser.

Defect and Morphology Characterization - L. Robins, L. Cook

Facility consists of a scanning electron microscope (SEM) equipped with mirrors for cathodoluminescence detection allowing for simultaneous electron and cathodoluminscence imaging. A spectrometer for optical spectrum analysis of the cathodoluminescence radiation is attached to the SEM.

Thin Film Deposition and Characterization - E. Farabaugh

Facility consists of an electron beam deposition system equipped with multiple sources for codeposition. Attached to the deposition system is surface analysis chamber with capabilities for Auger spectroscopy, electronic energy loss spectroscopy, X-ray photoelectron spectroscopy, and secondary ion mass spectroscopy. Facility includes a HP-1000 computer for data acquisition.

Metallorganic Chemical Vapor Deposition (MOCVD) System - D. Kaiser

The system has been designed for depositing selected oxide materials by the method of MOCVD. The materials that can be deposited depend on the availability of metallorganic precursor materials. At present precursors suitable for depositing titanium dioxide and barium oxide are available. The substrate area is approximately 1cm x 1cm.

APPENDIX

U.S.DEPARTMENT OF COMMERCE
National Institute of Standards and Technology

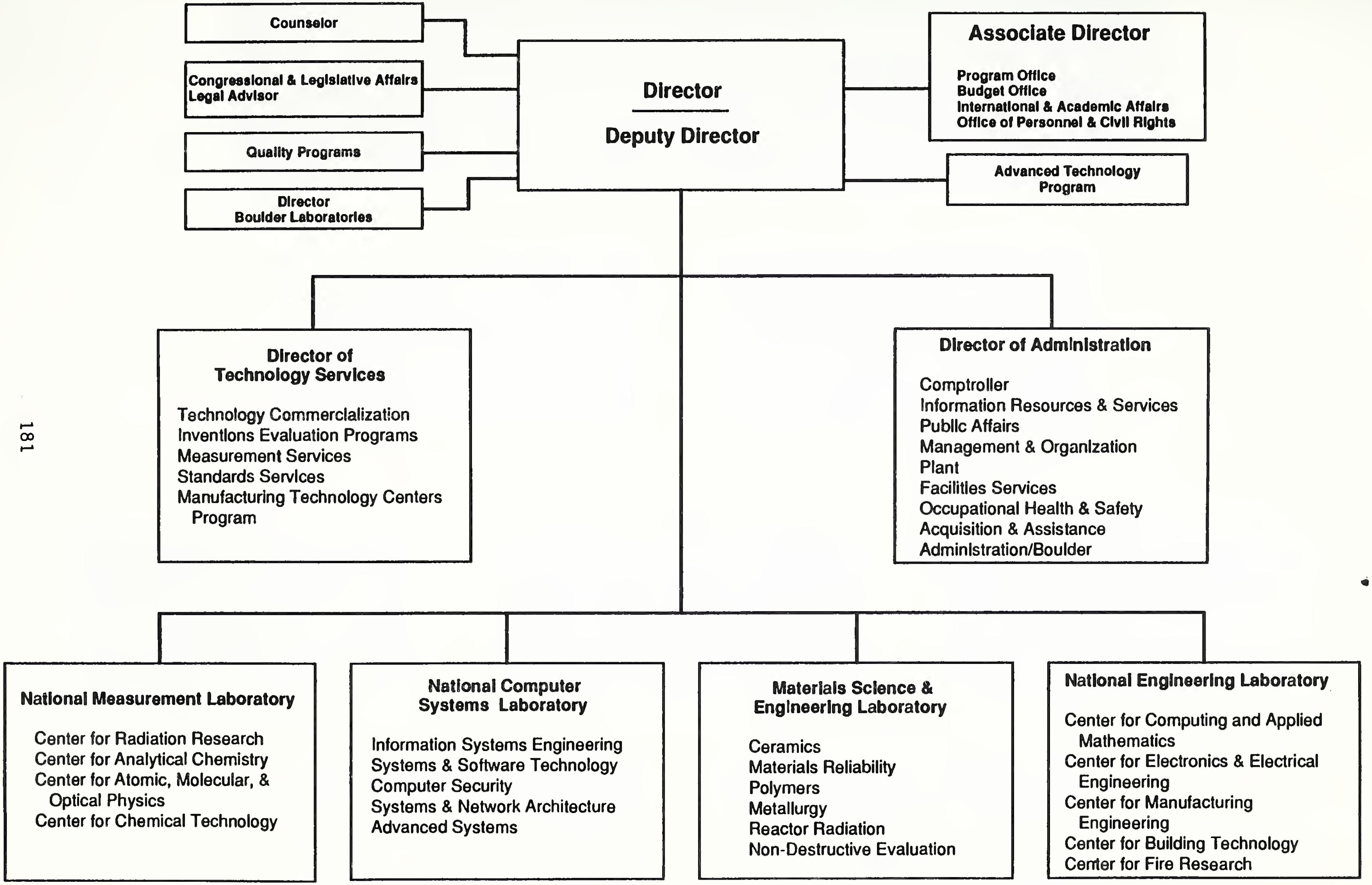

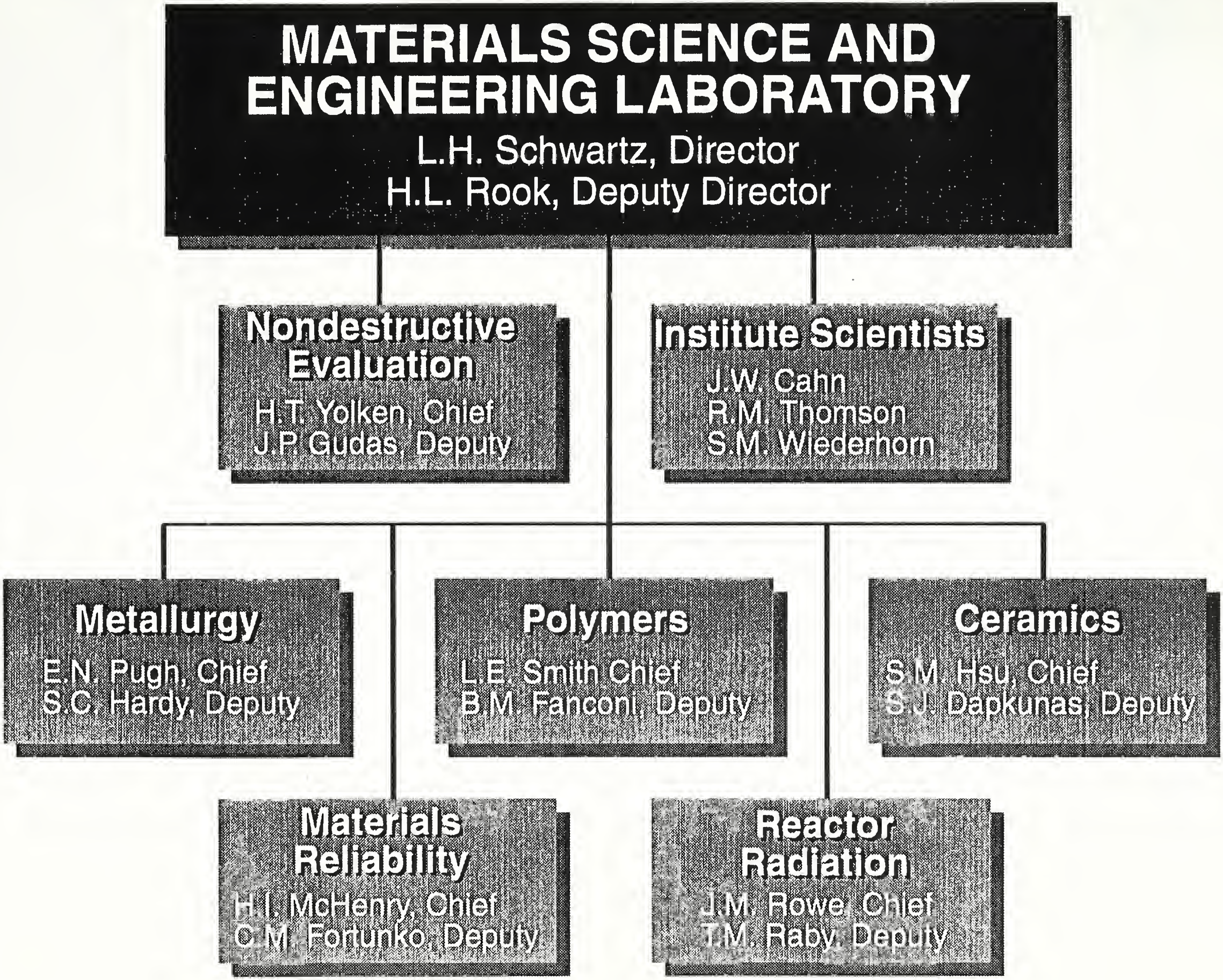

MATERIALS SCIENCE AND ENGINEERING LABORATORY

L.H. Schwartz, Director
H.L. Rook, Deputy Director

Nondestructive Evaluation
H.T. Yolken, Chief
J.P. Gudas, Deputy

Institute Scientists
J.W. Cahn
R.M. Thomson
S.M. Wiederhorn

Metallurgy
E.N. Pugh, Chief
S.C. Hardy, Deputy

Polymers
L.E. Smith Chief
B.M. Fanconi, Deputy

Ceramics
S.M. Hsu, Chief
S.J. Dapkunas, Deputy

Materials Reliability
H.I. McHenry, Chief
C.M. Fortunko, Deputy

Reactor Radiation
J.M. Rowe, Chief
T.M. Raby, Deputy

NIST-114A
(REV. 3-89)

U.S. DEPARTMENT OF COMMERCE
NATIONAL INSTITUTE OF STANDARDS AND TECHNOLOGY

BIBLIOGRAPHIC DATA SHEET

1. PUBLICATION OR REPORT NUMBER
NIST 4394

2. PERFORMING ORGANIZATION REPORT NUMBER

3. PUBLICATION DATE
November 1990

4. TITLE AND SUBTITLE
Ceramics Division - Technical Activities 1990

5. AUTHOR(S)
S. M. Hsu

6. PERFORMING ORGANIZATION (IF JOINT OR OTHER THAN NIST, SEE INSTRUCTIONS)

U.S. DEPARTMENT OF COMMERCE
NATIONAL INSTITUTE OF STANDARDS AND TECHNOLOGY
GAITHERSBURG, MD 20899

7. CONTRACT/GRANT NUMBER

8. TYPE OF REPORT AND PERIOD COVERED

9. SPONSORING ORGANIZATION NAME AND COMPLETE ADDRESS (STREET, CITY, STATE, ZIP)
NIST - Ceramics Division 420
Building 223/A256
Gaithersburg, MD 20899

10. SUPPLEMENTARY NOTES

☐ DOCUMENT DESCRIBES A COMPUTER PROGRAM; SF-185, FIPS SOFTWARE SUMMARY, IS ATTACHED.

11. ABSTRACT (A 200-WORD OR LESS FACTUAL SUMMARY OF MOST SIGNIFICANT INFORMATION. IF DOCUMENT INCLUDES A SIGNIFICANT BIBLIOGRAPHY OR LITERATURE SURVEY, MENTION IT HERE.)

Current programs of the Ceramics Division are reviewed.

12. KEY WORDS (6 TO 12 ENTRIES; ALPHABETICAL ORDER; CAPITALIZE ONLY PROPER NAMES; AND SEPARATE KEY WORDS BY SEMICOLONS)
Advanced Ceramics; Data Bases; Electronic Ceramics; Mechanical Properties; Optical Materials; Powder Characterization and Processing; Tribology; Superconductors; Synchrotron Radiation

13. AVAILABILITY
☒ UNLIMITED
☐ FOR OFFICIAL DISTRIBUTION. DO NOT RELEASE TO NATIONAL TECHNICAL INFORMATION SERVICE (NTIS).
☐ ORDER FROM SUPERINTENDENT OF DOCUMENTS, U.S. GOVERNMENT PRINTING OFFICE, WASHINGTON, DC 20402.
☒ ORDER FROM NATIONAL TECHNICAL INFORMATION SERVICE (NTIS), SPRINGFIELD, VA 22161.

14. NUMBER OF PRINTED PAGES
166

15. PRICE
A08

ELECTRONIC FORM